Molecular Mechanism and Regulation of Autophagy in *Saccharomyces cerevisiae*

by

Zhiyuan Yao

A dissertation submitted in partial fulfillment
of the requirements for the degree of
Doctor of Philosophy
(Molecular, Cellular and Developmental Biology)
in the University of Michigan
2018

Doctoral Committee:

Professor Daniel J. Klionsky, Chair
Professor Laura Olsen
Professor Lois S. Weisman
Professor Haoxing Xu

Zhiyuan Yao

yzhiyuan@umich.edu

ORCID iD: 0000-0002-5759-9822

Dedication

This thesis is dedicated to my beloved wife Jie Li, and to my parents Cai Yao and Hexiang Liu for their unconditional support. This thesis is also dedicated to Saber, Artoria Pendragon, who always inspires me with her strong will and noble spirit.

Acknowledgements

First I want to thank my mentor, Dr. Daniel J. Klionsky, for his continuous support and patient guidance during my Ph.D. works. Dan is a great scientist as well as a wise advisor. His passion in science and helpful advice on my projects always encouraged me to plan ahead and consider potential problems before they develop. Five years' experience in one's 20s will greatly shape his view in both career and life, and I feel so lucky to have Dan as my example during my graduate life.

I also want to thank my thesis committee members, Professor Haoxing Xu, Professor Lois S. Weisman and Professor Laura Olsen. Your generous support and immense knowledge provided me with invaluable suggestions and criticisms for my research. Without all this help, I could not finish this thesis. Here I would like to express my sincere thanks for all of the efforts you made.

I would like to thank all current members and alumni in the Klionsky lab—thanks for your help both inside or outside the lab. I am so happy to have you guys around for the past five years. I enjoyed scientific discussions we had and lab activities we held. Specifically I want to thank Dr. Meiyan Jin and Dr. Xu Liu. Meiyan taught me most of the experimental methods when I was new in the lab and provided helpful suggestions when I encountered obstacles in my research. Xu provided countless suggestions during my graduate studies and offered generous help when I faced problems. Discussion with Xu is always a happy experience regardless of the topic. I learned a lot from both of them.

Finally I would like to thank my family for their unconditional support. Specifically I want to thank my wife Dr. Jie Li, who is playing Dota2 beside me while I am writing this acknowledgement. We have known each other over 16 years. Over this time you were my schoolmate, my classmate, my competitor, my girlfriend and finally you are my life mate. Thanks for supporting me both in life and in game, my thanks and love to you are far beyond what words can express. We shared a similar taste in food, and similar opinions of life, even though our Dota2 rank is not similar, I will be happy to help you rise up. Also, I want to thank our pet cat, Batman, for the happiness she gave us during these years.

Table of Contents

List of Tables

List of Figures

Abstract

Macroautophagy (hereafter autophagy), literally defined as a type of self-eating, is a dynamic cellular process in which cytoplasm is sequestered within a unique compartment termed the phagophore. Upon completion, the phagophore matures into a double-membrane autophagosome that fuses with the lysosome or vacuole, allowing degradation of the cargo. Autophagy is involved in various aspects of cell physiology, and its dysregulation is associated with a range of diseases. Thus, Understanding of molecular mechanism and the regulation of autophagy is important for exploring potential therapy of diseases.

The most prominent feature of autophagy is the formation of a double-membrane sequestering compartment, the phagophore; this transient organelle surrounds part of the cytoplasm and matures into an autophagosome, which subsequently fuses with the vacuole or lysosome to allow degradation of the cargo. Much attention has focused on the process involved in phagophore nucleation and expansion, but many questions remain. Here, we identified the yeast protein Icy2, which we now name Atg41, as playing a role in autophagosome formation. Atg41 interacts with the transmembrane protein Atg9, a key component involved in autophagosome biogenesis, and both proteins display a similar localization profile. Under autophagy-inducing conditions the expression level of Atg41 increases dramatically and is regulated by the transcription factor Gcn4. This work provides further insight into the mechanism of Atg9 function and the dynamics of sequestering membrane formation during autophagy.

Autophagy is a tightly controlled cellular process by which cytosolic proteins, Studies have revealed the molecular mechanism of transcriptional regulation of autophagy-related (*ATG*) genes upon nutrient deprivation. However, little is known about their translational regulation. Here we found that Dhh1, a DExD/H-box RNA helicase, is required for efficient translation of Atg1 and Atg13, two proteins essential for autophagy induction. Dhh1 directly associates with *ATG1* and *ATG13* mRNAs under nitrogen starvation conditions. The structured regions shortly after the start codons of the two mRNAs are necessary for their regulation by Dhh1. Moreover, Eap1, an EIF4E binding protein, physically interacts with Dhh1 to facilitate the delivery of the Dhh1-*ATG* mRNA complex to the translation initiation machinery. These results suggest a model for how some *ATG* genes bypass the general translational suppression that occurs during nitrogen starvation to maintain a proper level of autophagy.

The molecular mechansim of autophagosome formation has been an interesting topic over years due to its importance to autophagy process. This thesis enlarges the knowledge of Atg9 cycling system in yeast, which provides insight for understanding membrane donation process in autophagy. Diffterent levels of autophagy control are essential for cellular homestasis. This thesis, by investigating both transcriptional and translational regulation of autophagy, provides insight in understanding autophagy control. This will help further investigation on diseases resulting from autophagy dysfunction and their connections to autophagy regulation.

Chapter 1 Introduction[1]

Autophagy is a cellular process in which cytoplasmic contents are degraded within the lysosome/vacuole, and the resulting macromolecular constituents are recycled [1]. Macroautophagy is one type of autophagic process in which the substrates are sequestered within cytosolic double-membrane vesicles termed autophagosomes. The substrates of macroautophagy include superfluous and damaged organelles, cytosolic proteins and invasive microbes. Following degradation, the breakdown products are released back into the cytosol in order to recycle the macromolecular constituents and to generate energy to maintain cell viability under unfavorable conditions, and to protect the cell during various conditions of stress [2, 3]. Autophagy is highly conserved from yeast to mammals, both morphologically and with regard to the protein constituents that make up the core autophagy machinery.

1.1. Terms and structures

The most readily identifiable feature of macroautophagy is the sequestration of cargo within cytosolic doublemembrane vesicles, and many researchers still consider the analysis of macroautophagy by electron microscopy to be the "gold standard" for verifying

[1] This chapter is reprinted partly from Feng Y*, He D*, Yao Z*, Klionsky DJ. The machinery of macroautophagy. Cell Res 2014; 24:24 41 and partly from Feng Y*, Yao Z*, Klionsky DJ. How to control self-digestion: transcriptional, post-transcriptional, and post-translational regulation of autophagy. Trends in cell biology 25 (6), 354-363, with some modifications.

macroautophagy activity. Below, we present some of the most common terms describing the principle structures of macroautophagy (Figure 1.1).

Autophagic body: The inner-membrane-bound structure released into the vacuole lumen after the outer membrane of the autophagosome fuses with vacuolar membrane [4]. Note that autophagic bodies only appear in yeast and plants due to the large size of the vacuole, and are not found in mammalian lysosomes.

Autophagosome: The completed double-membrane bound compartment, the product of phagophore expansion and closure, which sequesters cytoplasmic cargos during macroautophagy [5, 6].

PAS: The phagophore assembly site; a peri-vacuolar location or compartment where the nucleation of the phagophore initiates. Most components of the macroautophagy core machinery locate at least transiently at the PAS in yeast; however, a mammalian equivalent of the PAS has not been identified [7-9].

Phagophore: The double-membrane structure that functions in the initial sequestering of cargo, and thus the active compartment of macroautophagy. The phagophore further elongates/expands and ultimately closes, generating a completed autophagosome [10].

1.2. The history of discovery

The term “autophagy” was coined by Christian de Duve at the CIBA Foundation Symposium on Lysosomes in 1963. This was based on his discovery of lysosomes in 1955, which won him the Nobel Prize in Physiology or Medicine in 1974 [11]. Autophagy was named morphologically by the observations from electron microscopy of rat hepatic cell lysosomes, where single membrane vesicles, containing cytoplasm or organelles such as mitochondria and endoplasmic reticulum (ER) were observed [12-15]. Based on Thomas

Ashford's and Keith Porter's early findings in 1962 that revealed the presence of sequestered organelles in rat hepatocytes following their exposure to glucagon [12], de Duve and his colleagues confirmed that this hormone can induce autophagy[16]. Subsequently, other researchers further examined the hormonal and enzymatic regulation of autophagy. For instance, Per Seglen and Paul Gordon discovered the inhibitory role of 3-methyladenine [17]. As de Duve mentioned in 1966 that autophagy could be selective [14], the specific sequestration of organelles including ER [18], mitochondria [19] and peroxisomes [20] by autophagy was demonstrated in the following decade. Although autophagy was initially revealed in mammalian systems, the molecular understanding of it was largely expanded and facilitated through genetic studies in yeast. Genetic screens of macroautophagy-defective mutants in *Saccharomyces cerevisiae* were carried out by the Ohsumi and Thumm laboratories [21, 22]. Shortly thereafter, the first autophagy-specific gene, APG1 (now ATG1 [23]), was identified, and the corresponding gene product, Apg1/Atg1, was characterized as a Ser/Thr protein kinase [24]. Multiple laboratories working on autophagy primarily in S. cerevisiae, Pichia pastoris and Hansenula polymorpha subsequently discovered more than forty autophagy related (ATG) genes. The molecular basis of autophagy was first connected to human diseases by Beth Levine's laboratory through the identification of BECN1/VPS30/ATG6 as a tumor suppressor gene [25]. Subsequently, a series of studies uncovered the connections between autophagy and pathophysiological conditions, such as pathogen infection [26-29] and neurodegeneration [30], and its dual role in cell growth and death [31, 32].

1.3. The types of autophagy

There are three primary types of autophagy: microautophagy, macroautophagy and a mechanistically unrelated process, chaperone-mediated autophagy that only occurs in mammalian cells. Both micro and macroautophagy can be selective or nonselective and these processes have been best characterized in yeast [33]. As noted above, the most distinguishing feature of macroautophagy (here-after autophagy) is the formation of the double-membrane bound phagophore and autophagosome (Figure 1.1). In contrast, during microautophagy the cargos are sequestered by direct invagination or protusion/septation of the yeast vacuole membrane [34]. Nonselective autophagy is used for the turnover of bulk cytoplasm under starvation conditions, whereas selective autophagy specifically targets damaged or superfluous organelles, including mitochondria and peroxisomes, as well as invasive microbes; each process involves a core set of machinery, as well as specific components, and accordingly is identified with a unique name — mitophagy for selective mitochondria degradation by autophagy, pexophagy for peroxisomes, xenophagy for microbes, etc. [35, 36].

1.4. Identification of the PAS and the origin of the phagophore membrane

1.4.1. Identification of the PAS

Atg8 was the first Atg protein characterized to mark the phagophore and autophagosome [37, 38]. Immunofluorescence microscopy revealed that in rich conditions, Atg8 is primarily dispersed in the cytoplasm as small puncta, while it forms larger puncta in the vicinity of the vacuole when yeast cells are switched to starvation conditions; the nature of the smaller puncta is not known, whereas the larger puncta correspond to nascent autophagosomes. Subsequent studies with green fluorescent protein (GFP)-tagged chimeras

demonstrated that most of the Atg proteins reside at this location, at least transiently [8]. Accordingly, this site is proposed to be where the phagophore assembles, and is thus termed the phagophore assembly site, or PAS [8, 9]. The precise nature of the PAS with regard to its protein and membrane composition, or the reason for its peri-vacuolar localization, is not known, but assembly of the Atg proteins at the PAS occurs in a hierarchical manner [39]. The PAS forms constitutively, and in vegetative conditions a key component that marks this site is Atg11; upon autophagy induction, the structure transitions into an autophagy specific PAS and the function of Atg11 is replaced by a ternary complex of Atg17-Atg31-Atg29 that assembles at the PAS along with Atg1 and Atg13 [40, 41]. Atg9, which shuttles between the PAS and peripheral sites, plays an important role in directing membrane to the PAS that is needed for autophagosome formation, and it localizes to the PAS at a similar time as the Atg1 kinase complex. Subsequently, the PtdIns3K and Atg12–Atg5-Atg16 complexes are recruited to the PAS; the latter acts in part as an E3 ligase to facilitate the formation of Atg8–PE, one of the last proteins that are recruited to the PAS. In mammalian cells, the colocalization of ATG proteins is observed at multiple sites [42-44], instead of a single PAS as in yeast.

1.4.2. Origin of the phagophore

Until recently, the dogma was that the phagophore and autophagosome formed de novo, meaning that the sequestering membrane does not form in “one step” from a pre-existing organelle already containing its cargo as occurs throughout the secretory pathway [45, 46]. Regardless of the specific mechanism, autophagosome formation is thought to occur by the expansion of the phagophore, that is, a sheet of membrane that would correspond to the size of a complete autophagosome does not separate from the endomembrane system and simply

curl up to form an autophagosome. Rather, after nucleation the phagophore grows through the addition of membrane from one or more donor sources [1, 47]; however, the origin of the phagophore membrane is still under debate. Various lines of data suggest a role for almost every membrane compartment in contributing to formation of the autophagosome, including the ER, mitochondria, the Golgi apparatus and the plasma membrane [48-52]. As discussed above, there is no absolute equivalent of the yeast PAS in mammalian cells. Instead, there is evidence that there may be at least two separate mechanisms for generating autophagosomes. One mechanism would involve the delivery of membrane from various organelles, as is thought to occur in yeast, and the second utilizes an omega-shaped membrane structure or cradle, derived from phosphatidylinositol-3-phosphate (PtdIns3P)-enriched ER subdomains, termed an omegasome [53].

1.5. Core molecular machinery of autophagosome formation

The transition of autophagy studies from morphology to molecular machinery relied on the identification of the ATG genes [23]. As mentioned above, genetic screens for autophagy-defective mutants in yeast have led to the identification of over 40 ATG genes [21-23, 54], many of which have known orthologs in higher eukaryotes.

Among these ATG genes, one subgroup, consisting of approximately 18 genes (Table 1.1), is shared among the various types of autophagy including nonselective macroautophagy, the cytoplasm-to-vacuole-targeting (Cvt) pathway (a biosynthetic autophagy-like pathway), mitophagy and pexophagy. More specifically, the corresponding gene products of this subgroup are required for autophagosome formation, and thus are termed the core autophagy machinery. The core Atg proteins can be divided into different functional subgroups: (A) the Atg1/ULK complex (Atg1, Atg11, Atg13, Atg17, Atg29 and Atg31) is

the initial complex that regulates the induction of autophagosome formation; (B) Atg9 and its cycling system (Atg23, Atg27, Atg2, Atg9 and Atg18) play a role in membrane delivery to the expanding phagophore after the assembly of the Atg1 complex at the PAS; (C) the PtdIns 3-kinase (PtdIns3K) complex (Vps34, Vps15, Vps30/Atg6, and Atg14) acts at the stage of vesicle nucleation, and is involved in the recruitment of PtdIns3P-binding proteins to the PAS; (D) two ubiquitin-like (Ubl) conjugation systems: the Atg12 (Atg5, Atg7, Atg10, Atg12 and Atg16) and Atg8 (Atg3, Atg4, Atg7 and Atg8) conjugation systems play roles in vesicle expansion [39, 55-57].

1.5.1 The Atg1/ULK complex

The Atg1 kinase complex regulates the magnitude of autophagy [58-62]. This complex also plays a role in mediating the retrieval of Atg9 from the PAS [63]. The Atg1 kinase complex is extensively regulated, receiving input from several signaling pathways. In yeast, much of the regulation centers around nutrient signaling and involves kinases that sense the nutritional status of the cell including the target of rapamycin (TOR), protein kinase A (PKA), Gcn2 and Snf1. The yeast Atg1 kinase complex includes Atg1, a Ser/Thr protein kinase, Atg13, a regulatory subunit, and the Atg17-Atg31-Atg29 complex, which may function in part as a scaffold. Atg1 is the only kinase of the core autophagy machinery; however, despite the fact that it was the first Atg protein to be identified, the key physiological substrate of yeast Atg1 is not known. Atg1 kinase activity is required for autophagosome formation and the Cvt pathway, although there are conflicting data concerning the changes in kinase activity when yeast cells shift from vegetative growth to autophagy-inducing conditions [24, 64, 65]. Atg1 recruitment to the PAS may be regulated

by PKA dependent phosphorylation [66]. TOR also phosphorylates Atg1, and autophosphorylation is important in regulating Atg1 kinase activity [67, 68].

Atg13 is required for Atg1 kinase activity. Atg13 is hyperphosphorylated under nutrient-rich conditions, and its phosphorylation is regulated by TOR complex 1 (TORC1) [69] and/or PKA [70]. Atg13 is rapidly, but only partially, dephosphorylated upon autophagy induction[71]. These data, coupled with affinity isolation studies, led to a model suggesting that the interaction between Atg1 and Atg13 is controlled by Atg13 phosphorylation-dephosphorylation would lead to the formation of an Atg1-Atg13 complex, and subsequent activation of Atg1 kinase activity [61]. Recent data, however, suggest that Atg1 and Atg13 interact in a constitutive manner [72],which is similar to the situation in other organisms.

Atg17-Atg31-Atg29 exists as a stable complex under both vegetative and starvation conditions, suggesting that formation of the complex is not involved in autophagy induction. Atg31 bridges Atg17 and Atg29, Atg17 binds Atg13, and Atg29 binds Atg11; the latter is a scaffold protein that may also be considered part of the Atg1 kinase complex because it binds Atg1 and is involved in the transition of the PAS that occurs during the switch from vegetative to starvation conditions [40, 41, 58, 73-75]. Both Atg29 and Atg31 are phosphoproteins. The phosphorylation of Atg29 appears to be involved in regulation and is proposed to alter the conformation of an inhibitory C-terminal peptide to allow the protein to become active [41].

The mammalian ULK1/2 complex includes ULK1/2 (mammalian homologs of Atg1), ATG13 (a homolog of yeast Atg13), RB1CC1/FIP200 (a putative Atg17 homolog) and C12orf44/ATG101 (the latter component is not conserved in S. cerevisiae) [76-80]. ULK1/2 interact with ATG13, which directly binds RB1CC1 and mediates the latter's interaction

with the ULKs [76, 81]. In mammalian cells, ULK1 kinase can be activated by both AMP-activated protein kinase (AMPK)-dependent (glucose starvation) and -independent (amino acid starvation) processes [82]. The ULK1/2-ATG13-RB1CC1 interaction is nutrient independent, forming a complex even in nutrient-rich conditions [80]. In this situation, MTORC1 phosphorylates and inhibits ULK1/2 and ATG13, disrupting the interaction between ULK1 and AMPK [82]. In contrast, under autophagy-inducing conditions, MTOR is released from the complex, resulting in activation of ULK1/2, which phosphorylates, and presumably activates, ATG13 and RB1CC1. AMBRA1 and BECN1, components of the autophagy-promoting PtdIns3K complexes, are also phosphorylated by ULK1; these modifications result in localization of the lipid kinase complex to the ER and its activation [83, 84].

1.5.2. The Atg9 Complex

In yeast cells, Atg9 is a transmembrane protein that transits between the PAS and peripheral sites; the latter have been termed Atg9 reservoirs or tubulovesicular clusters, and are proposed to represent sites from which membrane is delivered to the forming phagophore [49, 63, 85], although the exact role of Atg9 in this process is not clear. Atg9 is proposed to consist of six transmembrane domains, with both the amino and carboxyl termini exposed in the cytosol. Atg9 self-interacts and may exist in a complex [85, 86].

Atg9 localization to the PAS from the peripheral sites (referred to as anterograde transport) depends on Atg11, Atg23 and Atg27 [63, 87-89]. Return to the peripheral sites (retrograde movement) requires Atg1-Atg13, Atg2 and Atg18; PAS recruitment of the latter involves binding to PtdIns3P and thus necessitates the function of Atg14 and the class III PtdIns3K

complex [63]. Atg27 is a type I integral transmembrane protein, while the other components involved in Atg9 movement are soluble and/or peripherally associated with membranes.

The mammalian Atg9 homolog ATG9A localizes to the trans-Golgi network and late endosomes in nutrient-rich conditions [44]; another Atg9 ortholog, ATG9B, displays a similar localization, but is expressed only in the placenta and pituitary gland, whereas ATG9A is expressed ubiquitously [43]. ATG9 appears to have a conserved role in coordinating membrane transport from donor sources to the phagophore and displays a cycling pattern similar to that seen in yeast [44, 90]. ATG9 and ATG16L1 also appear to traffic at least in part on vesicles derived from the plasma membrane, which are delivered to the recycling endosome; the two proteins are initially present in separate vesicular populations that subsequently fuse as part of the process of autophagosome formation [91]. ATG9 movement is dependent on the activity of the ULK1 and PIK3C3/VPS34 kinases, as well as WIPI2 (a homolog of yeast Atg18).

1.5.3. PtdIns3K complexes

In yeast, Vps15 (a putative regulatory protein kinase that is required for Vps34 membrane association), Vps30/Atg6, Vps34 (the PtdIns3K), Atg14 and Atg38, form the autophagy-specific class III PtdIns3K complex I, which localizes at the PAS [92-94]. One key role of the PtdIns3K complex, the generation of PtdIns3P, is presumably to recruit PtdIns3P-binding proteins such as Atg18 to the PAS. Vps15, Vps34 and Vps30 are present in a second complex that includes Vps38 instead of Atg14. Thus, the latter protein appears to determine the specificity of the PtdIns3K complex I for macroautophagy.

Mammalian cells have both a class I phosphoinositide 3-kinase and a class III PtdIns3K; the class III enzyme complexes consist of homologs of Vps34 (PIK3C3), Vps15 (PIK3R4) and Vps30 (BECN1) [95]. These core components are part of at least three different complexes [96, 97]. The ATG14 complex contains ATG14 and is regulated by the binding of BECN1 to AMBRA1 and BCL2, which stimulate and inhibit the complex, respectively. This complex functions similarly to the yeast PtdIns3K complex I. The UVRAG complex replaces ATG14 and AMBRA1 with UVRAG and its positive regulator SH3GLB1, and participates in both endocytosis and macroautophagy. In the third complex, SH3GLB1 is replaced with KIAA0226/Rubicon, which inhibits UVRAG; this complex acts to negatively regulate macroautophagy.

1.5.4. Ubiquitin-like (Ubl) conjugation systems

There are two Ubl protein conjugation systems that participate in macroautophagy in yeast[48]. These include two Ubl proteins, Atg8 and Atg12, which are used to generate the conjugation products Atg8–PE and Atg12–Atg5, respectively. The Ubl conjugation systems participate in phagophore expansion, although their functions are not fully understood. The Atg12–Atg5 conjugate, along with a third component, Atg16, may act in part as an E3 ligase to facilitate the conjugation of Atg8 to PE, and the amount of Atg8 can regulate the size of autophagosomes [98]; however, Atg8 also functions in cargo binding during selective autophagy [99]. Yeast Atg8 is initially synthesized with a C-terminal arginine residue that is removed by Atg4, a cysteine protease [38, 100]. During autophagy, Atg8 is released from Atg8–PE by a second Atg4-dependent cleavage referred to as deconjugation [101], whereas there is no similar cleavage that separates Atg12 from Atg5. Both of the Ubl

protein conjugation systems share a single E1-like activating enzyme, Atg7 [100, 102-104]. The E2-like conjugating enzymes are Atg3 for Atg8, and Atg10 for Atg12 [102, 105].

The Ubl protein conjugation systems are highly conserved from yeast to mammals [106-109]. One of the primary differences is the existence of multiple homologs of yeast Atg8, which are divided into two subfamilies, LC3 and GABARAP. LC3 functions at the stage of phagophore elongation, whereas GABARAP proteins act at a later stage of maturation [110]. There are four mammalian ATG4 homologs, with ATG4B carrying out the primary role in macroautophagy [111]. As in yeast, this enzyme cleaves after the C-terminal glycine of proLC3 to form cytosolic LC3-I, followed by its subsequent conjugation to PE to generate the membrane-associated LC3-II form [112]. The GABARAP proteins undergo a similar type of posttranslational modification.

1.6. Regulation of autophagy

Autophagy is involved in normal aspects of cell development and physiology, and defects in this process are associated with a range of diseases in humans. Accordingly, there has been tremendous interest in manipulating autophagy for therapeutic purposes. One fundamental issue, however, is that either too little or too much autophagy can be deleterious. Therefore, the cell, and clinicians interested in modulating this process, need to ensure tight regulation of the induction and magnitude of autophagy. Thus, a thorough understanding of the mechanisms involved is crucial to allow the manipulation of autophagy for the treatment of disease. Regulation of autophagy can happened in different steps of Atg protein production, including transcriptional regulation, post transcriptional regulation and post-translational regulation.

1.6.1. Transcriptional regulation of autophagy

More and more transcriptional regulators have been identified recently either activate or suppress autophagy. Those regulators mainly manipulate autophagy through controlling *ATG* genes expression level. In yeast, Ume6 (Unscheduled Meiotic gene Expression) is part of a complex that includes the corepressor Sin3 (Switch IN dependent) and the histone deacetylase Rpd3 (Reduced Potassium Dependency), which acts as a negative regulator of *ATG8* transcription [113]. Another protein, Pho23, negatively controls the mRNA levels of *ATG1*, *ATG7*, *ATG8*, *ATG9*, and *ATG14* [114]. On the other hand, Gcn4, a master regulator in response to nutrient stress, was reported to activate multiple *ATG* genes expression [115-116].

In mammals, The transcription factor EB (TFEB), a master regulator of lysosome biogenesis, was found to regulate a variety of autophagic genes including UVRAG, WIPI, MAPLC3B, SQSTM1, VPS11, VPS18, and ATG9B [117]. Other examples includes FOXO (forkhead box O) family proteins, TP53 (tumor protein p53) and NFKB/NF-κB (nuclear factor of kappa light polypeptide gene enhancer in B-cells) [118-121]. However, these regulators seem to play dual roles in the regulation of autophagy. The detail mechanism needs further elucidation.

1.6.2. Post-transcriptional regulation of autophagy

Current knowledge about post-transcriptional regulation of autophagy focuses on two aspects: noncoding microRNAs (miRNA) regulation and mRNA decay through mRNA decapping machinery. miRNAs are a class of small endogenous regulatory RNAs that control gene expression at the post-transcriptional level, typically by translational arrest or mRNA cleavage, through interaction mainly at the 3'-untranslated regions (UTRs) of the

target mRNAs. Mir20a and Mir106b, two members of the Mir17 microRNA family, suppress ULK1 expression in C2C12 myoblasts [122]. In addition, MIR885-3p regulates autophagy through its putative recognition sequence present in the 5'-UTR of ULK2, which results in ULK2 downregulation [123].

Recently, studies started to show the importance of mRNA decay to autophagy regulation. Dcp2, the decapping enzyme, was found to degrade the *ATG* mRNA only in nutrient rich condition. The activity of Dcp2 is controlled by TOR phosphorylation and the association of specific RNA helicase. More than twenty *ATG* mRNAs are affected by Dcp2 to ensure the low level of autophagy under nutrient rich regulation [124].

1.6.3. Post-translational regulation of autophagy

Although translational control of autophagy is still under the myth, the post-translational control of autophagy is well studied. Atg proteins are phorphorylated, ubiqutinated or acetylated during autophagy, affecting their function, stability and localization.

Phosphorylation of ATG proteins is the most well studied post-translational modifications (PTMs). In yeast, TOR participates in the regulation of Atg1 through the direct phosphorylation of the regulatory Atg13 subunit, which is also inhibited by PKA (cAMP-dependent protein kinase A). The phosphorylation of Atg13 affects both the nature of its interaction with Atg1 and its localization to the phagophore assembly site. Atg1 is also a direct substrate of PKA, and phosphorylation regulates Atg1 localization to the PAS. Phosphorylation of the PtdIns3K complex, another part of the autophagy core machinery, which is responsible for producing PtdIns3P, also regulates autophagy [125-126]. In mammals, PIK3C3/VPS34 is the catalytic subunit of a class III PtdIns3K that provides the core function of the complex. PIK3C3 is functional in autophagy when it interacts with

BECN1, which in turn is inhibited by anti-apoptotic proteins such as BCL2 [127]. Thus, any PTM that disrupts the interaction between BECN1 and its inhibitory partners has the potential for stimulating autophagy and vice versa. For example, DAPK (death-associated protein kinase) phosphorylates BECN1 and MAPK8/ JNK1 (mitogen-activated protein kinase 8) phosphorylates BCL2 [125,128-129]. In both cases the interaction between BECN1 and BCL2 is disrupted, allowing BECN1 to associate with PIK3C3 and induce autophagy.

Ubiquitination is another type of PTM that regulates autophagy. In general ubiquitination can affect the stability of Atg proteins and their upstream regulators. Ubiquitination of the autophagy core machinery can either affect protein function or stability. TRAF6 (TNF receptor-associated factor 6, E3 ubiquitin protein ligase), a RING finger-containing ligase, can ubiquitinate both BECN1 and ULK1 [130-131]. The Lys63 (K63)-linked ubiquitination of BECN1 by TRAF6 is required for the induction of autophagy by TLR4 (toll-like receptor 4), a protein that plays a role in activation of the innate immune system in response to bacterial antigen. By contrast, the deubiquitinating enzyme TNFAIP3/A20 (tumor necrosis factor, alpha-induced protein 3) antagonizes TRAF6 regulation by deubiquitinating BECN1 and repressing autophagy.

ATG proteins are also regulated by direct acetylation [132]. During serum starvation, the acetyltransferase KAT5/TIP60 [K(lysine) acetyltransferase 5] is activated by GSK3 (glycogen synthase kinase 3) and it directly acetylates ULK1 [133]. This acetylation is required for ULK1 activation and autophagy initiation. Another example of regulatory acetylation/deacetylation in autophagy is seen with EP300/p300 (E1A binding protein p300)

and SIRT1 (sirtuin 1). The EP300 acetyltransferase acetylates a variety of autophagy proteins including ATG5, ATG7, LC3, and ATG12.

1.7. References

1. Klionsky DJ, Baehrecke EH, Brumell JH, et al. A comprehensive glossary of autophagy-related molecules and processes (2nd edition). Autophagy 2011; 7:1273-1294.
2. Klionsky DJ. The molecular machinery of autophagy: unanswered questions. J Cell Sci 2005; 118:7-18.
3. Yorimitsu T, Klionsky DJ. Autophagy: molecular machinery for self-eating. Cell Death Differ 2005; 12:1542-1552.
4. Baba M, Osumi M, Ohsumi Y. Analysis of the membrane structures involved in autophagy in yeast by freeze-replica method. Cell Struct Funct 1995; 20:465-471.
5. Fimia GM, Stoykova A, Romagnoli A, et al. Ambra1 regulates autophagy and development of the nervous system. Nature 2007; 447:1121-1125.
6. Dunn WA Jr. Studies on the mechanisms of autophagy: maturation
of the autophagic vacuole. J Cell Biol 1990; 110:1935-1945.
7. He C, Klionsky DJ. Atg9 trafficking in autophagy-related pathways. Autophagy 2007; 3:271-274.
8. Suzuki K, Kirisako T, Kamada Y, et al. The pre-autophagosomal structure organized by concerted functions of APG genes is essential for autophagosome formation. EMBO J 2001; 20:5971-5981.
9. Kim J, Huang WP, Stromhaug PE, Klionsky DJ. Convergence of multiple autophagy and cytoplasm to vacuole targeting components to a perivacuolar membrane compartment prior to de novo vesicle formation. J Biol Chem 2002; 277:763-773.
10. Seglen PO, Gordon PB, Holen I. Non-selective autophagy.
Semin Cell Biol 1990;1:441-448.
11. de Duve C, Pressman BC, Gianetto R, Wattiaux R, Appelmans F. Tissue fractionation studies. (6). Intracellular distributionpatterns of enzymes in rat-liver tissue. Biochem J 1955;60:604-617.
12. Ashford TP, Porter KR. Cytoplasmic components in hepaticcell lysosomes. J Cell Biol 1962;12:198-202.
13. Clark SL Jr. Cellular differentiation in the kidneys of newborn mice studied with the electron microscope. J Biophys Biochem Cytol 1957; 3:349-362.
14. de Duve C, Wattiaux R. Functions of lysosomes. Annu Rev
Physiol 1966; 28:435-492.
15. Novikoff AB. The proximal tubule cell in experimental hydronephrosis. J Biophys Biochem Cytol 1959; 6:136-138.
16. Deter RL, Baudhuin P, de Duve C. Participation of lysosomes in cellular autophagy induced in rat liver by glucagon. J Cell Biol 1967; 35:C11-C16.

17. Seglen PO, Gordon PB. 3-Methyladenine: specific inhibitor of autophagic/lysosomal protein degradation in isolated rat hepatocytes. Proc Natl Acad Sci USA 1982; 79:1889-1892.
18. Bolender RP, Weibel ER. A morphometric study of the removal of phenobarbital-induced membranes from hepatocytes after cessation of threatment. J Cell Biol 1973; 56:746-761.
19. Beaulaton J, Lockshin RA. Ultrastructural study of the normal degeneration of the intersegmental muscles of Anthereae polyphemus and Manduca sexta (Insecta, Lepidoptera) with particular reference of cellular autophagy. J Morphol 1977; 154:39-57.
20. Veenhuis M, Douma A, Harder W, Osumi M. Degradation and turnover of peroxisomes in the yeast Hansenula polymorpha induced by selective inactivation of peroxisomal enzymes. Arch Microbiol 1983; 134:193-203.
21. Thumm M, Egner R, Koch B, et al. Isolation of autophagocytosis mutants of *Saccharomyces cerevisiae*. FEBS Lett 1994; 349:275-280.
22. Tsukada M, Ohsumi Y. Isolation and characterization of autophagy-defective mutants of *Saccharomyces cerevisiae*. FEBS Lett 1993; 333:169-174.
23. Klionsky DJ, Cregg JM, Dunn WA Jr, et al. A unified nomenclature for yeast autophagy-related genes. Dev Cell 2003; 5:539-545.
24. Matsuura A, Tsukada M, Wada Y, Ohsumi Y. Apg1p, a novel protein kinase required for the autophagic process in *Saccharomyces cerevisiae*. Gene 1997; 192:245-250.
25. Liang XH, Jackson S, Seaman M, et al. Induction of autophagy and inhibition of tumorigenesis by beclin 1. Nature 1999; 402:672-676.
26. Rikihisa Y. Glycogen autophagosomes in polymorphonuclear leukocytes induced by rickettsiae. Anat Rec 1984; 208:319-327.
27. Liang XH, Kleeman LK, Jiang HH, et al. Protection against fatal Sindbis virus encephalitis by beclin, a novel Bcl-2-interacting protein. J Virol 1998; 72:8586-8596.
28. Orvedahl A, Alexander D, Tallóczy Z, et al. HSV-1 ICP34.5 confers neurovirulence by targeting the Beclin 1 autophagy protein. Cell Host Microbe 2007; 1:23-35.
29. Tallóczy Z, Virgin HW IV, Levine B. PKR-dependent autophagic degradation of herpes simplex virus type 1. Autophagy 2006; 2:24-29.
30. Rubinsztein DC, DiFiglia M, Heintz N, et al. Autophagy and its possible roles in nervous system diseases, damage and repair. Autophagy 2005; 1:11-22.
31. Boya P, Gonzalez-Polo RA, Casares N, et al. Inhibition of macroautophagy triggers apoptosis. Mol Cell Biol 2005;25:1025-1040.
32. Yu L, Alva A, Su H, et al. Regulation of an ATG7-beclin 1 program of autophagic cell death by caspase-8. Science 2004; 304:1500-1502.
33. Shintani T, Klionsky DJ. Autophagy in health and disease: a double-edged sword. Science 2004; 306:990-995.
34. Kunz JB, Schwarz H, Mayer A. Determination of four sequential stages during microautophagy in vitro. J Biol Chem 2004; 279:9987-9996.
35. Deffieu M, Bhatia-Kissova I, Salin B, et al. Glutathione participates in the regulation of mitophagy in yeast. J Biol Chem 2009; 284:14828-14837.

36. Dunn WA Jr, Cregg JM, Kiel JAKW, et al. Pexophagy: the selective autophagy of peroxisomes. Autophagy 2005; 1:75-83.
37. Huang W-P, Scott SV, Kim J, Klionsky DJ. The itinerary of a vesicle component, Aut7p/Cvt5p, terminates in the yeast vacuole via the autophagy/Cvt pathways. J Biol Chem 2000;
275:5845-5851.
38. Kirisako T, Baba M, Ishihara N, et al. Formation process of autophagosome is traced with Apg8/Aut7p in yeast. J Cell Biol 1999; 147:435-446.
39. Suzuki K, Kubota Y, Sekito T, Ohsumi Y. Hierarchy of Atg proteins in pre-autophagosomal structure organization. Genes Cells 2007; 12:209-218.
40. Cheong H, Klionsky DJ. Dual role of Atg1 in regulation of autophagy-specific PAS assembly in *Saccharomyces cerevisiae*. Autophagy 2008; 4:724-726.
41. Mao K, Chew LH, Inoue-Aono Y, et al. Atg29 phosphorylation regulates coordination of the Atg17-Atg31-Atg29 complex with the Atg11 scaffold during autophagy initiation. Proc Natl Acad Sci USA 2013; 110:E2875-E2884.
42. Mizushima N, Yamamoto A, Hatano M, et al. Dissection of autophagosome formation using Apg5-deficient mouse embryonic stem cells. J Cell Biol 2001; 152:657-668.
43. Yamada T, Carson AR, Caniggia I, et al. Endothelial nitricoxide synthase antisense (NOS3AS) gene encodes an autophagy-related protein (APG9-like2) highly expressed in trophoblast. J Biol Chem 2005; 280:18283-18290.
44. Young ARJ, Chan EYW, Hu XW, et al. Starvation and ULK1-dependent cycling of mammalian Atg9 between the TGN and endosomes. J Cell Sci 2006; 119:3888-3900.
45. Noda T, Suzuki K, Ohsumi Y. Yeast autophagosomes: de novo formation of a membrane structure. Trends Cell Biol 2002; 12:231-235.
46. Kovács AL, Palfia Z, Rez G, Vellai T, Kovács J. Sequestration revisited: integrating traditional electron microscopy, de novo assembly and new results. Autophagy 2007; 3:655-662.
47. Gordon PB, Seglen PO. Prelysosomal convergence of autophagic and endocytic pathways. Biochem Biophys Res Commun 1988; 151:40-47.
48. Geng J, Klionsky DJ. The Atg8 and Atg12 ubiquitin-like conjugation systems in macroautophagy. EMBO Rep 2008;9:859-864.
49. Mari M, Griffith J, Rieter E, et al. An Atg9-containing compartment that functions in the early steps of autophagosome biogenesis. J Cell Biol 2010; 190:1005-1022.
50. van der Vaart A, Griffith J, Reggiori F. Exit from the Golgi is required for the expansion of the autophagosomal phagophore in yeast *Saccharomyces cerevisiae*. Mol Biol Cell 2010; 21:2270-2284.
51. Yen W-L, Shintani T, Nair U, et al. The conserved oligomeric Golgi complex is involved in double-membrane vesicle formation during autophagy. J Cell Biol 2010; 188:101-114.
52. Taylor R Jr, Chen PH, Chou CC, Patel J, Jin SV. KCS1 deletion in *Saccharomyces cerevisiae* leads to a defect in translocation of autophagic proteins and reduces autophagosome formation. Autophagy 2012; 8:1300-1311.

53. Axe EL, Walker SA, Manifava M, et al. Autophagosome formation from membrane compartments enriched in phosphatidylinositol 3-phosphate and dynamically connected to the endoplasmic reticulum. J Cell Biol 2008; 182:685-701.
54. Harding TM, Morano KA, Scott SV, Klionsky DJ. Isolation and characterization of yeast mutants in the cytoplasm to vacuole protein targeting pathway. J Cell Biol 1995;131:591-602.
55. Mizushima N. Autophagy: process and function. Genes Dev 2007; 21:2861-2873.
56. Mizushima N, Yoshimori T, Ohsumi Y. The role of Atg proteins in autophagosome formation. Annu Rev Cell Dev Biol 2011; 27:107-132.
57. Xie Z, Klionsky DJ. Autophagosome formation: core machinery and adaptations. Nat Cell Biol 2007; 9:1102-1109.
58. Cheong H, Yorimitsu T, Reggiori F, et al. Atg17 regulates the magnitude of the autophagic response. Mol Biol Cell 2005;16:3438-3453.
59. Kabeya Y, Kamada Y, Baba M, et al. Atg17 functions in cooperation with Atg1 and Atg13 in yeast autophagy. Mol Biol Cell 2005; 16:2544-2553.
60. Kabeya Y, Kawamata T, Suzuki K, Ohsumi Y. Cis1/Atg31 is required for autophagosome formation in *Saccharomyces cerevisiae*. Biochem Biophys Res Commun 2007; 356:405-410.
61. Kamada Y, Funakoshi T, Shintani T, et al. Tor-mediated induction of autophagy via an Apg1 protein kinase complex. J Cell Biol 2000; 150:1507-1513.
62. Kawamata T, Kamada Y, Suzuki K, et al. Characterization of a novel autophagy-specific gene, ATG29. Biochem Biophys Res Commun 2005; 338:1884-1889.
63. Reggiori F, Tucker KA, Stromhaug PE, Klionsky DJ. The Atg1-Atg13 complex regulates Atg9 and Atg23 retrieval transport from the pre-autophagosomal structure. Dev Cell 2004; 6:79-90.
64. Abeliovich H, Zhang C, Dunn WA Jr, Shokat KM, Klionsky DJ. Chemical genetic analysis of Apg1 reveals a non-kinase role in the induction of autophagy. Mol Biol Cell 2003;14:477-490.
65. Nair U, Klionsky DJ. Molecular mechanisms and regulation of specific and nonspecific autophagy pathways in yeast. J Biol Chem 2005; 280:41785-41788.
66. Stephan JS, Yeh YY, Ramachandran V, Deminoff SJ, Herman PK. The Tor and PKA signaling pathways independently target the Atg1/Atg13 protein kinase complex to control autophagy. Proc Natl Acad Sci USA 2009; 106:17049-17054.
67. Yeh YY, Wrasman K, Herman PK. Autophosphorylation within the Atg1 activation loop is required for both kinase activity and the induction of autophagy in *Saccharomyces cerevisiae*. Genetics 2010; 185:871-882.
68. Kijanska M, Dohnal I, Reiter W, et al. Activation of Atg1 kinase in autophagy by regulated phosphorylation. Autophagy 2010; 6:1168-1178.
69. Kamada Y, Yoshino K, Kondo C, et al. Tor directly controls the Atg1 kinase complex to regulate autophagy. Mol Cell Biol 2010; 30:1049-1058.
70. Budovskaya YV, Stephan JS, Deminoff SJ, Herman PK. An evolutionary proteomics approach identifies substrates of the cAMP-dependent protein kinase. Proc Natl Acad Sci USA

2005; 102:13933-13938.
71. Scott SV, Nice DC, III, Nau JJ, et al. Apg13p and Vac8p are part of a complex of phosphoproteins that are required for cytoplasm to vacuole targeting. J Biol Chem 2000; 275:25840-25849.
72. Kraft C, Kijanska M, Kalie E, et al. Binding of the Atg1/ULK1 kinase to the ubiquitin-like protein Atg8 regulates autophagy.EMBO J 2012; 31:3691-3703.
73. Cao Y, Nair U, Yasumura-Yorimitsu K, Klionsky DJ. A multiple ATG gene knockout strain for yeast two-hybrid analysis.Autophagy 2009; 5:699-705.
74. Kabeya Y, Noda NN, Fujioka Y, et al. Characterization of the Atg17-Atg29-Atg31 complex specifically required for starvation-induced autophagy in *Saccharomyces cerevisiae*. Biochem Biophys Res Commun 2009; 389:612-615.
75. Ragusa MJ, Stanley RE, Hurley JH. Architecture of the Atg17 complex as a scaffold for autophagosome biogenesis. Cell 2012; 151:1501-1512.
76. Hosokawa N, Hara T, Kaizuka T, et al. Nutrient-dependent mTORC1 association with the ULK1-Atg13-FIP200 complex required for autophagy. Mol Biol Cell 2009; 20:1981-1991.
77. Mizushima N. The role of the Atg1/ULK1 complex in autophagy regulation. Curr Opin Cell Biol 2010; 22:132-139.
78. Hosokawa N, Sasaki T, Iemura S, et al. Atg101, a novel mammalian autophagy protein interacting with Atg13. Autophagy 2009; 5:973-979.
79. Mercer CA, Kaliappan A, Dennis PB. A novel, human Atg13 binding protein, Atg101, interacts with ULK1 and is essential for macroautophagy. Autophagy 2009; 5:649-662.
80. Hara T, Takamura A, Kishi C, et al. FIP200, a ULK-interacting protein, is required for autophagosome formation in mammalian cells. J Cell Biol 2008; 181:497-510.
81. Jung CH, Jun CB, Ro SH, et al. ULK-Atg13-FIP200 complexes mediate mTOR signaling to the autophagy machinery. Mol Biol Cell 2009; 20:1992-2003.
82. Kim J, Kundu M, Viollet B, Guan KL. AMPK and mTOR regulate autophagy through direct phosphorylation of Ulk1. Nat Cell Biol 2011; 13:132-141.
83. Di Bartolomeo S, Corazzari M, Nazio F, et al. The dynamic interaction of AMBRA1 with the dynein motor complex regulates mammalian autophagy. J Cell Biol 2010; 191:155-168.
84. Russell RC, Tian Y, Yuan H, et al. ULK1 induces autophagy by phosphorylating Beclin-1 and activating VPS34 lipid kinase. Nat Cell Biol 2013; 15:741-750.
85. Reggiori F, Shintani T, Nair U, Klionsky DJ. Atg9 cycles between mitochondria and the pre-autophagosomal structure in yeasts. Autophagy 2005; 1:101-109.
86. He C, Baba M, Cao Y, Klionsky DJ. Self-interaction is critical for Atg9 transport and function at the phagophore assembly site during autophagy. Mol Biol Cell 2008; 19:5506-5516.
87. He C, Song H, Yorimitsu T, et al. Recruitment of Atg9 to the preautophagosomal structure by Atg11 is essential for selective autophagy in budding yeast. J Cell Biol 2006; 175:925-935.
88. Legakis JE, Yen W-L, Klionsky DJ. A cycling protein complex required for selective autophagy. Autophagy 2007;3:422-432.

89. Yen WL, Legakis JE, Nair U, Klionsky DJ. Atg27 is required for autophagy-dependent cycling of Atg9. Mol Biol Cell 2007; 18:581-593.
90. Orsi A, Razi M, Dooley HC, et al. Dynamic and transient interactions of Atg9 with autophagosomes, but not membrane integration, are required for autophagy. Mol Biol Cell 2012;23:1860-1873.
91. Puri C, Renna M, Bento CF, Moreau K, Rubinsztein DC. Diverse autophagosome membrane sources coalesce in recycling endosomes. Cell 2013; 154:1285-1299.
92. Obara K, Sekito T, Ohsumi Y. Assortment of phosphatidylinositol 3-kinase complexes–Atg14p directs association of complex I to the pre-autophagosomal structure in *Saccharomyces cerevisiae*. Mol Biol Cell 2006; 17:1527-1539.
93. Kihara A, Noda T, Ishihara N, Ohsumi Y. Two distinct Vps34 phosphatidylinositol 3-kinase complexes function in autophagy and carboxypeptidase Y sorting in *Saccharomyces cerevisiae*. J Cell Biol 2001; 152:519-530.
94. Araki Y, Ku WC, Akioka M, et al. Atg38 is required for autophagy-specific phosphatidylinositol 3-kinase complex integrity. J Cell Biol 2013; 203:299-313.
95. Itakura E, Kishi C, Inoue K, Mizushima N. Beclin 1 forms two distinct phosphatidylinositol 3-kinase complexes with mammalian Atg14 and UVRAG. Mol Biol Cell 2008;19:5360-5372.
96. Yang Z, Klionsky DJ. Mammalian autophagy: core molecular machinery and signaling regulation. Curr Opin Cell Biol 2010; 22:124-131.
97. Parzych KR, Klionsky DJ. An overview of autophagy: Morphology, mechanism, and regulation. Antioxid Redox Signal 2013 Aug 2. doi:10.1089/ars.2013.5371
98. Xie Z, Nair U, Klionsky DJ. Atg8 controls phagophore expansion during autophagosome formation. Mol Biol Cell 2008; 19:3290-3298.
99. Shintani T, Huang W-P, Stromhaug PE, Klionsky DJ. Mechanism of cargo selection in the cytoplasm to vacuole targeting pathway. Dev Cell 2002; 3:825-837.
100. Kim J, Dalton VM, Eggerton KP, Scott SV, Klionsky DJ. Apg7p/Cvt2p is required for the cytoplasm-to-vacuole targeting, macroautophagy, and peroxisome degradation pathways. Mol Biol Cell 1999; 10:1337-1351.
101. Kirisako T, Ichimura Y, Okada H, et al. The reversible modification regulates the membrane-binding state of Apg8/Aut7 essential for autophagy and the cytoplasm to vacuole targeting pathway. J Cell Biol 2000; 151:263-276.
102. Ichimura Y, Kirisako T, Takao T, et al. A ubiquitin-like system mediates protein lipidation. Nature 2000; 408:488-492.
103. Mizushima N, Noda T, Yoshimori T, et al. A protein conjugation system essential for autophagy. Nature 1998; 395:395-398.
104. Tanida I, Mizushima N, Kiyooka M, et al. Apg7p/Cvt2p: A novel protein-activating enzyme essential for autophagy. Mol Biol Cell 1999; 10:1367-1379.
105. Shintani T, Mizushima N, Ogawa Y, et al. Apg10p, a novel protein-conjugating enzyme essential for autophagy in yeast. EMBO J 1999; 18:5234-5241.
106. Mizushima N, Sugita H, Yoshimori T, Ohsumi Y. A new protein conjugation system in human. The counterpart of the yeast Apg12p conjugation system essential for autophagy. J Biol Chem 1998; 273:33889-33892.

107. Tanida I, Tanida-Miyake E, Ueno T, Kominami E. The human homolog of *Saccharomyces cerevisiae* Apg7p is a protein-activating enzyme for multiple substrates including human Apg12p, GATE-16, GABARAP, and MAP-LC3. J Biol Chem 2001; 276:1701-1706.
108. Mizushima N, Yoshimori T, Ohsumi Y. Mouse Apg10 as an Apg12-conjugating enzyme: analysis by the conjugation-mediated yeast two-hybrid method. FEBS Lett 2002; 532:450-454.
109. Mizushima N, Kuma A, Kobayashi Y, et al. Mouse Apg16L, a novel WD-repeat protein, targets to the autophagic isolation membrane with the Apg12-Apg5 conjugate. J Cell Sci 2003; 116:1679-1688.
110. Weidberg H, Shvets E, Shpilka T, et al. LC3 and GATE-16/GABARAP subfamilies are both essential yet act differently in autophagosome biogenesis. EMBO J 2010; 29:1792-1802.
111. Li M, Hou Y, Wang J, et al. Kinetics comparisons of mammalian Atg4 homologues indicate selective preferences toward diverse Atg8 substrates. J Biol Chem 2011; 286:7327-7338.
112. Kabeya Y, Mizushima N, Yamamoto A, et al. LC3, GABARAP and GATE16 localize to autophagosomal membrane depending on form-II formation. J Cell Sci 2004; 117:2805-2812.
113. Bartholomew CR, Suzuki T, Du Z, Backues SK, Jin M, Lynch-Day MA, Umekawa M, Kamath A, Zhao M, Xie Z, et al. Ume6 transcription factor is part of a signaling cascade that regulates autophagy. Proc Natl Acad Sci USA 2012; 109:11206-10;
114. Jin M, He D, Backues SK, Freeberg MA, Liu X, Kim JK, Klionsky DJ. Transcriptional regulation by Pho23 modulates the frequency of autophagosome formation. Curr Biol 2014; 24:1314-22;
115. Bernard, A., et al., A large-scale analysis of autophagy-related gene expression identifies new regulators of autophagy. Autophagy, 2015. 11(11): p. 2114-2122.
116. Yao, Z., et al., Atg41/Icy2 regulates autophagosome formation. Autophagy, 2015. 11(12): p. 2288-99.
117. Settembre, C., et al., TFEB links autophagy to lysosomal biogenesis. Science, 2011. 332(6036): p. 1429-33.
118. Kreuzaler PA, et al. Stat3 controls lysosomal-mediated cell death in vivo. Nat Cell Biol. 2011; 13:303–309.
119. Guerriero JL, et al. Non-apoptotic routes to defeat cancer. Oncoimmunology. 2012; 1:94–96.
120. Jiang L, et al. Decision making by p53: life versus death. Mol Cell Pharmacol. 2010; 2:69–77.
121. Sengupta A, et al. FoxO transcription factors promote autophagy in cardiomyocytes. J Biol Chem. 2009; 284:28319–28331.
122. Wu H, et al. MiR-20a and miR-106b negatively regulate autophagy induced by leucine deprivation via suppression of ULK1 expression in C2C12 myoblasts. Cell Signal. 2012; 24:2179–2186.

123. Huang Y, et al. Phospho-DeltaNp63alpha/miR-885-3p axis in tumor cell life and cell death upon cisplatin exposure. Cell Cycle. 2011; 10:3938–3947.
124. Hu, G., et al., A conserved mechanism of TOR-dependent RCK-mediated mRNA degradation regulates autophagy. Nat Cell Biol, 2015. 17(7): p. 930-942.
125. Boya P, et al. Emerging regulation and functions of autophagy. Nat Cell Biol. 2013; 15:713–720.
126. Marino G, et al. Self-consumption: the interplay of autophagy and apoptosis. Nat Rev Mol Cell Biol. 2014; 15:81–94.
127. Feng Y, et al. The machinery of macroautophagy. Cell Res. 2014; 24:24–41.
128. Xu P, et al. JNK regulates FoxO-dependent autophagy in neurons. Genes Dev. 2011;25:310–322.
129. Zalckvar E, et al. DAP-kinase-mediated phosphorylation on the BH3 domain of beclin 1 promotes dissociation of beclin 1 from Bcl-XL and induction of autophagy. EMBO Rep. 2009; 10:285–292.
130. Nazio F, et al. mTOR inhibits autophagy by controlling ULK1 ubiquitylation, self-association and function through AMBRA1 and TRAF6. Nat Cell Biol. 2013; 15:406–416.
131. Shi CS, Kehrl JH. Traf6 and A20 differentially regulate TLR4-induced autophagy by affecting the ubiquitination of Beclin 1. Autophagy. 2010; 6:986–987.
132. Banreti A, et al. The emerging role of acetylation in the regulation of autophagy. Autophagy. 2013; 9:819–829.
133. Lin SY, et al. GSK3-TIP60-ULK1 signaling pathway links growth factor deprivation to autophagy. Science. 2012; 336:477–481.

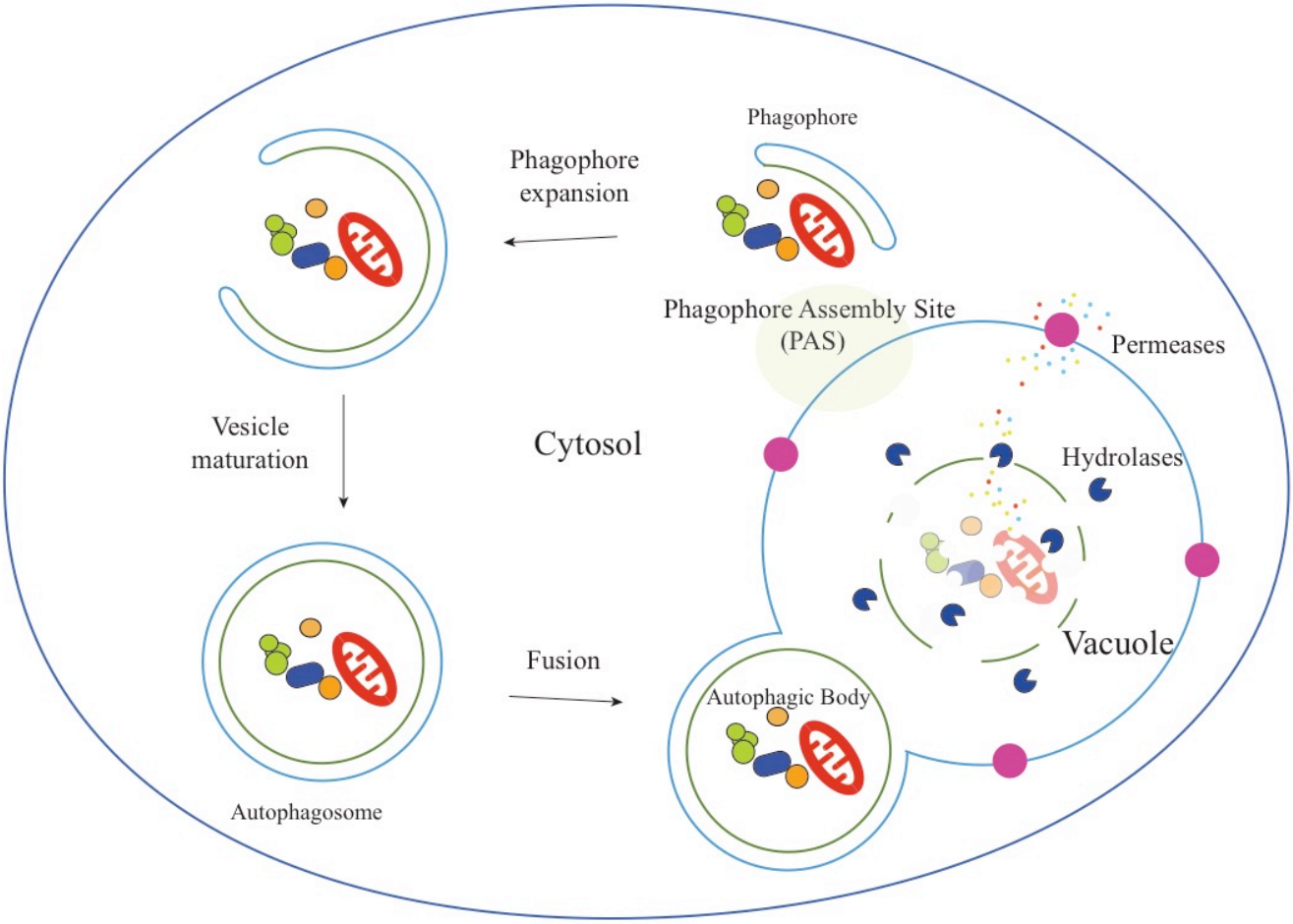

Figure 1.1. Schematic depiction of the macroautophagy in yeast.
In macroautophagy, random cytoplasm and dysfunctional organelles are sequestered by the expanding phagophore, leading to the formation of the autophagosome. The autophagosome subsequently fuses with the vacuole membrane, releasing the autophagic body into the vacuole lumen. Eventually, the sequestered cargos are degraded or processed by vacuolar hydrolases.

Table 1.1. Atg/ATG proteins in the core machinery of autophagosome formation.

	Yeast	Mammals	Characteristics and functions
Atg1/ULK complex	Atg1	ULK1/2	Ser/Thr protein kinase; phosphorylated by M/TORC1; recruitment of Atg proteins to the PAS
	Atg13	ATG13	Regulatory subunit through phosphorylation by M/TORC1 and/or PKA, linker between Atg1 and Atg17
	Atg17	RB1CC1/FIP200 (functional homolog)	Scaffold protein, ternary complex with Atg29 and Atg31; Phosphorylated by ULK1; scaffold for ULK1/2 and ATG13
	Atg29		Ternary complex with Atg17 and Atg31
	Atg31		Ternary complex with Atg17 and Atg29
	Atg11		Scaffold protein in selective autophagy for PAS organization
		C12orf44/Atg101	Component of the complex with ATG13 and RB1CC1
Atg9 and its cycling system	Atg2	ATG2	Interacts with Atg18
	Atg9	ATG9A/B	Transmembrane protein, directs membrane to the phagophore
	Atg18	WIPI1/2	PtdIns3P-binding protein
	Atg23		Interacts with Atg9 and Atg27
	Atg27		Interacts with Atg9 and Atg23
PtdIns3K complex	Vps34	PIK3C3/VPS34	PtdIns 3-kinase
	Vps15	PIK3R4/VPS15	Ser/Thr protein kinase
	Vps30/Atg6	BECN1	Component of PtdIns3K complex I and II
	Atg14	ATG14	Component of PtdIns3K complex I
Atg8 Ubl conjugation system	Atg8	LC3A/B/C, GABARAP, GABARAPL1/2	Ubl, conjugated to PE
	Atg7	ATG7	E1-like enzyme
	Atg3	ATG3	E2-like enzyme
	Atg4	ATG4A/B/C/D	Deconjugating enzyme, cysteine proteinase
Atg12 Ubl conjugation system	Atg12	ATG12	Ubl
	Atg7	ATG7	E1-like enzyme
	Atg10	ATG10	E2-like enzyme
	Atg16	ATG16L1	Interacts with Atg5 and Atg12
	Atg5	ATG5	Conjugated by Atg12

Chapter 2 Atg41/Icy2 regulates autophagosome formation[2]

2.1. Abstract

Macroautophagy (hereafter autophagy) is one of the major degradation systems in eukaryotic cells, and its dysfunction may result in diseases ranging from neurodegeneration to cancer. Although most of the autophagy-related (Atg) proteins that function in this pathway were first identified in yeast, many were subsequently shown to have homologs in higher eukaryotes including humans, and the overall mechanism of autophagy is highly conserved. The most prominent feature of autophagy is the formation of a double-membrane sequestering compartment, the phagophore; this transient organelle surrounds part of the cytoplasm and matures into an autophagosome, which subsequently fuses with the vacuole or lysosome to allow degradation of the cargo. Much attention has focused on the process involved in phagophore nucleation and expansion, but many questions remain. Here, we identified the yeast protein Icy2, which we now name Atg41, as playing a role in autophagosome formation. Atg41 interacts with the transmembrane protein Atg9, a key component involved in autophagosome biogenesis, and both proteins display a similar localization profile. Under autophagy-inducing conditions the expression level of Atg41 increases dramatically and is regulated by the transcription factor Gcn4. This work provides

[2] This chapter is reprinted partly from Z Yao, E Delorme-Axford, SK Backues, DJ Klionsky. Atg41/Icy2 regulates autophagosome formation. *Autophagy* 11 (12), 2288-2299, with some modifications.

further insight into the mechanism of Atg9 function and the dynamics of sequestering membrane formation during autophagy.

2.2. Introduction

Autophagy is involved in numerous aspects of cellular homeostasis, and autophagic dysfunction is associated with a range of diseases in humans [1]. Part of the reason that autophagy is connected to a wide array of physiological pathways has to do with the unique process of sequestration involving the phagophore. In contrast to the secretory pathway, where vesicles bud off from organelles already containing their cargo, the phagophore is generated through an expansion process that provides tremendous cargo flexibility. Thus, autophagy is the primary mechanism through which cells can eliminate damaged or superfluous organelles. For this reason, the mechanism of phagophore nucleation and expansion, including the origin of the donor membranes, has been the subject of intense focus.

The biogenesis of the phagophore is thought to initiate at a nucleating site, named the phagophore assembly site (PAS). Most of the Atg proteins transiently reside at the PAS, although the ultrastructure of this site and the interactions among the Atg proteins during phagophore formation are not known. One of the key proteins that functions in formation and/or expansion of the phagophore is Atg9. This protein is predicted to contain 6 transmembrane domains, and to transit from the endoplasmic reticulum to the Golgi apparatus [2-3]; Atg9 subsequently localizes to peri-mitochondrial sites that are termed Atg9 peripheral structures, Atg9 reservoirs or tubulovesicular clusters [4]. As a membrane protein, Atg9 is considered to play a role in delivering or directing membrane from a donor site(s) to the PAS. In addition, Atg9 may move between these sites in successive rounds of

trafficking [4-5]. Anterograde movement to the PAS requires Atg11, Atg23 and Atg27, whereas retrograde movement involves Atg1-Atg13 and Atg2-Atg18 [5-6]. The details of Atg9 trafficking, however, are not understood.

Molecular genetic studies in *Saccharomyces cerevisiae* have contributed substantially to our understanding of autophagy at the molecular level [7]. Genetic screens for autophagy-defective mutants have identified a series of genes whose products are involved primarily or exclusively in autophagy. These Atg proteins act at different steps of the autophagy process. Even though 40 different Atg proteins have been reported in yeast, new ones continue to be identified. Atg41 is a small protein identified in yeast as being upregulated during heat shock [8], but the structural and functional information for this protein is limited and its cellular function is not known [9-11].

Here, we report that Atg41 plays a role in autophagosome formation; *atg41Δ* cells display a severe defect in autophagy activity. We found that *ATG41* is upregulated at the transcriptional level, resulting in a substantial increase in the protein amount under autophagy-inducing conditions, and this upregulation is required for efficient autophagy. The association between Atg41 and Atg9 suggest that this protein is part of the Atg9 complex that plays a role in determining the frequency of autophagosome formation.

2.3. Result

2.3.1 Atg41/Icy2 is required for nonselective autophagy

We identified *icy2Δ* in a large-scale screen for mutants defective in mitophagy, the selective autophagic degradation of mitochondria [12]. To determine whether Icy2 plays a role in nonselective autophagy, we carried out the GFP-Atg8 processing assay. Atg8 is required for autophagosome formation and the phosphatidylethanolamine (PE)-conjugated form of the

protein initially lines both sides of the phagophore; Atg8–PE on the outer surface of the mature autophagosome is released, whereas the population inside the autophagosome is delivered to the vacuole and degraded [3]. When fused to GFP, Atg8 is still degraded in the vacuole lumen, but the GFP moiety is relatively stable. Thus, the generation of free GFP can be used to monitor autophagic delivery to the vacuole [13]. We monitored the processing of GFP-Atg8 expressed under the control of the endogenous ATG8 promoter. In growing conditions there is a low level of GFP-Atg8, and the protein is upregulated following autophagy induction (Fig. 2.1A). We observed a substantial decrease of free GFP in *icy2Δ* cells after 2 h of autophagy induced by nitrogen starvation compared to the wild type (Fig. 2.1 A-B), suggesting that autophagy flux was reduced in the mutant.

The GFP-Atg8 processing assay reflects the surface area of the inner autophagosome vesicle, which is referred to as an autophagic body once it is released into the vacuole lumen. A more quantitative measure of autophagic capacity can be achieved with the Pho8Δ60 assay, which measures the volume of the autophagosome/autophagic body. Pho8 is a vacuolar phosphatase that is synthesized as a zymogen; it is delivered to the vacuole via part of the secretory pathway and is subsequently activated in the vacuolar lumen by proteolytic removal of a C-terminal propeptide [14]. Pho8Δ60 lacks the N-terminal transmembrane domain that serves as an internal, uncleaved signal sequence; the truncated protein remains in the cytosol and is only delivered to the vacuole by autophagy. Thus, autophagy activity can be measured by monitoring Pho8Δ60-dependent phosphatase activity in a strain lacking the endogenous *PHO8* gene [15].

The wild-type strain showed the expected increase in autophagy activity following nitrogen starvation (Fig. 2.1C). In contrast, an *atg9Δ* strain displayed essentially a complete block in

Pho8Δ60-dependent phosphatase activity. Consistent with the GFP-Atg8 processing assay, the *icy2Δ* strain showed a significant reduction in autophagy activity compared to the wild type. Yeast express a paralog of Icy2, Icy1, and we extended the analysis by examining the requirement for this protein in autophagy. In contrast to the *icy2Δ* strain, however, there was no significant difference between the autophagy activity in the *icy1Δ* and wildtype cells. To verify that the defect seen in the *icy2Δ* mutant was not due to an unknown secondary mutation we transformed the null strain with a plasmid encoding the wild-type *ICY2* gene under the control of its endogenous promoter. The wild-type gene fully restored the autophagy activity of the null strain suggesting that the mutant phenotype was indeed the result of deleting *ICY2* (Fig. S2.1A).

We decided to examine whether Icy2 was sufficient to induce autophagy by overexpressing it during nutrient-rich conditions. We took advantage of the *ZEO1* promoter, which allows constitutive expression of the downstream gene before and after starvation. However, overexpressing *ICY2* by replacing its endogenous promoter with the *ZEO1* promoter did not induce autophagy in growing conditions (Fig. S2.1B), and in fact caused a partial decrease in activity in starvation conditions. The inability to induce autophagy by overexpression in growing conditions likely reflects the need for the upregulation of other Atg proteins including Atg7, Atg8 and Atg9 to achieve a higher level of autophagy activity [16-18]. To rule out the possibility that Icy2 affects the transcription of other *ATG* genes we examined the expression of the *ATG7* and *ATG9* genes in the *icy2Δ* mutant after starvation. We found that the expression of either gene was not affected by the absence of Icy2 (Fig. S2.1C). Similarly, the amount of the Atg9 protein was unaffected (Fig. S2.1D), indicating that Icy2

was not required for Atg9 translation; we do not have antibody to the endogenous Atg7 protein.

Next, to investigate whether Icy2 affects selective autophagy, we examined processing of precursor aminopeptidase I (prApe1). The precursor form of Ape1 is the major cargo of the cytoplasmto-vacuole targeting (Cvt) pathway, a biosynthetic type of selective autophagy.19 Upon delivery to the vacuole, the propeptide of prApe1 is proteolytically cleaved and the resulting molecular weight shift can be detected by western blot. We observed a defect in prApe1 processing in the absence of Icy2 (Fig. S2.1E), indicating that this protein is required for an efficient Cvt pathway. Taken together, these data indicate that Icy2 is required for normal autophagy flux. Because of the autophagy-defective phenotype of the *icy2Δ* strain based on the GFP-Atg8 processing and Pho8Δ60 assays, and the block in the Cvt pathway, we concluded that Icy2 is involved in both selective and nonselective autophagy. We are not able to identify a previous publication describing Icy2, and therefore refer to the protein as Atg41 hereafter.

2.3.2 An increased Atg41 expression level during starvation is required for autophagy

Either insufficient or excessive autophagy can be detrimental to cell physiology. Accordingly, autophagy activity is regulated at many levels, including through transcriptional control [16-18,20]. To determine whether the expression level of Atg41 changed between nutrient-rich and nitrogen starvation conditions we first examined the *ATG41* mRNA level by real-time quantitative PCR (RT-qPCR; Fig. 2.2A). A dramatic increase of *ATG41* mRNA was observed after 1 h of nitrogen starvation. To determine whether the *ATG41* transcriptional expression increase leads to a corresponding translational upregulation, we integrated epitope tags at the *ATG41* chromosomal locus

using either GFP or protein A (PA) to generate C-terminal fusions. A Pho8Δ60 assay of the *ATG41-GFP* strain showed a comparable autophagy activity level to the wild type, indicating that the C-terminal tagging of *ATG41* did not disrupt protein function (Fig. S2.2A). Cells expressing tagged Atg41 were harvested from cultures in growing and nitrogen starvation conditions and protein extracts were examined by western blot (Fig. 2.2B-C). In agreement with the RT-qPCR results, the protein level of Atg41 detected in either of the tagged strains increased substantially during nitrogen starvation. We could not detect *Atg41-GFP* in growing conditions with a short-time exposure, but could observe a low level of *Atg41-PA*. The inability to detect the GFP-tagged protein in growing conditions probably reflects the low expression level of Atg41 during vegetative growth and the different sensitivity of the respective antibodies.

We took advantage of the GFP tag to examine the expression of Atg41 by fluorescence microscopy. Consistent with the western blot results, dramatically increased fluorescence intensity was observed after 2-h nitrogen starvation (Fig. S2.2B). To investigate the stability of the Atg41 protein, we performed the western blot equivalent of a pulse-chase experiment, relying on the low expression level observed in growing conditions (Fig. S2.2C). Cells expressing Atg41-GFP were first starved for nitrogen and then shifted back to rich medium conditions (YPD). Protein extracts were collected at different time points and examined by western blot. The Atg8 level was also monitored for comparison because Atg8 shows a similar dramatic increase in expression under starvation conditions. We found that the Atg41 level decreased back to the pre-starvation level within 30 min after shifting the cultures back to growing conditions, indicating that Atg41 is unstable or rapidly degraded when the cells are not under autophagy inducing conditions. In contrast, Atg8 levels

displayed a steady but slow decline consistent with the turnover of the part of the Atg8 population that was present within autophagic bodies.

The increased expression of Atg41 was of a greater magnitude than that seen for any of the characterized Atg proteins, with the exception of Atg8. In the case of Atg7, Atg8 and Atg9 the increases in protein levels are important for efficient autophagy [16-18]. Accordingly, we next wanted to determine whether the increase in Atg41 was required for robust autophagy activity. Accordingly, we replaced the endogenous *ATG41* promoter in the genome with the *COF1* promoter. We determined empirically that the *COF1* promoter drives relatively low protein expression; in addition, the expression pattern of genes under the control of the *COF1* promoter showed relatively little difference between vegetative and starvation conditions (data not shown).

Thus, by replacing the endogenous *ATG41* promoter (*ATG41p*) with that of *COF1* we were able to maintain a similar, low *ATG41* expression level before and after nitrogen starvation (Fig. 2.3A). We used the C-terminal GFP-tagged strain to allow us to detect the Atg41-GFP protein level; in fact, the primary purpose of using this strain in addition to the null mutant was that it allowed us to verify the reduced level of Atg41 with a positive signal. The *atg41Δ*, *ATG41p-ATG41-GFP* and *COF1p-ATG41-GFP* cells were grown to mid-log phase and shifted to starvation conditions; aliquots were collected and protein extracts were analyzed by the Pho8Δ60 assay. The wild-type and *ATG41p-ATG41-GFP* strains displayed a robust induction of autophagy activity during nitrogen starvation (Fig. 2.3B). In contrast, the *COF1p-ATG41-GFP* cells showed a substantial reduction in autophagy activity, close to that of the *atg41Δ* null strain. These data suggest that the large increase in Atg41 protein seen under starvation conditions is required for normal autophagy activity.

2.3.3 Atg41 protein levels correlate with autophagosome number

A decrease in the number and/or size of autophagosomes can result in impaired autophagy activity [21-22]. Therefore, we used transmission electron microscopy to determine the effect of decreased Atg41 protein levels with regard to autophagosome formation, by measuring the number and size of autophagic bodies[23]. We used a *pep4Δvps4Δ* strain background for this analysis. *PEP4* encodes proteinase A, which is required to activate multiple vacuolar hydrolases; deleting *PEP4* causes the accumulation of intact autophagic bodies in the vacuole. VPS4 edcodes a AAA-ATPase involved in multivesicular body protein sorting, and deletion of this gene reduces the vesicular background content of the vacuole. We analyzed the *atg41Δ*, *ATG41p-ATG41-GFP* and *COF1p-ATG41-GFP* strains with regard to autophagic body number and size (Fig. 2.3C-E). Quantitative analysis of the images revealed that the number of autophagic bodies was reduced in the *atg41Δ* and *COF1p-ATG41-GFP* strains (Fig. 3D), whereas there was essentially no difference in autophagic body size (Fig. 2.3E). Using an algorithm to estimate total autophagic body number and size within the vacuole [23], the electron microscopy analysis indicated that the total autophagy flux in the *COF1p- ATG41-GFP* and *atg41Δ* strains was reduced by approximately 50% compared to the *ATG41p-ATG41-GFP* wild type (Table S2.1), which is consistent with the Pho8Δ60 assay results. These data further support our finding that the increased Atg41 level is required for a maximal autophagic response. Finally, because the lower autophagy activity was due to decreased autophagosome numbers, these results also suggest that the Atg41 level is important in determining the rate of autophagosome formation.

2.3.4 Atg41 localizes to Atg9 peripheral structures and associates with Atg9

Reduced levels of Atg41 affected the number of autophagosomes formed during starvation, and we next wanted to determine the relationship of Atg41 to other components of the Atg core machinery, those proteins that are needed for autophagosome formation [24]. Information on protein subcellular location can often provide useful informative with regard to protein function, and most of the Atg proteins have discrete localization patterns. Accordingly, we examined the localization of Atg41-GFP. Our analysis of Atg41 expression based on the visualization of the Atg41-GFP chimera showed a unique distribution pattern for this protein (Fig. S2.2B), which was reminiscent of the overall morphology of yeast mitochondria. Accordingly, we used Mito-Tracker Red to stain the mitochondria of cells expressing Atg41-GFP and examined them by fluorescence microscopy. We observed substantial colocalization of Atg41-GFP and Mito- Tracker Red (Fig. 2.4A). A peri-mitochondrial distribution is similar to that displayed by Atg9-GFP [4]. In addition, Atg41 does not contain a mitochondrial targeting sequence or transmembrane domain, suggesting that Atg41-GFP distributes around the mitochondria rather than being directly associated with the organelle.

Considering that Atg41 had a similar subcellular distribution to that of Atg9, and a decrease in either protein correlated with a reduced number of autophagic bodies, we decided to investigate the relationship between these 2 proteins. We first tagged Atg9 with mCherry, and Atg41 with GFP to see if these 2 proteins displayed a close proximity under fluorescence microscopy (Fig. 2.4B). The results indicated a partial co-localization of Atg9 and Atg41. To further examine whether a potential transient interaction exists, we took advantage of the bimolecular fluorescence complementation (BiFC) assay [25]. In this assay, Venus YFP is split into 2 parts, the N terminus (VN) and C terminus (VC). We genomically

tagged the C terminus of Atg41 with VC and the C terminus of Atg9 with VN, generating an *ATG41-VC ATG9-VN* strain. The YFP fluorescence signal in this strain can only be observed when VN and VC are in close proximity. For comparison, we also constructed *ATG41-VC ATG2-VN* and *ATG41-VC ATG27-VN* strains. Atg2 and Atg27 both function in Atg9 trafficking between the peripheral sites and the PAS, in retrograde and anterograde trafficking, respectively. We observed bright fluorescent dots in the cells expressing Atg41-VC Atg9-VN, but not in the other strains (Fig. 2.4C-D). Furthermore, we could only detect a fluorescent signal between Atg41-VC and Atg9-VN under starvation conditions; however, this may simply reflect the extremely low level of Atg41 expression during growing conditions (Fig. 2.2). This result suggests that Atg41 associates with (or is located in proximity to) Atg9, but not necessarily other Atg proteins involved in Atg9 trafficking.

To confirm the BiFC result, we also performed the yeast two hybrid assay (Fig. 2.4E). *AD-ATG41* and *BD-ATG9* were cotransformed into cells, while the *AD* empty vector and *BD-ATG9* were co-transformed as controls. The results showed that only cells with *AD-ATG41* and *BD-ATG9* could grow under minus histidine selection, indicating an association between Atg41 and Atg9. Since Atg9 is proposed to function in donating or directing membrane to the expanding phagophore by trafficking from donor sites to the PAS, we next investigated whether Atg41 controlled autophagy via an effect on Atg9 movement. Previous studies indicated that in the absence of Atg1 the retrograde trafficking of Atg9 was largely blocked resulting in accumulation of the protein at the PAS [5]. We took advantage of this phenotype to carry out a kinetic analysis of Atg9 anterograde movement in cells expressing a temperature sensitive allele of ATG1 (Atg1ts); the strain also expressed Atg9-3GFP and RFP-Ape1 as a PAS marker. When autophagy was induced at the permissive temperature,

Atg9–3GFP could shuttle between the PAS and peripheral sites, resulting in a low level of co-localization between Atg9 and prApe1 (data not shown). Similarly, the cells displayed a low level of co-localization in growing conditions (Fig. 2.4F). Following a shift of the Atg1ts strain to the non-permissive temperature, Atg9–3GFP accumulated at the PAS resulting in a substantial increase in co-localization with RFP-Ape1. In the *atg41Δ* strain there was a significant decrease in the co-localization between these 2 proteins compared to the wild type. The Atg41 protein level in the Atg1ts strain was comparable to that in the wild-type strain after 1 h of starvation at the non-permissive temperature (Fig. S2.3A), indicating that the defect in Atg9 trafficking reflected the absence of Atg41 specifically in the *atg41Δ* (Atg1ts) strain and not the *ATG41* wild-type (Atg1ts) strain. This result indicated a kinetic defect in Atg9 anterograde trafficking in the absence of Atg41.

Because fluorescence microscopy, bimolecular fluorescence complementation and yeast two-hybrid data suggested that Atg41 associated with Atg9, we wanted to map the region of Atg41 that is required for this interaction, which would then allow us to examine the effect of specifically disrupting this association. We started the analysis with a computerized prediction of intrinsically disordered regions (IDRs) in Atg41. For many proteins IDRs participate in dynamic binding interactions. Furthermore, we determined that many of the yeast Atg proteins contain IDRs [26], and this appears to be conserved up to humans [27]. We used PONDR-FIT [28], an algorithm that combines several individual disorder predictors that evaluate the tendency for intrinsic disorder based on the target sequence, to identify putative IDRs in Atg41 (Fig. 2.5A). Based on the analysis, Atg41 contains at least 4 regions above the threshold level. Two of these potential IDRs are located at or near the N terminus. Because deletions of this part of the protein were more likely to affect folding of

the remainder of the protein we focused our initial analysis on the 2 C-terminal IDRs and generated strains expressing Atg41(*Δ91–110*) and Atg41(*Δ127–136*). The C termini of these strains were tagged with VC, and Atg9 was tagged with VN to allow us to carry out the BiFC assay.

Based on the bimolecular fluorescence complementation assay after autophagy induction we could still detect a fluorescent signal with Atg9-VN and Atg41(*Δ91–110*)-VC, similar to the results with full-length Atg41 (Fig. 2.5B-C). In contrast, deletion of the extreme 10 C-terminal residues in Atg41(*Δ127–136*)-VC abrogated the association between the 2 proteins. Because of the relatively small size of the deletion, and its location at the extreme C terminus, this mutation is unlikely to affect the stability of Atg41; indeed, analysis of Atg41(*Δ127–136*)-GFP by microscopy indicated that the truncation did not affect the stability of the protein relative to the wild type (Fig. 2.5D). Similarly, western blot indicated that Atg41(*Δ127-136*)-GFP was stable (Fig. S2.3B). Therefore, these data suggest that the extreme C-terminal region of Atg41 is important for associating with Atg9.

Having identified a region in Atg41 that was needed for its association with Atg9, we next utilized the Pho8Δ60 assay to examine the phenotypic consequence of disrupting this association (Fig. 2.5E). Cells expressing Atg41-VC displayed a wild-type level of autophagy activity, which was also the case for cells expressing Atg41(*Δ91–110*)-VC. In contrast, the Atg41(*Δ127–136*)-VC protein, which no longer interacted with Atg9, had a reduction of Pho8Δ60 activity similar to that seen with the atg41Δ strain. Finally, we examined the distribution pattern of the Atg41(*Δ127–136*) mutant. In contrast to the peri-mitochondrial localization seen with wild-type Atg41-GFP, Atg41(*Δ127–136*)-GFP showed a diffuse distribution pattern (Fig. 2.5D). Taken together, these results indicate the very C-

terminal region of Atg41 is important for its association with Atg9, its correct subcellular distribution and normal autophagy activity.

2.3.5 The Gcn4 transcription factor regulates ATG41 expression

Because the Atg41 expression level changed considerably between growing and starvation conditions, we wanted to determine the mechanism involved in the transcriptional regulation of *ATG41*. High-throughput analysis indicates that Gcn4, the master regulator of gene expression during amino acid starvation, modulates the transcriptional level of multiple ATG genes [29]. Moreover, combining the previous study and an online yeast transcriptional database, Yeastract (www.yeastract.com), indicated that the *ATG41* 5' untranslated region (5'UTR) contains 2 putative Gcn4 binding regions [30]. Therefore, we decided to investigate the possible role of Gcn4 in regulating *ATG41* expression. We examined the *ATG41* mRNA level by RT-qPCR. As we observed previously (Fig. 2.2A), there was a strong increase in *ATG41* mRNA in the wild-type strain following autophagy induction by nitrogen starvation. In contrast, there was a significant reduction relative to the wild type in a *gcn4Δ* strain (Fig. 2.6A). Next, we tagged Atg41 with protein A in the *gcn4Δ* mutant and monitored the protein level of Atg41-PA by western blot. In agreement with the RT-qPCR results, the protein level of Atg41-PA was reduced by approximately 40% in the *gcn4Δ* background (Fig. 2.6B and C). Next, we used the Pho8Δ60 assay to determine whether the absence of Gcn4 caused an autophagy defect (Fig. 2.6D). We found a clear decrease of autophagy activity in the *gcn4Δ* background, suggesting that Gcn4-dependent regulation is necessary for optimal autophagy activity. To test whether overexpression of Atg41 in starvation conditions could rescue the *gcn4Δ* phenotype, we replaced the *ATG41* endogenous promoter with the *ZEO1* promoter in the *gcn4Δ* background; Gcn4 does not

regulate the *ZEO1* promoter. The Pho8Δ60 assay of *ZEO1p-ATG41* showed a significantly increased autophagy activity compared to *gcn4Δ*, indicating a partial rescue of the *gcn4Δ* autophagy defect (Fig.2.6E). The observation that the *ZEO1p-ATG41* strain did not display a complete restoration of autophagy likely reflects a role for Gcn4 in regulating other genes whose products are required for full autophagy activity. Taken together, these data suggest that Gcn4 positively regulates *ATG41* and that this regulation is important for autophagy.

Finally, we wanted to determine whether Gcn4 regulates ATG41 by direct binding to its promoter or indirectly by activating other transcription factors. To address this question we carried out a chromatin immunoprecipitation (ChIP) experiment using a Gcn4-PA strain. We designed 9 pairs of primers (*ATG41–1* to *ATG41–9*) each spanning approximately 130 to 170 nucleotides of the ATG41 promoter region to ensure complete coverage including 2 potential Gcn4 binding regions predicted by computer and database analysis (Fig. 2.6F). In addition, we used a previously identified site in the *HIS5* gene as a positive control [29] and the *TFC1* gene, which lacks any predicted Gcn4 binding sites, as a negative control. The RT-qPCR analysis indicated binding at the HIS5 promoter, but no binding at the TFC1 promoter as expected (Fig.2.6G). For the *ATG41* promoter region, we detected enrichment (at least 50% the level of the positive control) of the PCR product using primers *ATG41–1* to *ATG41–5*, with the regions detected by primers *ATG41–3* and *ATG41–4* showing an even higher enrichment than the *HIS5* positive control. This result is in agreement with the prediction that one of the potential Gcn4 binding sites is located in the region covered by these primers. The second predicted binding site, covered by the primer pair *ATG41–8* did not show a strong enrichment. This second site is located almost 800 nucleotides away from the translational start site (compared to approximately 300 nucleotides for the enriched site),

which is generally outside the region of yeast promoters, and is therefore unlikely to function in transcriptional control of *ATG41*. Taken together, these results indicated that Gcn4 binds directly to the promoter region of *ATG41* and transcriptionally activates expression of this gene.

2.4. Discussion

In this report we identified Atg41 as a novel component of the autophagy machinery in yeast. The absence of Atg41 results in a severe defect in autophagy activity due to a decreased rate of autophagosome formation. Icy1, a paralog of Atg41/Icy2, has low sequence similarity to Atg41/Icy2, which likely explains why Icy1 does not appear to play a role in autophagy. Many of the Atg proteins are upregulated during starvation, but only Atg8 and Atg41 display a greater than 10-fold increase in protein level. Both Atg8 and Atg41 are relatively small proteins, and Atg8 functions in phagophore expansion; lower levels of Atg8 correspond to smaller autophagosomes[21]. In contrast, Atg41 does not appear to play a role in determining the size of autophagosomes, but rather influences their formation rate, similar to Atg9 [17]. Along these lines, the localization of Atg41 shows a peri-mitochondrial distribution similar to Atg9. Furthermore, our results showed an association between Atg9 and Atg41. Considering all of these data, we propose that Atg41 is part of the Atg9 complex and is involved in the delivery of donor membrane to the expanding phagophore.

We also identified Gcn4 as a positive regulator of autophagy in agreement with previous studies [31]. *ATG41* mRNA levels only increased approximately 8-fold in the *gcn4Δ* strain compared to the nearly 60-fold increase seen in the wild type, indicating that Gcn4 plays a primary role in transcriptional regulation of *ATG41*. Although *ATG41* transcripts increased

at 6- to 7-fold higher levels in the wild type compared to the *gcn4Δ* strain, the protein levels only increased approximately 2-fold. This difference may reflect the role of other potential positive regulators, or translational silencing. The *gcn4Δ* strain displayed an approximately 50% decrease in autophagy activity, which further supports our hypothesis that a large increase in the amount of the Atg41 protein is required for normal autophagy activity. Cells do not maintain elevated levels of autophagy indefinitely, although the mechanisms involved in down-regulating autophagy under inducing conditions are not fully understood. For example, at present we do not know what controls the turnover of Atg41. We have not detected this protein within the vacuole (data not shown), suggesting that it may be degraded by the proteasome. Expression from the *COF1* promoter is predicted to be constant under growing and starvation conditions, yet we observed a clear decrease in Atg41-GFP when expressed at low levels (Fig. 2.3A), which may correspond to degradation of the protein. Future studies may provide further information on the mechanism(s) involved in regulating the expression and stability of Atg41 and in determining its role in autophagy. Although homologs of Atg41/Icy2 are found in different fungal species, no homolog is reported in higher eukaryotes based on sequence analysis. Even though many Atg proteins are conserved from yeast to mammals, a number of Atg proteins in yeast lack the corresponding homologs in mammals; however, in many cases the potential functional counterparts of these Atg proteins in mammals exist. One example is seen with Atg17 and RB1CC1, the latter of which is considered as the mammalian counterpart. Although RB1CC1 is much larger than Atg17 (1594 amino acids compared to 417 amino acids), both proteins bind to the Atg1/ULK1 kinase and play important roles in autophagy induction [32]. In yeast, Atg17, Atg29 and Atg31 form a stable complex, whereas RB1CC1 can

interact with ULK1 alone. It is thus possible in this case that in mammals one protein combines the functions of several yeast proteins. We speculate that Atg41 also falls into this category. That is, it is possible that a functional counterpart exists in mammals, and this protein either functions similarly to Atg41 or combines the functions of Atg41 and at least one other yeast protein.

2.5. Materials and Methods

2.5.1 Yeast strains, media and growth conditions

Yeast strains used in this paper are listed in Table S2.2. Yeast cells are grown in rich medium (YPD: 1% [wt/vol] yeast extract [ForMedium, YEM04], 2% [wt/vol] peptone [ForMedium, PEP04], 2% [wt/vol] glucose; or SMD: 0.67% yeast nitrogen base [ForMedium, CYN0410], 2% [wt/vol] glucose, 0.5% casamino acids [ForMedium, CAS03], 1× complete amino acids and vitamins supplement (see Table S2.3 for details), 2% glucose). Autophagy was induced by shifting mid-log phase cells from rich medium to nitrogen starvation medium (SD-N: 0.17% yeast nitrogen base without ammonium sulfate or amino acids [For-Medium,CYN0501], 2% [wt/vol] glucose) for the indicated times.

2.5.2 Antibodies and antisera

Anti-YFP antibody, which detects GFP, was from Clontech (JL-8; 63281), and anti-Pgk1 was a generous gift from Dr. Jeremy Thorner (University of California, Berkeley). Antibodies to Ape1 and Atg9 were described previously [33-34]. The protein A tag was detected with a nonspecific commercial antibody that is no longer available.

2.5.3 Plasmids

pRS405-GFP-ATG8 contains the *GFP-ATG8* open reading frame with the endogenous ATG8 promoter. This plasmid was linearized and integrated into the corresponding strains

listed in Table S2.2. *pRS414-ATG41* contains 1,000 nucleotides of the *ATG41* 5' UTR, the *ATG41* open reading frame and 500 nucleotides of the 3' UTR. *pRS414-ATG1-ts* contains the ATG1 open reading frame with the endogenous *ATG1* promoter, and L88H, F112L and S158P mutations that confer a temperature sensitive phenotype [35].

2.5.4 Fluorescence microscopy

Yeast cells were grown to mid-log phase in rich medium and then shifted to SD-N for autophagy induction. Cells were then examined by microscopy (Olympus; Delta Vision, GE Healthcare Life Sciences, Pittsburgh, PA, USA) using a 100× objective, and a CCD camera (CoolSnap HQ; Photometrics, Tucson, AZ, USA). Twelve-image stacks were taken for each picture with a 0.3-μm distance between 2 images.

2.5.5 Mitochondria staining

MitoTracker Red CMXRos (Molecular Probes/ThermoFisher Scientific, M-7512) was dissolved in DMSO. The dye was added to mid-log cells growing in rich medium with a final working concentration of 200 nM and a final DMSO concentration of 0.02%. After approximately 45 min, cells were washed and grown in rich medium for another 1 h. Cells were then shifted to SD-N for autophagy induction and microscopy analysis.

2.5.6 Real-time quantitative PCR

Yeast cells were cultured in YPD to mid-log phase and then shifted to SD-N for autophagy induction. Cells were then collected and frozen in liquid nitrogen. Total RNA was extracted using an RNA extraction kit (NucleoSpin RNA II; Clontech, 740955.50). Reverse transcription was carried out using the High Capacity cDNA Reverse Transcription Kit (Applied Biosystems/ThermoFisher Scientific, ILT4368814). RT-qPCR was performed

using the Power SYBR Green PCR Master Mix (Applied Biosystems/ThermoFisher Scientific, ILT4367659). All primer information can be found in Table S2.4.

2.5.7 Chromatin immunoprecipitation

The protocol for ChIP was slightly modified from one described previously [36]. After induction of autophagy, formaldehyde was added to the cells for DNA-protein cross-linking. Samples were then harvested, lysed and chromatin was isolated. DNA was then sheared by sonication and the sheared chromatin was immunoprecipitated. The protein-DNA complex was eluted from the beads and reverse cross-linking was performed. DNA was then purified and examined by quantitative PCR. All primer information can be found in Table S2.4.

2.5.8 Other methods

Western blot, Pho8Δ60, GFP-Atg8 processing, and prApe1 processing assays, and transmission electron microscopy were performed as described previously [13,15,23,37]. Gene deletion, truncation or integration was performed based on a standard method [38]. Genome tagging and genomic promoter exchange were performed based on a standard method [39].

2.6. References

1. Shintani T, Klionsky DJ. Autophagy in health and disease: a double-edged sword. Science 2004; 306:990-5.
2. Mari M, Griffith J, Rieter E, Krishnappa L, Klionsky DJ, Reggiori F. An Atg9-containing compartment that functions in the early steps of autophagosome biogenesis. J Cell Biol 2010; 190:1005-22.
3. Feng Y, He D, Yao Z, Klionsky DJ. The machinery of macroautophagy. Cell Res 2014; 24:24 41.
4. Reggiori F, Shintani T, Nair U, Klionsky DJ. Atg9 cycles between mitochondria and the pre-autophagosomal structure in yeasts. Autophagy 2005; 1:101-9.
5. Reggiori F, Tucker KA, Stromhaug PE, Klionsky DJ. The Atg1-Atg13 complex regulates Atg9 and Atg23 retrieval transport from the pre-autophagosomal structure. Dev Cell 2004; 6:79-90.

6. Yen WL, Legakis JE, Nair U, Klionsky DJ. Atg27 is required for autophagy-dependent cycling of Atg9. Mol Biol Cell 2007; 18:581-93.
7. Tsukada M, Ohsumi Y. Isolation and characterization of autophagy-defective mutants of *Saccharomyces cerevisiae*. FEBS Lett 1993; 333:169-74.
8. Jones DL, Petty J, Hoyle DC, Hayes A, Oliver SG, Riba-Garcia I, Gaskell SJ, Stateva L. Genome-wide analysis of the effects of heat shock on a *Saccharomyces cerevisiae* mutant with a constitutively activated cAMPdependent pathway. Comp Funct Genomics 2004.
9. Kuhn KM, DeRisi JL, Brown PO, Sarnow P. Global and specific translational regulation in the
genomic response of *Saccharomyces cerevisiae* to a rapid transfer from a fermentable to a nonfermentable carbon source. Mol Cell Biol 2001; 21:916-27.
10. Ubersax JA, Woodbury EL, Quang PN, Paraz M, Blethrow JD, Shah K, Shokat KM, Morgan DO. Targets of the cyclin-dependent kinase Cdk1. Nature 2003; 425:859-64.
11. Byrne KP, Wolfe KH. The Yeast Gene Order Browser: combining curated homology and syntenic context reveals gene fate in polyploid species. Genome Res 2005; 15:1456-61.
12. Kanki T, Wang K, Baba M, Bartholomew CR, Lynch-Day MA, Du Z, Geng J, Mao K, Yang Z, Yen WL, et al. A genomic screen for yeast mutants defective in selective mitochondria autophagy. Mol Biol Cell 2009; 20:4730-8.
13. Shintani T, Klionsky DJ. Cargo proteins facilitate the formation of transport vesicles in the cytoplasm to vacuole targeting pathway. J Biol Chem 2004; 279:29889-94.
14. Klionsky DJ, Emr SD. Membrane protein sorting: biosynthesis, transport and processing of yeast vacuolar alkaline phosphatase. Embo J 1989.
15. Noda T, Klionsky DJ. The quantitative Pho8Delta60 assay of nonspecific autophagy. Methods Enzymol 2008; 451:33-42.
16. Bartholomew CR, Suzuki T, Du Z, Backues SK, Jin M, Lynch-Day MA, Umekawa M, Kamath A, Zhao M, Xie Z, et al. Ume6 transcription factor is part of a signaling cascade that regulates autophagy. Proc Natl Acad Sci U S A 2012; 109:11206-10.
17. Jin M, He D, Backues SK, Freeberg MA, Liu X, Kim JK, Klionsky DJ. Transcriptional regulation by Pho23 modulates the frequency of autophagosome formation. Curr Biol 2014; 24:1314-22.
18. Bernard A, Jin M, Gonzalez-Rodriguez P, Fullgrabe J, Delorme-Axford E, Backues SK, Joseph B, Klionsky DJ. Rph1/KDM4 Mediates Nutrient-Limitation Signaling that Leads to the Transcriptional Induction of Autophagy. Curr Biol 2015; 25(5):546-55.
19. Lynch-Day MA, Klionsky DJ. The Cvt pathway as a model for selective autophagy. FEBS Lett 2010; 584:1359-66.
20. Kang YA, Sanalkumar R, O'Geen H, Linnemann AK, Chang CJ, Bouhassira EE, Farnham PJ, Keles S, Bresnick EH. Autophagy driven by a master regulator of hematopoiesis. Mol Cell Biol 2012; 32:226-39.
21. Xie Z, Nair U, Klionsky DJ. Atg8 controls phagophore expansion during autophagosome formation. Mol Biol Cell 2008; 19:3290-8.
22. Jin M, Klionsky DJ. Transcriptional regulation of ATG9 by the Pho23-Rpd3 complex modulates the frequency of autophagosome formation. Autophagy 2014; 10:1681-2.

23. Backues SK, Chen D, Ruan J, Xie Z, Klionsky DJ. Estimating the size and number of autophagic bodies by electron microscopy. Autophagy 2014; 10:155-64.
24. Xie Z, Klionsky DJ. Autophagosome formation: core machinery and adaptations. Nat Cell Biol 2007; 9:1102-9.
25. Sung MK, Huh WK. Bimolecular fluorescence complementation analysis system for in vivo detection of protein-protein interaction in *Saccharomyces cerevisiae*. Yeast 2007; 24:767-75.
26. Popelka H, Uversky VN, Klionsky DJ. Identification of Atg3 as an intrinsically disordered polypeptide yields insights into the molecular dynamics of autophagyrelated proteins in yeast. Autophagy 2014; 10:1093-104.
27. Mei Y, Su M, Soni G, Salem S, Colbert CL, Sinha SC. Intrinsically disordered regions in autophagy proteins. Proteins 2014; 82:565-78.
28. Xue B, Dunbrack RL, Williams RW, Dunker AK, Uversky VN. PONDR-FIT: a meta-predictor of intrinsically disordered amino acids. Biochim Biophys Acta 2010; 1804:996-1010.
29. Natarajan K, Meyer MR, Jackson BM, Slade D, Roberts C, Hinnebusch AG, Marton MJ. Transcriptional profiling shows that Gcn4p is a master regulator of gene expression during amino acid starvation in yeast. Mol Cell Biol 2001; 21:4347-68.
30. Fedorova AV, Chan IS, Shin JA. The GCN4 bZIP can bind to noncognate gene regulatory sequences. Biochim Biophys Acta 2006; 1764:1252-9.
31. Yang Z, Geng J, Yen WL, Wang K, Klionsky DJ. Positive or negative roles of different cyclin-dependent kinase Pho85-cyclin complexes orchestrate induction of autophagy in *Saccharomyces cerevisiae*. Mol Cell 2010; 38:250-64.
32. Hara T,Mizushima N. Role of ULK-FIP200 complex in mammalian autophagy: FIP200, a counterpart of yeast Atg17? Autophagy 2009; 5:85-7.
33. Klionsky DJ, Cueva R, Yaver DS. Aminopeptidase I of *Saccharomyces cerevisiae* is localized to the vacuole independent of the secretory pathway. J Cell Biol 1992; 119:287-99.
34. Noda T, Kim J, Huang WP, Baba M, Tokunaga C, Ohsumi Y, Klionsky DJ. Apg9p/Cvt7p is an integral membrane protein required for transport vesicle formation in the Cvt and autophagy pathways. J Cell Biol 2000; 148:465-80.
35. Suzuki K, Kirisako T, Kamada Y, Mizushima N, Noda T, Ohsumi Y. The pre-autophagosomal structure organized by concerted functions of APG genes is essential for autophagosome formation. EMBO J 2001; 20:5971-81.
36. Govin J, Dorsey J, Gaucher J, Rousseaux S, Khochbin S, Berger SL. Systematic screen reveals new functional dynamics of histones H3 and H4 during gametogenesis. Genes Dev 2010; 24:1772-86.
37. Klionsky DJ, Abdalla FC, Abeliovich H, Abraham RT, Acevedo-Arozena A, Adeli K, Agholme L, Agnello M, Agostinis P, Aguirre-Ghiso JA, et al. Guidelines for the use and interpretation of assays for monitoring autophagy. Autophagy 2012; 8:445-544.
38. Gueldener U, Heinisch J, Koehler GJ, Voss D, Hegemann JH. A second set of loxP marker cassettes for Cremediated multiple gene knockouts in budding yeast. Nucleic Acids Res 2002; 30:e23.

39. Longtine MS, McKenzie A, 3rd, Demarini DJ, Shah NG, Wach A, Brachat A, Philippsen P, Pringle JR. Additional modules for versatile and economical PCR-based gene deletion and modification in *Saccharomyces cerevisiae*. Yeast 1998; 14:953-61.

Table S2.1. Detailed analysis of TEM data.

Strain	**Autophagic body size**				
	Measured cross sections		Estimated original		
	Mean rad[a]	SD rad	Mean rad	SD rad	Volume[b]
ATG41-GFP	187.065	54.430	219.400	37.065	4.81E+07
COF1p-ATG41-GFP	173.260	47.824	202.738	30.962	3.74E+07
atg41Δ	187.273	52.571	221.008	32.479	4.82E+07
Strain	**Vacuole size**				
	Measured cross sections		Estimated original		
	Mean rad	SD rad	Mean rad	SD rad	
ATG41-GFP	882.267	251.897	952.992	238.480	
COF1p-ATG41-GFP	859.125	268.753	895.624	258.352	
atg41Δ	865.867	266.114	904.460	260.716	
Strain	**Autophagic body number**				
	Measured cross sections/ cell		Estimated bodies/cell		
ATG41-GFP	7.330		25.640		
COF1p-ATG41-GFP	4.539		15.862		
atg41Δ	4.331		14.185		
Strain	**Total flux (%)[c]**		**Number of cells analyzed**		
ATG41-GFP	100		183		
COF1p-ATG41-GFP	48.07		170		
atg41Δ	55.41		136		

[a]Rad, radius in nm.
[b]Expressed in nm3.
[c]Total flux was calculated as (the estimated average autophagic body volume) × (the estimated autophagic body number per cell). The values were normalized to the *ATG41-GFP* sample, which was set to 100%.

Table S2.2. Strains used in this study.

Name	Genotype	Ref
SEY6210	MATα *leu2-3,112 ura3-52 his3-Δ200 trp1-Δ901 suc2-Δ9 lys2-801 GAL*	[1]
PJ69-4A	MATa trp1-901 leu2-3,112 ura3-52 his3-200 gal4Δ gal80Δ LYS2::GAL1-HIS GAL2-ADE2 met2::GAL7-lacZ	[2]
FRY143	SEY6210 *vps4Δ::TRP1 pep4Δ::LEU2*	[3]
SKB171	*atg1Δ::ble atg9::KAN ATG9-3GFP::LEU2 RFP-Ape1::URA3* SEY6210	This study
WLY176	SEY6210 *pho13Δ pho8Δ60*	[4]
ZYY101	WLY176 *pRS405-GFP-ATG8::LEU2*	This study
ZYY102	WLY176 *pRS405-GFP-ATG8::LEU2 icy2Δ::HIS3*	This study
ZYY103	WLY176 *pRS405-GFP-ATG8::LEU2 atg3Δ::HIS3*	This study
ZYY104	WLY176 *atg9Δ::LEU2*	This study
ZYY105	WLY176 *icy2Δ::HIS3*	This study
ZYY106	WLY176 *icy1Δ::LEU2*	This study
ZYY107	WLY176 *ICY2-GFP::HIS3*	This study
ZYY108	WLY176 *ICY2-PA::HIS3*	This study
ZYY109	WLY176 *PCOF1::KAN-ICY2-GFP:;HIS3*	This study
ZYY110	FRY143 *icy2Δ::HIS3*	This study
ZYY111	FRY143 *PCOF1::KAN-ICY2-GFP:;HIS3*	This study
ZYY112	FRY143 *ICY2-GFP::HIS3*	This study
ZYY113	WLY176 *ICY2-VC::HIS3 ATG9-VN::TRP1*	This study
ZYY114	WLY176 *ICY2-VC::HIS3 ATG2-VN::TRP1*	This study
ZYY115	WLY176 *ICY2-VC::HIS3 ATG27-VN::TRP1*	This study
ZYY116	WLY176 *ICY2-VC::HIS3*	This study
ZYY117	WLY176 *icy2Δ(91-110)-VC::HIS3*	This study
ZYY118	WLY176 *icy2Δ(127-136)-VC::HIS3*	This study
ZYY119	WLY176 *icy2Δ(91-110)-VC::HIS3 ATG9-VN::TRP1*	This study
ZYY120	WLY176 *icy2Δ(127-136)-VC::HIS3 ATG9-VN::TRP1*	This study
ZYY121	WLY176 *icy2Δ(127-136)-GFP::HIS3*	This study
ZYY122	WLY176 *gcn4Δ::LEU2*	This study
ZYY123	WLY176 *gcn4Δ::LEU2 ICY2-PA::HIS3*	This study
ZYY124	WLY176 *GCN4-PA::LEU2*	This study
ZYY125	WLY176 *ICY2-GFP::HIS3; ATG9-mCherry::TRP1*	This study
ZYY126	SKB171 *icy2Δ::HIS3*	This study
ZYY127	WLY176 *PZEO1::HIS3-ICY2 gcn4Δ::LEU2*	This study
ZYY128	WLY176 *PZEO1::HIS3-ICY2*	This study
ZYY129	WLY176 *ICY2-GFP::HIS3 atg1Δ::LEU2*	This study

1. Robinson JS, Klionsky DJ, Banta LM, Emr SD. Protein sorting in *Saccharomyces cerevisiae*: isolation of mutants defective in the delivery and processing of multiple vacuolar hydrolases. Mol Cell Biol 1988; 8:4936-48.
2. James P, Halladay J, Craig EA. Genomic libraries and a host strain designed for highly efficient two-hybrid selection in yeast. Genetics 1996; 144:1425-36.
3. Cheong H, Yorimitsu T, Reggiori F, Legakis JE, Wang C-W, Klionsky DJ. Atg17 regulates the magnitude of the autophagic response. Mol Biol Cell 2005; 16:3438-53.
4. Kanki T, Wang K, Baba M, Bartholomew CR, Lynch-Day MA, Du Z, Geng J, Mao K, Yang Z, Yen W-L. A genomic screen for yeast mutants defective in selective mitochondria autophagy. Mol Biol Cell 2009; 20:4730-8.

Table S2.3. Amino acid, nucleoside and vitamin stock solutions.

20×amino acid and nucleic acid base complete stock
(1 L in distilled H2O); store at 4°C.

Amino acid or base	Concentration (%)
Adenine	0.06
Histidine	0.04
Leucine	0.10
Lysine	0.06
Tryptophan	0.10
Uracil	0.04

200x vitamins (1 L in distilled H2O); filter sterilize and store at store at 4°C or -20°C.

Vitamin or precursor	Concentration
4-Aminobenzoic acid (p-Aminobenzoic acid)	0.3 mM
Biotin (vitamin H)	2.0 μM
Ca pantothenate (vitamin B5)	330 μM
Folic acid (vitamin B9)	1.0 μM
Inositol (myo-inositol; vitamin B8)	2.22 mM
Niacin (nicotmic acid, vitamin B3)	0.65 mM
Pyridoxine HCl (vitamin B6)	0.4 mM
Riboflavin (vitamin B2)	0.1 mM
Thiamine HCl (vitamin B1)	0.24 mM

Table S2.4. Primers used in qPCR, ChIP and promoter replacement.

NAME	SEQUENCE	PURPOSE
ATG41-CHIP1-F	GCGGCTCTGCGTAAAAAGGT	CHIP-qPCR
ATG41-CHIP2-F	CGGAAAGGGTCTGGAGCAAC	CHIP-qPCR
ATG41-CHIP3-F	GCGCGAAGATGACACATTGC	CHIP-qPCR
ATG41-CHIP4-F	CCGTCCGGAAATCTACAGAA	CHIP-qPCR
ATG41-CHIP5-F	CCAAGAAGTCCCTTGGGGTT	CHIP-qPCR
ATG41-CHIP6-F	ACACCATACCCACTGTCCTG	CHIP-qPCR
ATG41-CHIP7-F	TCTCCCTTCCGGGTAAGCAC	CHIP-qPCR
ATG41-CHIP8-F	GCTCTCCCCCAAAGCTAGTT	CHIP-qPCR
ATG41-CHIP9-F	GTTCTTTCACCAGAGCCAAG	CHIP-qPCR
ATG41-CHIP1-R	TTGGTTGGTTTGGTGTAGCC	CHIP-qPCR
ATG41-CHIP2-R	GGGGGAAGATTCCACAGAGG	CHIP-qPCR
ATG41-CHIP3-R	ACCTTTTTACGCAGAGCCGC	CHIP-qPCR
ATG41-CHIP4-R	GCAATGTGTCATCTTCGCGC	CHIP-qPCR
ATG41-CHIP5-R	TTCTGTAGATTTCCGGACGG	CHIP-qPCR
ATG41-CHIP6-R	AACCCCAAGGGACTTCTTGG	CHIP-qPCR
ATG41-CHIP7-R	CAGGACAGTGGGTATGGTGT	CHIP-qPCR
ATG41-CHIP8-R	GTGCTTACCCGGAAGGGAGA	CHIP-qPCR
ATG41-CHIP9-R	AACTAGCTTTGGGGGAGAGC	CHIP-qPCR
HIS5-F	TGGTATAGTGACGTAGTTAGTGC	CHIP-qPCR
HIS5-R	GAACAGAACTGTGTGCATCC	CHIP-qPCR
TFC1-F	CCCCATCTTTAAGCTCTGCT	CHIP-qPCR, *ATG41* mRNA LEVEL CHECK
TFC1-R	AAGACCAAAAGCGAAGAAGC	CHIP-qPCR, ATG41 mRNA LEVEL CHECK
ATG41_F1	CGAGTACTGAAGACGATTGCAT	*ATG41* mRNA LEVEL CHECK
ATG41_R1	TGCGACATTGGCAAAGGCAT	*ATG41* mRNA LEVEL CHECK
ATG41_F2	GCACGCACACTAAAGATAAGACG	*ATG41* mRNA LEVEL CHECK
ATG41_R2	ACTTGCAAAGGCAAACCCAG	*ATG41* mRNA LEVEL CHECK
ATG41_COF1-P-F	CTTGTTTTATTCTTGAGAAAACCA AACTAAATTGGCTACAGAATTCGA GCTCGTTTAAAC	*COF1* PROMOTER CHANGE

ATG41_COF1-P-R	CTTCATAGCGCGAGATGGGGGAAGATTCCACAGAGGACATCTTCTTTTGTTAGTTTTTTG	*COF1* PROMOTER CHANGE
ATG41-ZEO1-P-F	CTTGTTTTATTCTTGAGAAAACCAAACTAAATTGGCTACAGAATTCGAGCTCGTTTAAAC	*ZEO1* PROMOTER CHANGE
ATG41-ZEO1-P-R	CTTCATAGCGCGAGATGGGGGAAGATTCCACAGAGGACATAATTAATTGATATAAACGTA	*ZEO1* PROMOTER CHANGE
ATG7-F	ATGAGCATTGTCCAGCATGTAG	*ATG7* mRNA LEVEL CHECK
ATG7-R	GACCTCCTGCTTTATGACTGAC	*ATG7* mRNA LEVEL CHECK
ATG9-F	CGTACTAACAGAGTCTTTCCTTG	*ATG9* mRNA LEVEL CHECK
ATG9-R	CTAAGACACCACCCTTATTGAG	*ATG9* mRNA LEVEL CHECK

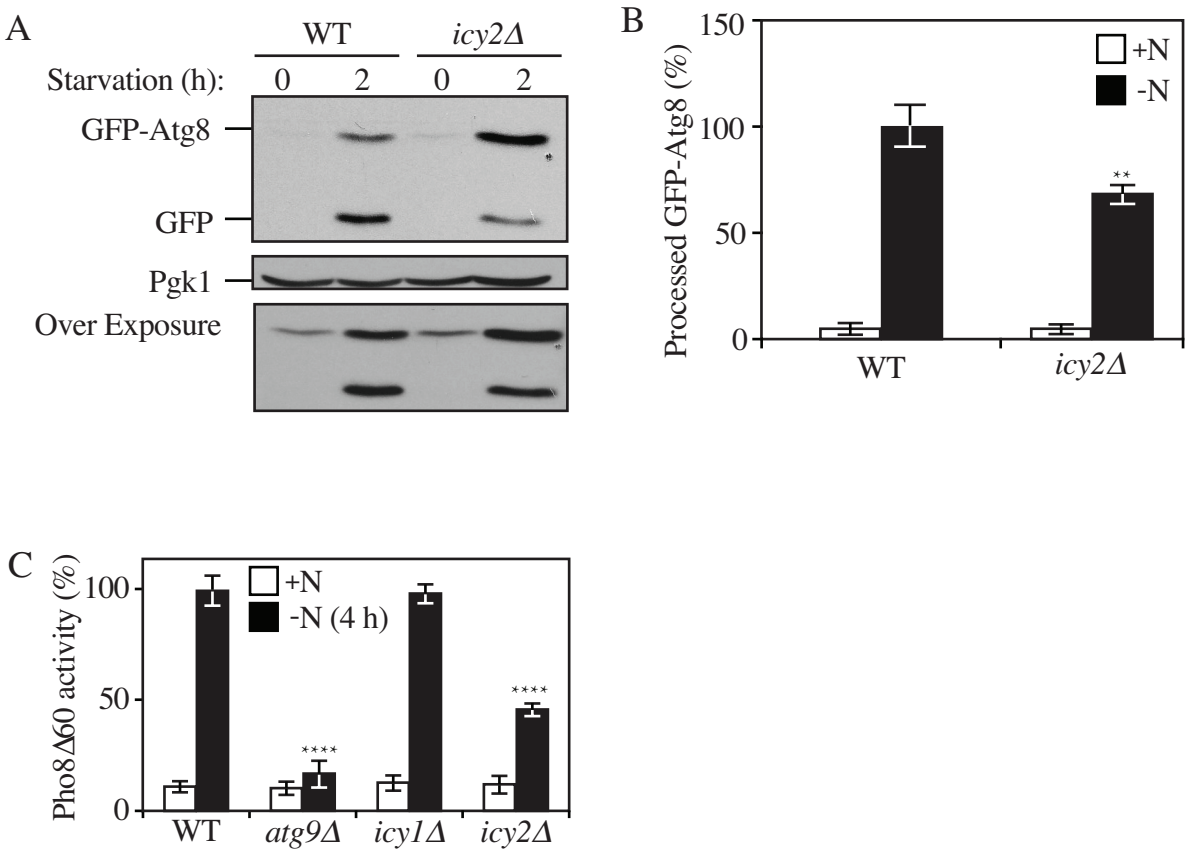

Figure 2.1. Icy2 is required for nonselective autophagy.
(A) GFP-Atg8 processing assay for samples prepared from wild-type (WT; ZYY101) and *icy2Δ* (ZYY102) strains. Both growing samples (0 h; mid-log phase in YPD) and starvation samples (2 h; SD-N medium) were collected. Proteins were resolved by SDS-PAGE and detected by western blot with anti-YFP antibody and anti-Pgk1 (loading control) antiserum. A long exposure of a separate blot is included to show the GFP-Atg8 bands in growing conditions. (B) Quantitative analysis of processed GFP for the experiment in (A) Error bars represent the SD of 3 independent experiments. The result is examined by 2-way analysis of variance (ANOVA). P values derived from the Sidak post test are reported for the comparison between wild type and mutant. **, p<0 .01. (C) Pho8Δ60 assay for the WT (WLY176), *atg9Δ* (ZYY104), *icy1Δ* (ZYY106) and *icy2Δ* (ZYY105) strains. Samples were collected from growing cells (+N; mid-log phase in YPD) and after starvation (-N; SD-N medium). The Pho8Δ60 activity in the WT was set to 100% and the other samples were normalized. The error bars indicate the SD of 3 independent experiments. The result is examined by ANOVA. p values derived from the Sidak post test are reported for the comparison between wild type and mutant. ****, p < 0 .0001.

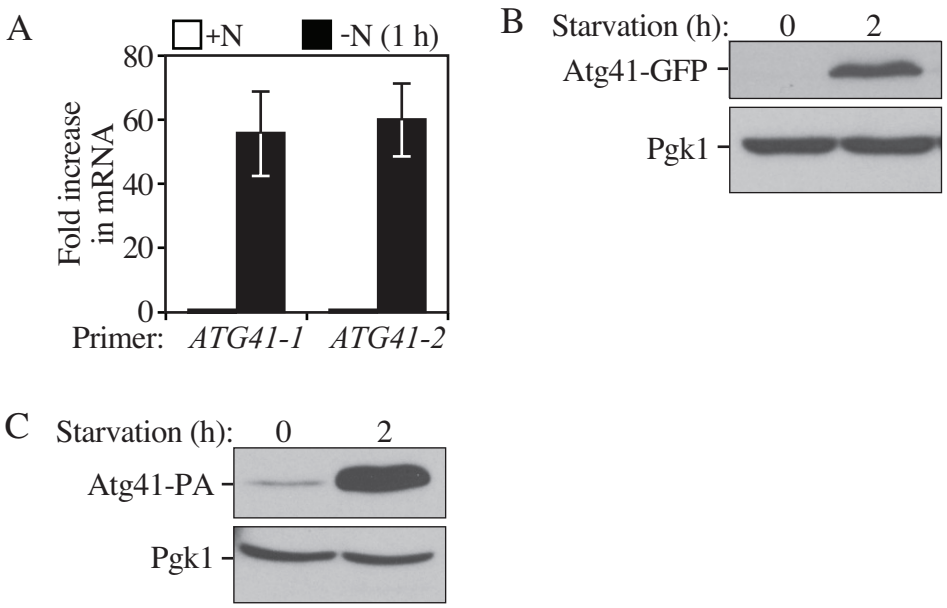

Figure 2.2. The Atg41 expression level increases after autophagy is induced.
(A) The mRNA level of ATG41 was measured by RT-qPCR in the wild-type strain (WT; WLY176) before and after nitrogen starvation with 2 pairs of independent *ATG41* primers. The error bars represent the SD from 3 independent experiments. (B) The protein level of Atg41-GFP was detected by western blot. Both growing (mid-log phase in YPD) and starvation (SD-N medium) samples of Atg41-GFP were collected, protein extracts resolved by SDS-PAGE and blots probed with anti-YFP antibody and anti-Pgk1 (loading control) antiserum. (C) The protein level of Atg41-PA was detected by western blot as described in B.

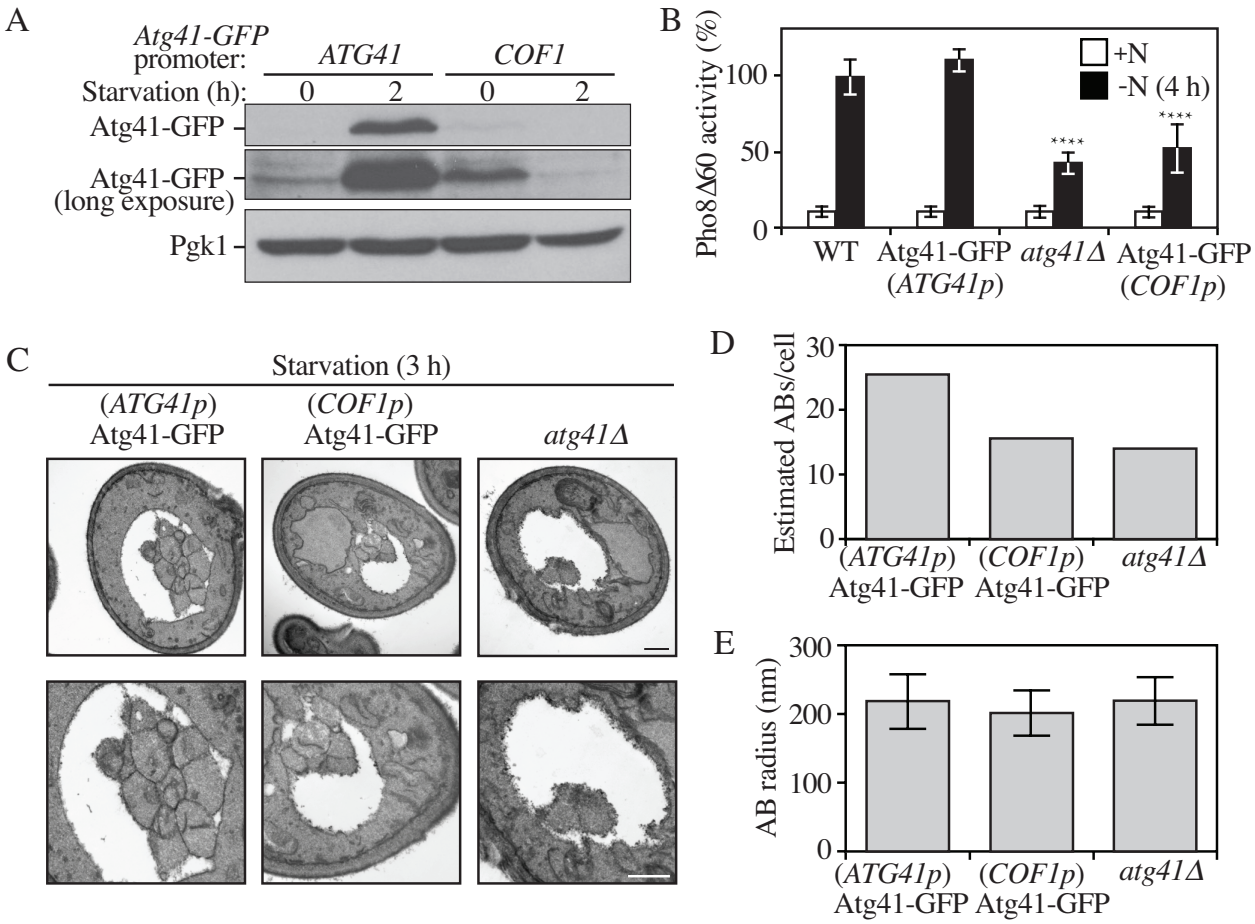

Figure 2.3. The increase in Atg41 protein level is required for autophagy.
(A) The *COF1* promoter was used to clamp Atg41/Icy2 expression at the basal level. Both *ATG41p-ATG41-GFP* (ZYY107) and *COF1p-ATG41-GFP* (ZYY109) cells were collected before and after nitrogen starvation, and protein extracts were analyzed by western blot as in Figure 2.1. A long exposure is shown to visualize Atg41 in growing conditions. (B) Pho8Δ60 assay of *ATG41p-ATG41-GFP* (ZYY107) and *COF1p-ATG41-GFP* (ZYY109). The activity in the wild-type strain (WT; WLY176) was set to 100% and other values were normalized. Error bars represent the SD of 3 independent experiments. The result is examined by 2-way analysis of variance (ANOVA). p values derived from the Sidak post test are reported for the comparison between wild type and mutant. ****, $p < 0.0001$. (C) Representative TEM images of *ATG41p-ATG41-GFP*, *COF1p-ATG41-GFP* and *atg41Δ* cells after starvation (SD-N medium). Autophagic bodies are seen as clustered vesicles in the vacuole lumen, which appears white. The lower panels provide a higher magnification of the cells in the upper panels. Scale bar: 500 nm. (D, E) Estimated average number (D) or average radius (E) of of autophagic bodies per cell for the strains in C. Estimations were based on the number (D) or the radius (E) of autophagic body cross sections observed by TEM in a sample size of more than 100 cells. The error bars indicate SD of the sample cells' radius estimated and calculated by the mathematic algorithm.

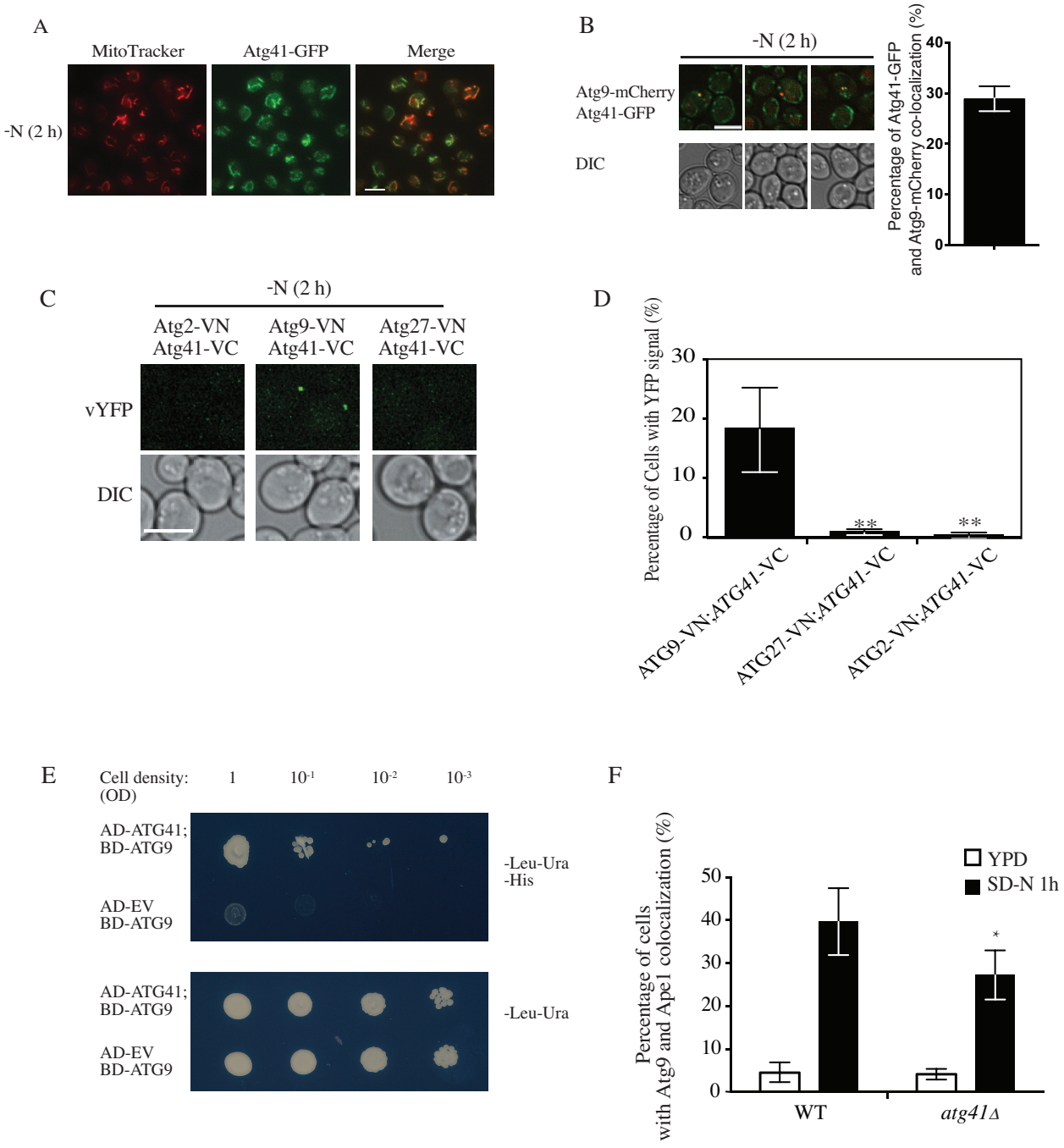

Figure 2.4. Atg41 localizes to peripheral Atg9-containing sites.
(A) Representative images for co-localization of Atg41 and MitoTracker Red. *ATG41-GFP* (ZYY107) cells were grown to mid-log phase and stained with MitoTracker Red in YPD medium. Cells were then washed and shifted to starvation conditions (SD-N) before fluorescence microscopy analysis; images are representative pictures from single Z-sections. Scale bar: 5µm. (B) Representative images and the quantification for Atg41-GFP and Atg9-mCherry (ZYY125) co-localization. Cells were starved in SD-N medium prior to microscopy. Scale bar: 5µm. (C) Representative images for a BiFC assay of strains

expressing Atg41-VC and either Atg2-VN (ZYY114), Atg9-VN (ZYY113) or Atg27-VN (ZYY115). Cells were starved in SD-N medium prior to microscopy. Scale bar: 5μm. (D) Quantitative analysis of cells showing BiFC signals described in (C). The result was examined by 2-way analysis of variance (ANOVA). p values derived from the Sidak post test are reported for the comparisons between ZYY113 and 2 other strains. **, p<0 .01. (E) Images for the yeast 2-hybrid result. The *ATG41-AD* and *AD* empty prey plasmids were co-transformed with the *ATG9-BD* bait plasmid. Cells were grown on SMD –Leu –Ura plates selecting for the presence of both plasmids. Cells were also grown on SMD –Leu –Ura -His plates with 10-fold serial dilution for the selection of strains having protein interactions. (F) Quantitative analysis of Atg9 and prApe1 (PAS) colocalization. WT (SKB171) and mutant (ZYY126) cells were transformed with a plasmid expressing temperature-sensitive Atg1 and cultured at the permissive temperature (24°C) with SMD medium (+N) until the mid-log phase. Samples were then shifted to SD-N and cultured at the nonpermissive temperature (37°C) for 1 h. The co-localization of Atg9–3GFP and RFP-Ape1 were counted and the frequency was determined. The result was examined by ANOVA. P values derived from the Sidak post test are reported for the comparison between wild type and mutant. *, p < 0.05.

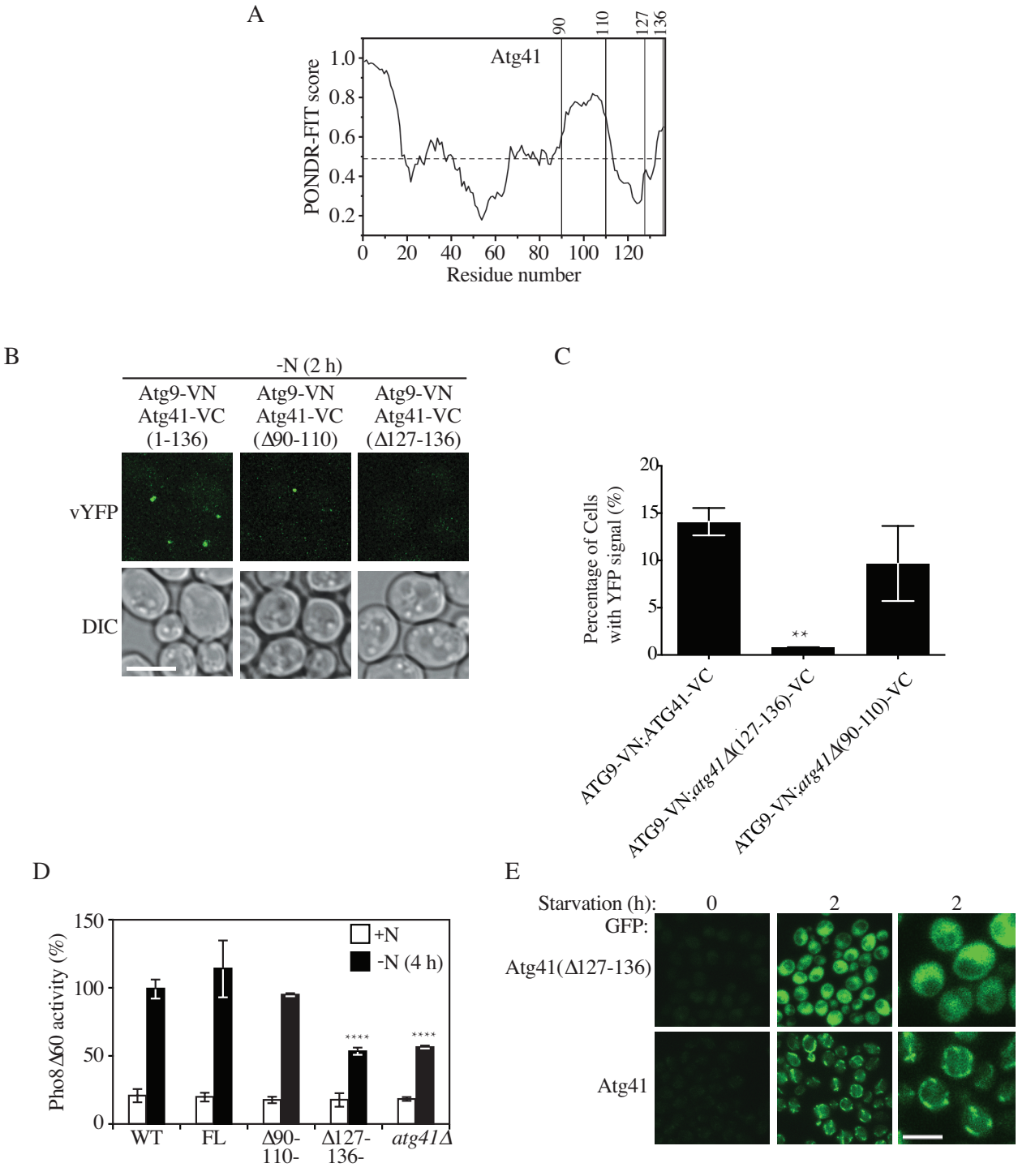

Figure 2.5. The C-terminal region of Atg41 is important for its function in autophagy. (A) Tendency of intrinsic disorder and probability of an Atg41 residue being in a disordered region, predicted by PONDR-FIT. Regions of the protein above the horizontal dashed line are predicted to be disordered. The vertical lines indicate the regions chosen for deletion analysis. (B) Representative images for a BiFC assay of Atg41-VC Atg9-VN cells

expressing full-length (1– 136) Atg41-VC (ZYY113), and deletion mutants Atg41 (*Δ91–110*)-VC (ZYY119) or Atg41 (*Δ127–136*)-VC (ZYY120). Cells were starved in SD-N medium before fluorescence microscopy analysis. Scale bar: 5μm. (C) Quantitative analysis of the BiFC assay described in (B). The result is examined by 2-way analysis of variance (ANOVA). p values derived from the Sidak post test are reported for the comparison between wild type and mutant. **, $p < 0.01$. (D) Representative images showing the distribution of Atg41-GFP (ZYY107) and Atg41 (*Δ127–136*)-GFP (ZYY121) in cells before and after starvation in SD-N medium prior to fluorescence microscopy analysis. The right column of panels corresponds to a higher magnification. Scale bar: 5μm. (E) Pho8Δ60 assay of a wild-type (WT; WLY176) or *atg41Δ* (ZYY105) strain, and strains expressing full-length (FL) Atg41-VC (ZYY116) and the indicated Atg41-VC deletion mutants (ZYY117 and ZYY118). Pho8Δ60 activity was set to 100% in the WT after starvation and normalized in the other samples. Error bar represented the SD of 3 independent experiments. The result is examined by 2-way analysis of variance (ANOVA). p values derived from the Sidak post test are reported for the comparison between wild type and mutant. ****, $p < 0.0001$.

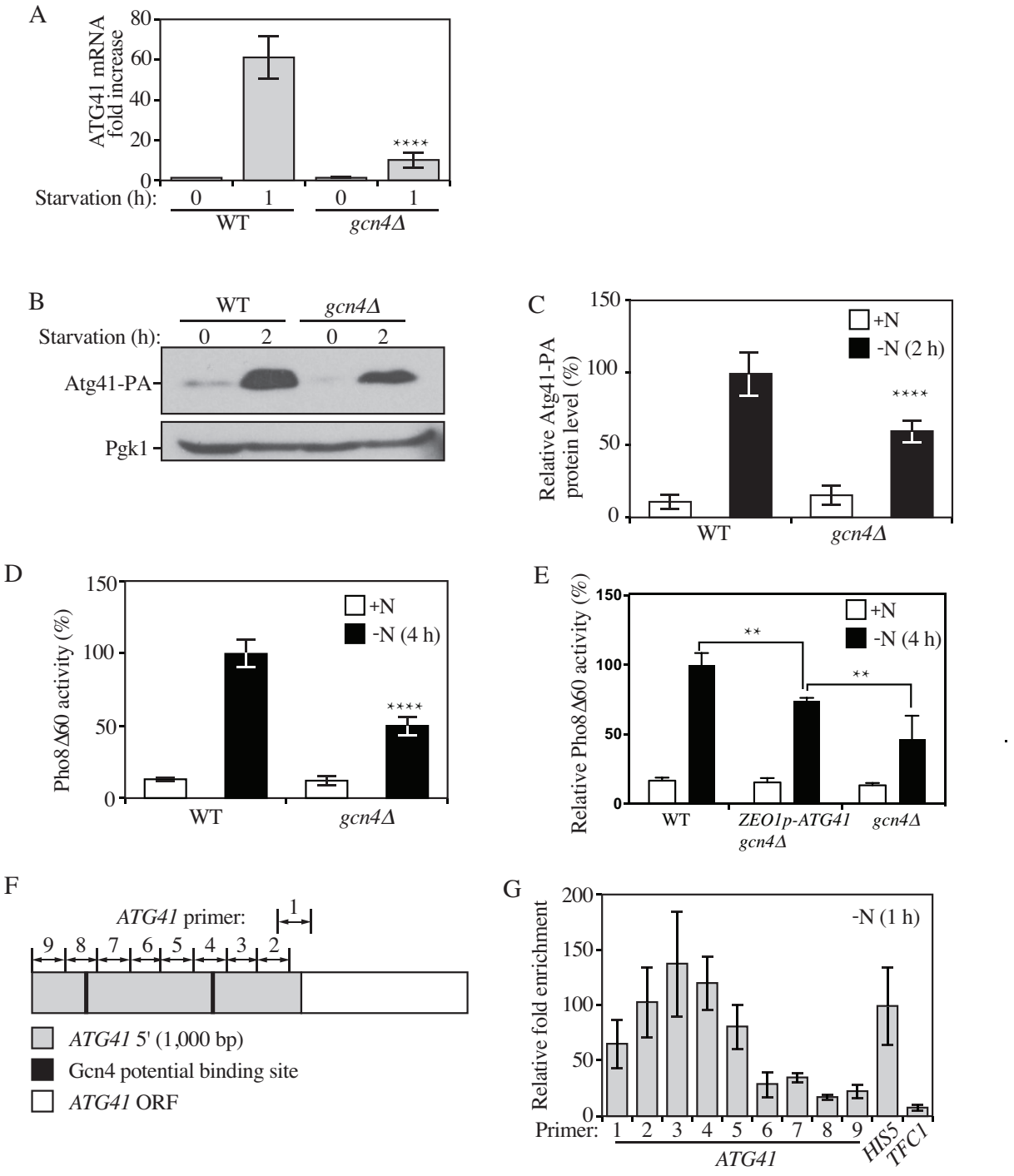

Figure 2.6. Gcn4 activates the transcription of *ATG41* during nitrogen starvation.
(A) The mRNA level of *ATG41* in the wild-type (WT; WLY176) and *gcn4Δ* (ZYY122) strains was measured by RT-qPCR. Samples were collected in both growing (YPD) and starvation (SD-N) conditions. Error bars represent the SD of 3 independent experiments. The result was examined by 2-way analysis of variance (ANOVA). p values derived from the Sidak post test are reported for the comparison between wild type and mutant. ****, p <

0 .0001. (B) The Atg41-PA level of WT (ZYY108) and *gcn4Δ* (ZYY123) strains was analyzed by western blot. Pgk1 served as a loading control. (C) Quantitative analysis of the protein levels from the samples in (B). The protein level in the WT strain in starvation conditions was set to 100% and other samples were normalized. Error bars indicate the SD of 3 independent experiments. The result is examined by ANOVA. P values derived from the Sidak post test are reported for the comparison between wild type and mutant. ****, $p <$ 0 .0001. (D) Pho8Δ60 assay for the WT and *gcn4Δ* strains. Cells were starved in SD-N. Error bars indicate the SD of 3 independent experiments. (E) Pho8Δ60 assay for the WT, *ZEO1p-ATG41 gcn4Δ* (ZYY127) and *gcn4Δ* strains. Cells were starved in SD-N. Error bars indicate the SD of 3 independent experiments. The result is examined by ANOVA. p values derived from the Sidak post test are reported for the comparison between ZYY127 and 2 other strains. **, $p < 0.01$. (F) Schematic picture showing the regions of the *ATG41* 5' UTR covered by the indicated primers for analysis by ChIP; "1" corresponds to the *ATG41–1* primer pair, etc. Gcn4 potential binding sites are shown as black lines. (G) RT-qPCR analysis of ChIP samples of the *GCN4-PA* strain (ZYY124). Numbers correspond to the primers illustrated in (F). The values were normalized to the positive control HIS5 (set to 100%). The error bars indicate the SD of 3 independent experiments.

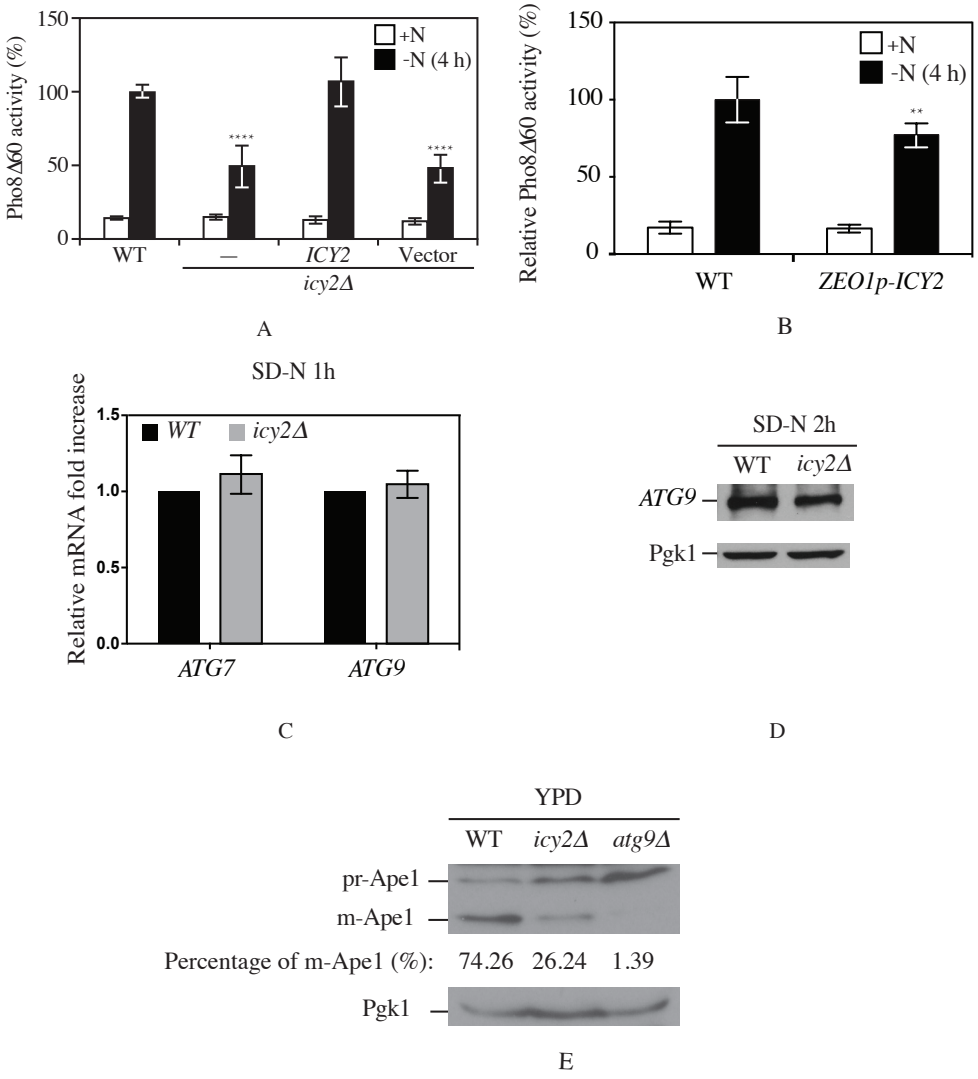

Figure S2.1. Exogenous *ICY2* can restore autophagy activity in the *icy2*Δ strain.
(A) Pho8Δ60 assay of the wild-type strain (WT; WLY176), the *icy2*Δ strain (ZYY105) or the *icy2*Δ strain transformed with a plasmid expressing *ICY2* or the corresponding empty vector. All samples were starved in SD-N. Autophagy activity in the WT was set to 100% and the other samples were normalized. Error bars indicate the SD of 3 independent experiments. (B) Pho8Δ60 assay of the wild-type strain and the *ZEO1p-ICY2* strain (ZYY128). Samples manipulation and data analysis are the same as described in (A). (C) The mRNA level of *ATG7* and *ATG9* was measured by RT-qPCR in the wild-type strain and the *icy2*Δ strain (ZYY102) after 1 h nitrogen starvation. The mRNA level of the WT strain was set to 1.0 and the *icy2*Δ strain was normalized. Error bars indicate the SD of 3 independent experiments. (D) Atg9 protein level after 2 h nitrogen starvation in the wild-type strain and the *icy2*Δ strain (ZYY102) was measured by western blot. Pgk1 served as

the loading control. (E) Precursor Ape1 processing assay of the wild-type, *icy2*Δ (ZYY102) and *atg9*Δ (ZYY104) strains; *atg9*Δ served as a negative control. The quantification was processed by ImageJ, Pgk1 served as the loading control.

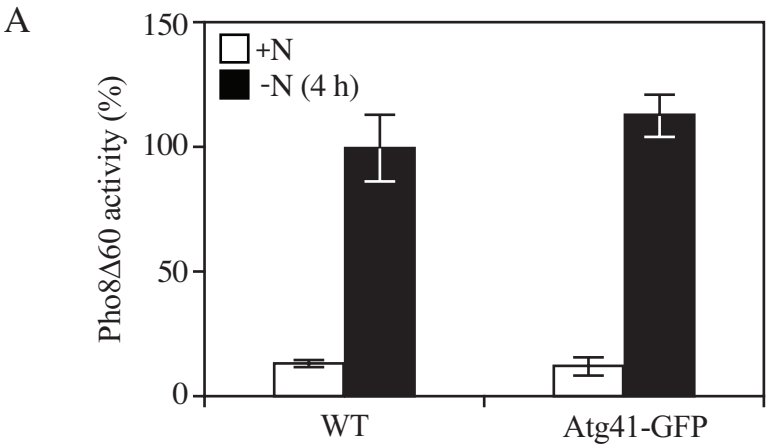
A
150
100
50
0
+N
-N (4 h)
Pho8Δ60 activity (%)
WT
Atg41-GFP

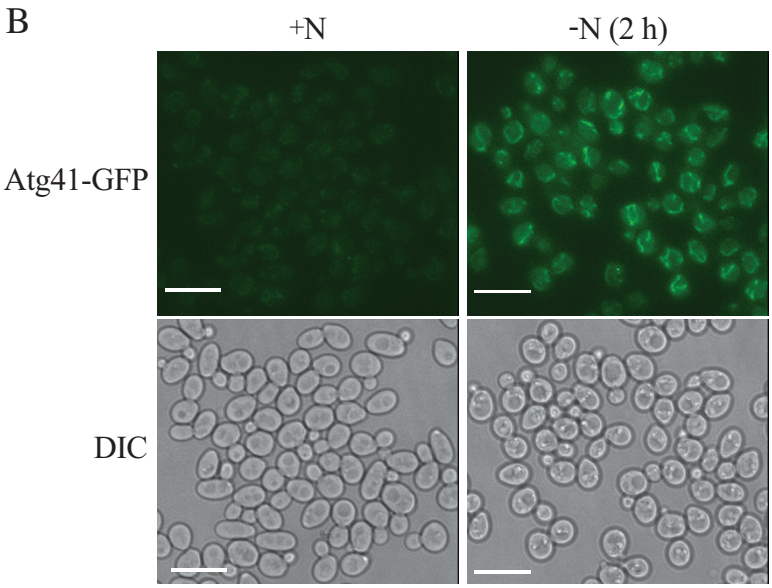
B
+N
-N (2 h)
Atg41-GFP
DIC

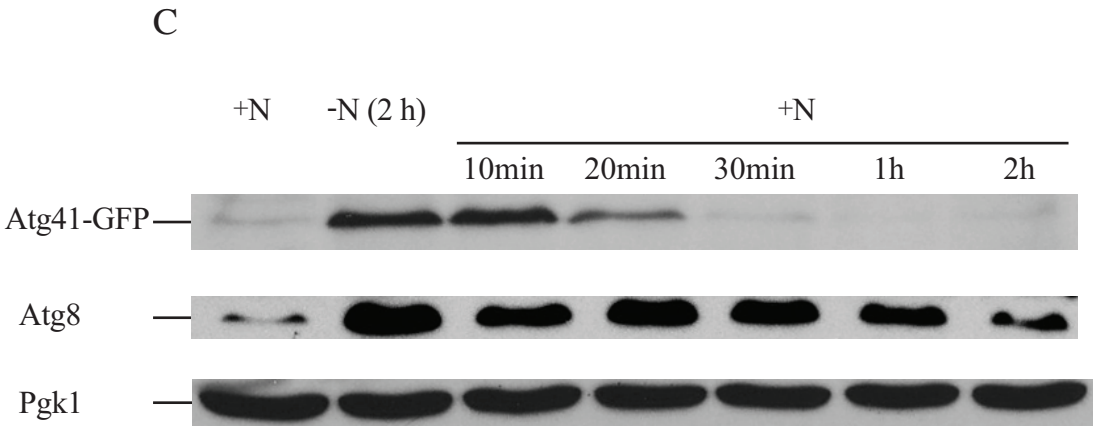
C
+N
-N (2 h)
+N
10min
20min
30min
1h
2h
Atg41-GFP
Atg8
Pgk1

Figure S2.2. The Atg41-GFP chimera is functional and the protein level increases after starvation.

(A) Pho8Δ60 assay of the wild-type (WT; WLY176) and *ATG41-GFP* (ZYY107) strains. Cells were starved in SD-N medium. Autophagy activity was set to 100% for the WT after starvation and other samples were normalized. Error bars indicate the SD of 3 independent experiments. (B) Microscopy analysis of Atg41-GFP fluorescence intensity after starvation. Samples were starved in SD-N. Scale bar: 5μm. (C) Stability of the *Atg41-GFP* protein when shifted from SD-N to nutrient-rich conditions. The protein level of Atg8 is also shown for comparison. Pgk1 served as a loading control.

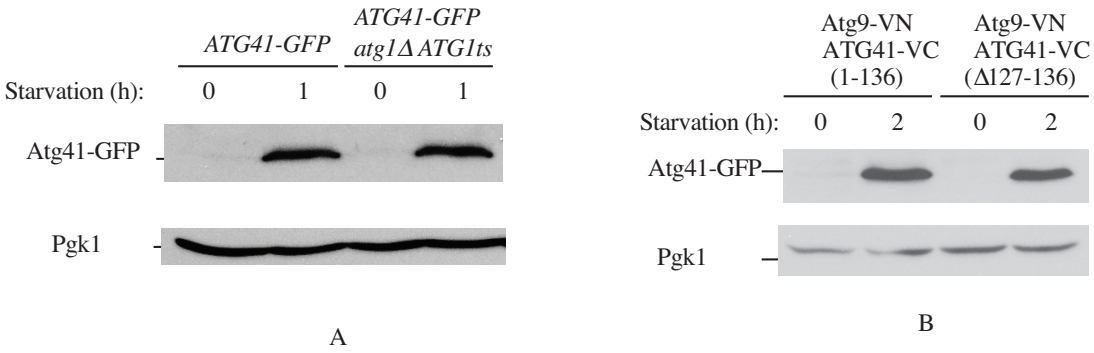

Figure S2.3. Atg41 and the corresponding deletion mutants are stable under nitrogen starvation conditions.

(A) The protein level of Atg41-GFP (ZYY107) and Atg41-GFP in an *atg1*Δ background (ZYY129) transformed with a plasmid expressing Atg1ts was measured before and after starvation. Pgk1 served as a loading control. (B) The protein level of full-length Atg41-VC in the presence of Atg9-VN (ZYY113) and the Δ*127-136* deletion mutant (ZYY120) was measured before and after nitrogen starvation. Pgk1 served as a loading control.

Chapter 3 Dhh1 promotes autophagy-related protein translation and autophagy during nitrogen starvation[3]

3.1. Abstract

Macroautophagy (hereafter autophagy) is a well-conserved cellular process through which cytoplasmic components are delivered to the vacuole/lysosome for degradation and recycling. Studies have revealed the molecular mechanism of transcriptional regulation of autophagy-related (*ATG*) genes upon nutrient deprivation. However, little is known about their translational regulation. Here we found that Dhh1, a DExD/H-box RNA helicase, is required for efficient translation of Atg1 and Atg13, two proteins essential for autophagy induction. Dhh1 directly associates with *ATG1* and *ATG13* mRNAs under nitrogen starvation conditions. The structured regions shortly after the start codons of the two mRNAs are necessary for their regulation by Dhh1. Moreover, Eap1, an EIF4E binding protein, physically interacts with Dhh1 to facilitate the delivery of the Dhh1-*ATG* mRNA complex to the translation initiation machinery. These results suggest a model for how some *ATG* genes bypass the general translational suppression that occurs during nitrogen starvation to maintain a proper level of autophagy.

---

[3] This chapter is reprinted partly from the manuscript X Liu*, Z Yao*, M Jin*, DJ Klionsky. Dhh1 promotes autophagy-related protein translation and autophagy during nitrogen starvation, with some modifications.

3.2. Introduction

Autophagy is a tightly controlled cellular process by which cytosolic proteins, protein aggregates, damaged or surplus organelles and invading pathogens are sequestered within a double-membrane vesicle (the autophagosome), then delivered to the vacuole/lysosome for degradation and recycling [1, 2]. Autophagy is highly conserved among eukaryotes. Malfunction of autophagy has been related to many human diseases, including cancer, myopathies, liver, heart and lung disease and neurodegeneration [3-6].

Studies in yeasts have identified more than 40 autophagy-related (*ATG*) genes involved in mediating autophagy [7]. Many of the corresponding gene products have homologs or functional counterparts in higher eukaryotes [2]. The expression levels of *ATG* genes are important for maintaining proper levels of autophagy activity [8, 9]. Expression of most *ATG* genes is upregulated under autophagy-inducing conditions such as nutrient deprivation [10]. The transcriptional regulation of *ATG* genes has been extensively investigated, and an increasing number of transcriptional activators and repressors involved in autophagy regulation are being characterized in both yeast and mammals [8, 10-14].

Two recent studies from our lab and collaborators showed that under nutrient-rich conditions *ATG* mRNAs are post-transciptionally regulated [15]. The main mRNA decapping enzyme, Dcp2, mediates the decapping of almost all major *ATG* mRNAs, while the RNA exoribonuclease, Xrn1, is responsible for the degradation of some of them. A subset of *ATG* mRNAs, especially *ATG8* mRNA, is conveyed to the decapping machinery by Dhh1, a DExD/H-box RNA helicase. These studies demonstrated that *ATG* mRNAs are post-transciptionally downregulated by decapping-mediated mRNA decay, so that their

expression is restricted to maintain autophagy activity at a basal level under nutrient-rich conditions.

However, it is not well known whether and how the expression of *ATG* genes is regulated post-transcriptionally and translationally when nutrients are limited. Under nutrient-deprivation conditions the translation of most genes across the genome is downregulated, while expression of most *ATG* genes are upregulated and maintained at relatively high levels to support the increased demands of autophagy activity. This suggests that there is likely to be a specialized post-transcriptional regulation mechanism, through which the *ATG* mRNAs escape the general translation inhibition when nutrients are depleted; conditions under which autophagy becomes essential.

In this study, we found that Dhh1 facilitates translation of *ATG1* and *ATG13* mRNAs under nitrogen starvation conditions, in contrast to its role as an autophagy inhibitor when nutrients are rich. Under nitrogen starvation, Dhh1 directly associates with *ATG1* and *ATG13* mRNAs, and it binds to *ATG1* mRNA through its 3'-untranslated region (UTR). The structured regions shortly after the start codons of *ATG1* and *ATG13* mRNAs are indispensible for the regulation by Dhh1. Moreover, Dhh1 interacts with an EIF4E binding protein, Eap1, which facilitates the delivery of *ATG1* and *ATG13* mRNAs to the translation initiation machinery. This mechanism acts to help Atg1 and Atg13 bypass the general translation repression after nitrogen starvation, to support the increased demand for autophagy activity.

3.3. Result

3.3.1 Dhh1 positively regulates autophay under nitrogen starvation conditions

The DExD/H-box-containing RCK family RNA helicases are highly conserved in eukaryotes [16]. These proteins play important roles in regulating mRNA degradation, storage, and translation. Recently others and we have shown that under nutrient-rich conditions Dhh1, a DExD/H-box protein, targets several *ATG* mRNAs, most significantly *ATG8* mRNA, for degradation through the Dcp2-mediated mRNA decapping pathway to restrict autophagy activity [15]. Consistently, deletion of the *DHH1* gene in yeast cells led to elevated *ATG8* expression and autophagy activity levels under both nutrient-rich and short-term nitrogen starvation conditions (Figure 3.1A). The *dhh1*Δ cells also displayed much lower viability compared to the wild-type cells after three days of nitrogen starvation (Figure 3.1B). However, we noticed that after longer periods of starvation, the Atg8 protein level and the autophagy activity in the *dhh1*Δ cells was not significantly different from that of wild-type cells, suggesting that the inhibitory effects of Dhh1 on *ATG8* expression and autophagy were released after prolonged nitrogen starvation (Figure 3.1A).

An obvious question then is what contributes to the significant lower viability of the *dhh1*Δ cells after prolonged nitrogen starvation, and does autophagy still play a role? To answer this, we needed to test autophagy activity in the *dhh1*Δ cells under conditions the prolonged nitrogen starvation. However, the commonly used autophagy flux assays in yeast [17], such as the GFP-Atg8 processing and Pho8Δ60 assays, are not suitable for this purpose, because the autophagy activity in the wild-type cells tested with these assays usually becomes saturated after 4 to 6 h of nitrogen starvation. Thus we developed a Pgi1-GFP processing assay to quantitatively monitor autophagy activity during prolonged nitrogen starvation. Pgi1 is a glycolytic long-lived cytosolic protein, which has a stable expression even upon prolonged nitrogen starvation conditions. As with most cytosolic proteins, we expect that,

upon starvation, the cytosolic Pgi1-GFP fusion protein is delivered to the vacuole for degradation through nonselective autophagy. The GFP moiety is relatively resistant to vacuolar degradation [18]; thus, consistent with our prediction, we observed an accumulation of the free GFP band in the wild-type cell lysates by western blot after autophagy induction (Figure 3.1C). There was no processing of Pgi1-GFP in *atg1*Δ cells that are defective for autophagy, demonstrating that the generation of free GFP was dependent on autophagic degradation of the chimera. In the *dhh1*Δ cells a substantially reduced amount of free GFP was detected after nitrogen starvation compared to the wild-type cells, suggesting autophagy was impaired in this mutant (Figure 3.1C). Similar results were observed when we examined the processing of another long-lived cytosolic fusion protein, Fba1-GFP (Figure S3.1). In sum, our observations suggest that Dhh1 is a bidirectional regulator of autophagy, whose role is controlled by nutrient conditions. Dhh1 acts as a negative regulator to direct some *ATG* mRNAs for degradation under nutrient-rich conditions. Here, our data imply a newly discovered role for Dhh1 to positively regulate autophagy under nitrogen starvation conditions.

3.3.2 Dhh1 promotes the translation of Atg1 and Atg13

The next question we would like to answer is how Dhh1 promotes autophagy during nitrogen starvation. Our previous analysis indicated that the levels of most *ATG* mRNAs in the *dhh1*Δ cells are similar to that in wild-type cells after 1 h starvation [15]; thus, it is less likely that Dhh1 regulates *ATG* mRNA stability under this condition. A recent genome-wide study suggested that Dhh1 is able to both suppress and promote mRNA translation [20]. However, this study was performed under nutrient-rich conditions when autophagy is not induced and it did not identify *ATG* mRNAs within the core autophagy molecular

machinery being directly translationally regulated by Dhh1. Accordingly, we specifically asked whether Dhh1 regulates mRNA translation under nitrogen starvation conditions, and if any *ATG* mRNAs are targets of Dhh1. The previous study [20] suggested that a feature of the mRNAs translationally activated by Dhh1 is that the nucleotides 50–120 after the start codons of these mRNAs show a high intrinsic tendency to form secondary structures. We used SPARCS (Structural Profile Assignment of RNA Coding Sequences) [21], a program to analyze structured regions in mRNA coding sequences, to predict if any of the *ATG* mRNAs are potential targets of Dhh1. Out of the 18 *ATG* mRNAs that comprise the core autophagy molecular machinery analyzed, only *ATG1*, *ATG6,* and *ATG13* mRNAs showed potential structured regions longer than 30 base pairs (bps) in the open reading frames (ORFs) shortly after the start codons (data not shown). Atg1 and Atg13 are the main components of a kinase complex essential for the autophagy process. In addition, the expression of the two proteins is highly induced after nitrogen starvation. Therefore, we decided to focus on investigating whether and how Dhh1 regulates Atg1 and Atg13 translation under autophagy-inducing conditions.

To test whether *ATG1* and *ATG13* mRNAs are bona fide targets of Dhh1, we first checked *ATG1* and *ATG13* expression when the *DHH1* gene is deleted. The Atg1 and Atg13-PA protein levels were substantially decreased in the *dhh1*Δ cells compare to the wild-type cells after 6 h nitrogen starvation (Figure 3.2A and 3.2B). Under nutrient-rich conditions, a higher Atg1 protein level was observed in the *dhh1*Δ cells compared to wild-type cells, consistent with the suggested role of Dhh1 in promoting decapping of some *ATG* mRNAs in this condition [15] (Figure 3.2A). By quantitative reverse transcription PCR (RT-qPCR), we found that there were no significant reductions in the *ATG1* and *ATG13* mRNA levels with

the deletion of *DHH1* under starvation conditions (Figure 3.2C). As a control, we also tested *ATG2* expression in the *dhh1*Δ cells and found that neither *ATG2* mRNA nor Atg2 protein level were decreased in the mutant compared to the wild-type cells under nitrogen starvation conditions (Figure S3.2). Taken together, these data suggest that Dhh1 promotes Atg1 and Atg13 translation during prolonged nitrogen starvation.

3.3.3 The structured regions in *ATG1* and *ATG13* ORFs are necessary for the translational regulation by Dhh1

Next, we further investigated whether the structured regions shortly after the start codons of *ATG1* and *ATG13* mRNAs are required for the regulation by Dhh1. We constructed plasmids expressing either $Atg1^{WT}$ or $Atg13^{WT}$-PA, or their mutant versions by changing the third base of the codons within the structured regions to make them unstructured without modifying the amino acid sequence (Figure 3.3A). These plasmids were integrated into the *atg1*Δ or *atg13*Δ cells, respectively. Subsequently, the *DHH1* gene was deleted in these strain backgrounds. In the cells expressing $Atg1^{WT}$ or $Atg13^{WT}$-PA, depletion of *DHH1* caused substantial decrease of the protein levels after nitrogen starvation (Figure 3.3B and 3.3C). In contrast, the $Atg1^{mut}$ and $Atg13^{mut}$-PA protein levels were not significantly affected by knocking out *DHH1* (Figure 3.3B and 3.3C). These results suggest that the structured region shortly after the start codons of *ATG1* and *ATG13* mRNAs are necessary for the translational regulation by Dhh1.

3.3.4 Dhh1 associates with *ATG1* and *ATG13* mRNAs

To further test our hypothesis that Dhh1 regulates Atg1 and Atg13 translation, we examined whether Dhh1 associates with these two mRNAs. The RNA immunoprecipitation assay has been utilized to investigate protein-RNA interactions (Figure 3.4A) [24]. We

immunoprecipitated Dhh1-PA with IgG-conjugated Sepharose beads from lysates prepared from cells starved for nitrogen. As a control, nitrogen-starved lysates from cells in which Dhh1 was not tagged were subjected to the same procedures in parallel. Subsequently, the affinity-isolated RNA fragments were analyzed by RT-qPCR. Through this approach, we found that, relative to the control group, significantly more *ATG1* and *ATG13* mRNA fragments were precipitated with Dhh1-PA (Figure 3.4B and 3.4C). In addition, Dhh1-PA showed a higher enrichment at both the 5'-UTR and the 3'-UTR regions of *ATG1* and *ATG13* mRNAs. This latter finding suggests that the captured *ATG1* and *ATG13* mRNAs are more likely in the "closed-loop" form (Figure 3.4B and 3.4C), which is suggested to be a feature of mRNAs that are actively being translated [25].

When we swapped the endogenous 3'-UTR of *ATG1* with that of the *ADH1* gene, making an *ATG1-ADH1*$^{3'UTR}$ mRNA, Dhh1-PA was not able to efficiently associate with the mRNA based on the RNA immunoprecipitation assay (Figure 3.4D). In addition, Dhh1-PA also did not show higher enrichment at the 5'-UTR of the mRNA, even though this region was endogenous. This result implies that the 3'-UTR was very likely the region bound by Dhh1. Moreover, deletion of the *DHH1* gene in the *ATG1-ADH1*$^{3'UTR}$ mRNA background did not result in a significant decrease in the Atg1 protein level compared to the control cells (Figure 3.4E). These results collectively suggest that Dhh1 is very likely to bind *ATG1* mRNAs through the 3'-UTR region to regulate its translation.

The residues in Dhh1 that are important for its RNA binding have been identified previously. For example, the Dhh1^{H369A} and Dhh1^{R370A} mutants bind RNAs less efficiently both in vitro and in yeast cells [26]. To further demonstrate that RNA binding of Dhh1 is required for its role in regulating *ATG* translation and autophagy, we generated a yeast

strain which stably expresses the Dhh1^{H369A,R370A}-PA mutant (Figure 3.4F). After nitrogen starvation the Atg1 protein level in the mutant cells was significantly lower than that in the cells expressing Dhh1^{WT}-PA (Figure 3.4F). The autophagy activity was also diminished in the Dhh1^{H369A,R370A}-PA mutant cells tested by the Pgi1-GFP processing assay (Figure 3.4G). Therefore, we conclude that Dhh1 binds to *ATG1* and *ATG13* mRNAs, and that the RNA binding is necessary for its role in promoting their translation and autophagy under nitrogen starvation conditions.

3.3.5 Eap1 interacts with Dhh1 and facilitates Atg1 and Atg13 translation during nitrogen starvation

In eukaryotic cells, translation occurs mostly in a cap-dependent manner, which requires the formation of the EIF4F complex, including EIF4A, EIF4E and EIF4G on the 5'-UTR of mRNAs. EIF4G, the scaffold for the complex, interacts with EIF4E, which directly binds to the 5' mRNA cap [27]. Dhh1 has recently been shown to associate with the translation initiation machinery [20], but it is not known whether Dhh1 directly binds to the translation initiation complex, nor it is clear how the association is regulated.

Eap1 is an EIF4E binding protein (EIF4EBP). Although EIF4EBPs generally inhibit translation through competing with EIF4G to bind EIF4E [27], they were recently shown to play positive roles in the translation of some mRNAs in breast cancer cells under hypoxic conditions [28]. In addition, *Thor/4E-BP1* null flies are more sensitive to starvation compared to wild-type flies [29]. These studies indicate that EIF4EBPs may function positively on certain mRNAs under specific conditions. Moreover, in yeast, Eap1 physically interacts with Dhh1 when nutrients are rich [30], leading us to propose that Eap1 also plays a role in regulating *ATG* mRNA translation by modulating the interaction between Dhh1

and the translation initiation machinery. First, we examined whether Eap1 interacts with Dhh1 under nitrogen starvation conditions. We immunoprecipitated Eap1-PA with IgG-conjugated Sepharose beads from lysates of cells subjected to nitrogen starvation. The Dhh1-3HA protein was affinity isolated together with Eap1-PA (Figure 3.5A). As a control, when the immunoprecipitation was performed with lysates from cells in which Eap1 was not tagged to PA, Dhh1-3HA was not co-precipitated. These results demonstrate that Dhh1 interacts with Eap1 under nitrogen starvation conditions.

Next we deleted the *EAP1* gene and checked its effects on *ATG1* and *ATG13* expression and autophagy activity. We observed lower Atg1 and Atg13-PA protein levels in the *eap1*Δ cells compared to the wild-type cells (Figure 3.5B and 3.5C), even though the *ATG1* and *ATG13* mRNA levels were not significantly affected (Figure 3.5D). Autophagy activity was also compromised in the *eap1*Δ cells based on the Pgi1-GFP processing assay (Figure 3.5E). These results imply that Eap1 promotes Atg1 and Atg13 translation and autophagy under nutrient depletion conditions possibly by facilitating the association of Dhh1 with the translation initiation machinery.

3.4. Discussion

The DExD/H-box RNA helicases, Dhh1 and its Vad1 homolog in *Cryptococcus neoformans*, have been shown to bind some *ATG* mRNAs and direct them to the decapping enzyme Dcp2 for degradation under nutrient-rich conditions, maintaining autophagy at a basal level [15]. When autophagy is induced by nutrient deprivation, inhibition of TOR leads to the loss of Dcp2 phosphorylation and a subsequent decrease in decapping activity. However, Vad1 or Dhh1 still show binding affinity towards some *ATG* mRNAs after nutrient deprivation, though to a lesser extent than that seen in nutrient-rich conditions [15]. Because

the *ATG* mRNA levels in the *dhh1*Δ cells are similar to that in wild-type cells, the binding of Dhh1 to the *ATG* mRNAs may not be related to mRNA stability. Here we found that Dhh1 promotes autophagy by targeting *ATG1* and *ATG13* mRNAs to the translation initiation machinery after nutrient deprivation, revealing the bidirectional roles of Dhh1 in regulating autophagy. These observations also suggest that Dhh1 is able to deliver mRNAs to different RNA processing machineries, resulting in distinct fates of the mRNAs.

What are the factors determining the outcomes of these mRNAs? Our analysis implicates that elements within the mRNAs are important. When the structured regions shortly after the start codons of *ATG1* and *ATG13* mRNAs were mutated to be unstructured or disordered, translation of the mRNAs were no longer promoted by Dhh1. The regions that Dhh1 binds to may also contribute to determining their fates. It was reported that DDX6, a DEAD box helicase protein in human cells, binds to the 3'-UTR in the mRNAs of positive regulators of proliferation/self-renewal such as *CDC1* and *EZH2*, to facilitate their translation in epidermal progenitor cells [31]. In contrast, DDX6 binds to the 5'-UTR of *KLF4*, which encodes a differentiation-inducing transcription factor to mediate its degradation through the decapping pathway. Therefore, some intrinsic feature(s) inside the regions Dhh1 binds to may also be critical for deciding what to do with the bound mRNAs. Conversely, regulation of interactions between Dhh1 and the different RNA function machineries may also be indispensible, though this is largely unexplored. Is it possible that post-translational modifications of Dhh1 are involved? Does the binding to mRNAs induce different conformational changes of Dhh1 that favor distinct protein-protein interactions?

Cap-dependent translation initiation requires formation of an EIF4F complex on mRNAs. The EIF4F complex is composed of three major components: EIF4A, EIF4E and EIF4G

[32]. EIF4EBPs inhibit translation initiation by competing with EIF4G to bind EIF4E [33]. TOR, an autophagy inhibitor, positively regulates cap-dependent translation by allowing the replacement of EIF4EBPs with EIF4G under nutrient-rich conditions [27]. Upon nutrient deprivation, TOR is inhibited, resulting in translational repression of ~98% of the cellular genes. This is partly due to dephosphorylation and activation of EIF4EBPs upon TOR inhibition, which in turn suppresses the complex formation between EIF4G and EIF4E [27, 34]. However, Eap1, a yeast EIF4EBP, counterintuitively promotes *ATG1* and *ATG13* mRNA translation under starvation conditions. Eap1 has a unique long C-terminal domain that is absent in its mammalian homologs. This domain may distinguish Eap1 as a positive regulator of *ATG1* and *ATG13* mRNAs. It would be interesting to identify the functional counterpart of the C-terminal part of Eap1 in higher eukaryotes. It is possible that the domain's function is executed by some unexplored protein(s) in mammals.

Eap1 was reported to physically interact with Dhh1, coordinating with the decapping complex to degrade the translationally suppressed mRNAs under nutrient-rich conditions [30]. However, the Eap1-Dhh1 complex facilitates the translation of *ATG1* and *ATG13* mRNAs upon nutrient deprivation. Nonetheless, the signaling that controls the switch of roles is unknown. It is very likely that the phosphorylation regulation of Eap1 by TOR and/or other kinases plays a role.

In summary, our study showed how *ATG1* and *ATG13* mRNA translation, which is crucial for maintaining autophagy activity and cell viability, is promoted under prolonged conditions of nitrogen starvation where general translation is inhibited. The future studies on the questions raised from this discovery will shed more light on how *ATG* genes are post-transcriptionally and translationally regulated.

3.5. Materials and Methods

3.5.1 Yeast strains, media and growth conditions

Yeast strains used in this study are listed in Table S1. For nutrient-rich conditions, yeast cells were grown in YPD medium (1% yeast extract, 2% peptone, 2% glucose). For nitrogen starvation, cells were cultured in SD-N medium (0.17% yeast nitrogen base without ammonium sulfate or amino acids, 2% glucose).

3.5.2 Plasmids

The pRS-*ATG1*(406) was made by a two-step cloning. The DNA fragments containing either 1000 bps upstream of the start codon together with the ORF of the *ATG1* gene, or 1000 bps downstream of the *ATG1* ORF were amplified by PCR from wild-type yeast genomic DNA. The fragments were then ligated into the KpnI and XhoI sites, and the XhoI and XmaI sites of the pRS406 vector, resulting in the pRS-*ATG1*(406) plasmid, based on which the pRS-*ATG1*^{mut}(406) contruct was made by site-directed mutagenesis.

The pRS-*ATG13-PA*(406) plasmid was made by fast cloning [35]. The DNA fragment containing 600 bps upstream of the start codon of *ATG13*, the ORF encoding *ATG13-PA*, and 423 bps downstream of the *ATG13* ORF, was amplified by PCR from the genomic DNA of a yeast strain where *ATG13* gene was C-terminal tagged with one copy of PA followed by the *ATG13* endogenous 3'-UTR. The fragment was inserted into the pRS406 vector by fast cloning as described previously [35]. The insertion takes place between EcoRI and BamHI sites. The pRS-*ATG13*^{mut}*-PA*(406) plasmid was made by site-directed mutagenesis based on the pRS-*ATG13-PA*(406) plasmid.

The pRS-*DHH1-PA*(405) plasmid was constructed by inserting a fragment containing the 675 bps upstream of the *DHH1* ORF, the *DHH1* ORF, the sequence encoding two tandem

repeats of PA, and the *ADH1* terminator into the XhoI and SpeI sites of pRS(405). This fragment was amplified by PCR from the genomic DNA of a yeast strain in which the *DHH1* gene was tagged with two tandem repeats of PA followed by the *ADH1* terminator. The pRS-*DHH1*(405) plasmid was made by deletion of the sequence encoding the two tandem repeats of PA in the pRS-*DHH1-PA*(405) plasmid via site-directed mutagenesis. The pRS-*DHH1*^{D195AE196A}-*PA*(405) and pRS-*DHH1*^{E196Q}-*PA*(405) plasmids were also made by site-directed mutagenesis based on pRS-*DHH1-PA*(405).

3.5.3 RNA immunoprecipitation assay

The RNA immunoprecipitation assay was adapted from the protocol described previously [24]. Dhh1-PA and Dhh1 untagged cells were cultured to mid-log phase in YPD and then were starved for 2 h in SD-N medium. The starved cells were subjected to cross-linking by 0.8% formaldehyde for 10 min before being harvested. The cross-linking was stopped by the addition of glycine. After washing with PBS, the samples were resuspended in FA lysis buffer (50 mM HEPES, pH 7.5, 150 mM NaCl, 1mM EDTA, 1% Triton X-100, 0.1% sodium deoxycholate, 0.1 % SDS). Before vortexing with glass beads to lyse the cells, PMSF (to 5 mM final concentration), 1 tablet of protease inhibitor cocktail (Roche) and RNasin® PLUS RNase inhibitor (Promega) were added into the buffer. The lysates were collected and sonicated at 4ºC with three rounds of 15-sec pulses with 45% amplitude. After centrifugation at 10000×g for 5 mins, the supernatants were recovered. An aliquot of each sample was stored in -80ºC as inputs for later use. The rest of the supernatants were incubated with IgG Sepharose™ beads (GE healthcare Life Sciences) overnight at 4ºC. IP fractions were washed with FA lysis buffer several times and one time with TE buffer (10 mM Tris-HCl, pH 7.5, 1 mM EDTA). Then the proteins and RNAs were eluted in RIP

elution buffer (50 mM Tris-HCl, pH 7.5, 10 mM EDTA, 1% SDS) with RNase inhibitor at 70ºC for 10 min. The IP elution and input samples were reverse cross-lined by incubation with proteinase K for 1 h at 42ºC, followed by 1 h at 65ºC. The RNAs in these samples were then recovered with acid-phenol:chloroform (pH=4.5) and subsequent ethanol precipitation. Glycogen (20 μg) was added to the samples to facilitate RNA precipitation. The pellets were washed with 70% ethanol and dried. The samples were next treated with the TURBO DNA free kit (Thermo Fisher Scientific) to remove residual DNA. The RNA samples were then subjected to analysis by RT-qPCR.

3.5.4 RT-qPCR

Yeast cells were cultured in YPD medium to mid-log phase. An aliquot was collected as the nutrient-rich sample. The other aliquot was shifted to SD-N medium for 6 h before the cells were collected. The total RNA for each sample was isolated using the RNeasy mini kit (Qiagen). One microgram of total RNA was subjected to reverse-transcription using the High Capacity cDNA Reverse Transcription Kit (Applied Biosystems). To analyze the cDNA levels, real-time PCR was performed with Power SYBR Green master mix (Applied Biosystems). The gene-specific primers for *ATG1, ATG2, ATG13,* and the reference gene *TAF10* are listed in a previous study [15].

The primers used for the RT-qPCR analysis for the RNA immunoprecipitation assays are listed in the supplemental materials.

3.5.5 Protein-protein co-immunoprecipitation assay

Yeast cells were cultured in YPD medium to mid-log phase. The cells were washed with sterile water one time before they were shifted to SD-N medium for 2 h starvation. Cells (50 OD units) for each sample were harvested and washed once with ice cold PBS. Cells were

lysed by vortexing them with glass beads in lysis buffer (10×PBS, 200 mM sorbitol, 1 mM MgCl2, 1% Tween 20, 1 mM DTT, 1 mM PMSF, protease inhibitor cocktail [Roche Diagnostic, 1 tablet for 500 µl solution]) at 4 °C. After spinning down the cell debris, 50 µl of the supernatant of each sample was saved as total lysate and 500 µl of the supernatant was subjected to immunoprecipitation. For total lysate, proteins were precipitated by adding 1 ml 10% TCA and the samples were kept on ice for 30 min before centrifugation. The pellets were washed with acetone once and then air dried. Next, 50 µl MURB (50 mM NaH_2PO_4, pH 7.0, 2.5 mM MES, pH 7.0, 1% SDS, 3 M Urea, 0.5% β-mercaptoethanol, 1 mM NaN_3, 0.2 mg/µl bromophenol blue) was added before the samples were heated at 55°C for 15 min. For immunoprecipitation, 40 µl IgG sepharose beads (GE healthcare Life Sciences) were prepared for each sample by washing them with IP buffer (10×PBS, 200 mM sorbitol, 1 mM $MgCl_2$, 1% Tween 20) 3 times. Supernatant (500 µl) was added to the beads. The total volume of each sample was made to 1 ml with IP buffer. The samples were incubated at 4°C on a shaker for 2 h. The IgG beads were then collected by centrifugation and washed 6 times with IP buffer. After the washing, 50 µl of MURB was added to the samples before they were heated at 55°C for 20 min. The input and IP samples were then analyzed by western blot.

3.5.6 Western blot

The western blot was performed as described previously [8]. The antisera to Pgk1 was generously provided by Dr. Jeremy Thorner (University of California, Berkeley) and used as described previously [8]. Antibody to YFP (Clontech, 632381) was used to detect GFP-tagged proteins. The antibody to PA (Jackson ImmunoResearch, 323-005-024) was used to

detect Atg13-PA, Dhh1-PA and Eap1-PA. The antibody to HA epitope (Sigma, H3663) was used to detect Dhh1-3HA. The endogenous antibody to Atg1 was described previously [36].

3.6. References

1. Xie, Z., and Klionsky, D.J. (2007). Autophagosome formation: core machinery and adaptations. Nat Cell Biol *9*, 1102-1109.
2. Yang, Z., and Klionsky, D.J. (2010). Mammalian autophagy: core molecular machinery and signaling regulation. Curr Opin Cell Biol *22*, 124-131.
3. Lynch-Day, M.A., Mao, K., Wang, K., Zhao, M., and Klionsky, D.J. (2012). The role of autophagy in Parkinson's disease. Cold Spring Harb Perspect Med *2*, a009357.
4. Levine, B., Mizushima, N., and Virgin, H.W. (2011). Autophagy in immunity and inflammation. Nature *469*, 323-335.
5. Klionsky, D.J., and Codogno, P. (2013). The mechanism and physiological function of macroautophagy. J Innate Immun *5*, 427-433.
6. Deretic, V., and Levine, B. (2009). Autophagy, immunity, and microbial adaptations. Cell Host Microbe *5*, 527-549.
7. Klionsky, D.J., Cregg, J.M., Dunn, W.A., Jr., Emr, S.D., Sakai, Y., Sandoval, I.V., Sibirny, A., Subramani, S., Thumm, M., Veenhuis, M., et al. (2003). A unified nomenclature for yeast autophagy-related genes. Dev Cell *5*, 539-545.
8. Jin, M., He, D., Backues, S.K., Freeberg, M.A., Liu, X., Kim, J.K., and Klionsky, D.J. (2014). Transcriptional regulation by Pho23 modulates the frequency of autophagosome formation. Curr Biol *24*, 1314-1322.
9. Xie, Z., Nair, U., and Klionsky, D.J. (2008). Atg8 controls phagophore expansion during autophagosome formation. Mol Biol Cell *19*, 3290-3298.
10. Bernard, A., Jin, M., Xu, Z., and Klionsky, D.J. (2015). A large-scale analysis of autophagy-related gene expression identifies new regulators of autophagy. Autophagy *11*, 2114-2122.
11. Bartholomew, C.R., Suzuki, T., Du, Z., Backues, S.K., Jin, M., Lynch-Day, M.A., Umekawa, M., Kamath, A., Zhao, M., Xie, Z., et al. (2012). Ume6 transcription factor is part of a signaling cascade that regulates autophagy. Proc Natl Acad Sci U S A *109*, 11206-11210.
12. Bernard, A., Jin, M., Gonzalez-Rodriguez, P., Fullgrabe, J., Delorme-Axford, E., Backues, S.K., Joseph, B., and Klionsky, D.J. (2015). Rph1/KDM4 mediates nutrient-limitation signaling that leads to the transcriptional induction of autophagy. Curr Biol *25*, 546-555.
13. Feng, Y., Yao, Z., and Klionsky, D.J. (2015). How to control self-digestion: transcriptional, post-transcriptional, and post-translational regulation of autophagy. Trends Cell Biol *25*, 354-363.
14. Settembre, C., Di Malta, C., Polito, V.A., Garcia Arencibia, M., Vetrini, F., Erdin, S., Erdin, S.U., Huynh, T., Medina, D., Colella, P., et al. (2011). TFEB links autophagy to lysosomal biogenesis. Science *332*, 1429-1433.

15. Hu, G., McQuiston, T., Bernard, A., Park, Y.D., Qiu, J., Vural, A., Zhang, N., Waterman, S.R., Blewett, N.H., Myers, T.G., et al. (2015). A conserved mechanism of TOR-dependent RCK-mediated mRNA degradation regulates autophagy. Nat Cell Biol *17*, 930-942.
16. Cordin, O., Banroques, J., Tanner, N.K., and Linder, P. (2006). The DEAD-box protein family of RNA helicases. Gene *367*, 17-37.
17. Klionsky, D.J., Abdelmohsen, K., Abe, A., Abedin, M.J., Abeliovich, H., Acevedo Arozena, A., Adachi, H., Adams, C.M., Adams, P.D., Adeli, K., et al. (2016). Guidelines for the use and interpretation of assays for monitoring autophagy (3rd edition). Autophagy *12*, 1-222.
18. Cheong, H., and Klionsky, D.J. (2008). Biochemical methods to monitor autophagy-related processes in yeast. Methods Enzymol *451*, 1-26.
19. Morawska, M., and Ulrich, H.D. (2013). An expanded tool kit for the auxin-inducible degron system in budding yeast. Yeast *30*, 341-351.
20. Jungfleisch, J., Nedialkova, D.D., Dotu, I., Sloan, K.E., Martinez-Bosch, N., Bruning, L., Raineri, E., Navarro, P., Bohnsack, M.T., Leidel, S.A., et al. (2017). A novel translational control mechanism involving RNA structures within coding sequences. Genome Res *27*, 95-106.
21. Zhang, Y., Ponty, Y., Blanchette, M., Lecuyer, E., and Waldispuhl, J. (2013). SPARCS: a web server to analyze (un)structured regions in coding RNA sequences. Nucleic Acids Res *41*, W480-485.
22. Pause, A., and Sonenberg, N. (1992). Mutational analysis of a DEAD box RNA helicase: the mammalian translation initiation factor eIF-4A. EMBO J *11*, 2643-2654.
23. Carroll, J.S., Munchel, S.E., and Weis, K. (2011). The DExD/H box ATPase Dhh1 functions in translational repression, mRNA decay, and processing body dynamics. J Cell Biol *194*, 527-537.
24. Selth, L.A., Gilbert, C., and Svejstrup, J.Q. (2009). RNA immunoprecipitation to determine RNA-protein associations in vivo. Cold Spring Harb Protoc *2009*, pdb prot5234.
25. Jackson, R.J., Hellen, C.U., and Pestova, T.V. (2010). The mechanism of eukaryotic translation initiation and principles of its regulation. Nat Rev Mol Cell Biol *11*, 113-127.
26. Cheng, Z., Coller, J., Parker, R., and Song, H. (2005). Crystal structure and functional analysis of DEAD-box protein Dhh1p. RNA *11*, 1258-1270.
27. Thoreen, C.C., Chantranupong, L., Keys, H.R., Wang, T., Gray, N.S., and Sabatini, D.M. (2012). A unifying model for mTORC1-mediated regulation of mRNA translation. Nature *485*, 109-113.
28. Braunstein, S., Karpisheva, K., Pola, C., Goldberg, J., Hochman, T., Yee, H., Cangiarella, J., Arju, R., Formenti, S.C., and Schneider, R.J. (2007). A hypoxia-controlled cap-dependent to cap-independent translation switch in breast cancer. Mol Cell *28*, 501-512.
29. Teleman, A.A., Chen, Y.W., and Cohen, S.M. (2005). 4E-BP functions as a metabolic brake used under stress conditions but not during normal growth. Genes Dev *19*, 1844-1848.
30. Blewett, N.H., and Goldstrohm, A.C. (2012). A eukaryotic translation initiation factor 4E-binding protein promotes mRNA decapping and is required for PUF repression. Mol Cell Biol *32*, 4181-4194.

31. Wang, Y., Arribas-Layton, M., Chen, Y., Lykke-Andersen, J., and Sen, G.L. (2015). DDX6 Orchestrates Mammalian Progenitor Function through the mRNA Degradation and Translation Pathways. Mol Cell *60*, 118-130.
32. Sonenberg, N., and Hinnebusch, A.G. (2009). Regulation of translation initiation in eukaryotes: mechanisms and biological targets. Cell *136*, 731-745.
33. Richter, J.D., and Sonenberg, N. (2005). Regulation of cap-dependent translation by eIF4E inhibitory proteins. Nature *433*, 477-480.
34. Ma, X.M., and Blenis, J. (2009). Molecular mechanisms of mTOR-mediated translational control. Nat Rev Mol Cell Biol *10*, 307-318.
35. Li, C., Wen, A., Shen, B., Lu, J., Huang, Y., and Chang, Y. (2011). FastCloning: a highly simplified, purification-free, sequence- and ligation-independent PCR cloning method. BMC Biotechnol *11*, 92.
36. Abeliovich, H., Zhang, C., Dunn, W.A., Jr., Shokat, K.M., and Klionsky, D.J. (2003). Chemical genetic analysis of Apg1 reveals a non-kinase role in the induction of autophagy. Mol Biol Cell *14*, 477-490.

Table S3.1. Yeast strains used in this study

Name	Genotype	Reference
BY4742	MATα *his3Δ1 leu2Δ0 lys2Δ0 ura3Δ0*	Invitrogen
JMY114	WLY176 *ATG13Δ::KAN*	This study
SEY6210	MATα *leu2-3,112 ura3-52 his3-Δ200 trp1-Δ901 suc2-Δ9 lys2-801 GAL*	[1]
WLY176	SEY6210 *pho13Δ pho8Δ60*	[2]
XLY301	SEY6210 *dhh1Δ::KANMX6*	This study
XLY306	BY4742 *PGI1-GFP::HIS3*	This study
XLY307	BY4742 *PGI1-GFP::HIS3 atg1Δ::URA3*	This study
XLY308	BY4742 *PGI1-GFP::HIS3 dhh1Δ::URA3*	This study
XLY310	BY4742 *PGI1-GFP::HIS3 eap1Δ::KANMX6*	This study
XLY312	SEY6210 *PGI1-GFP:TRP1*	This study
XLY314	SEY6210 *PGI1-GFP:TRP1 dhh1Δ::KANMX6*	This study
XLY316	SEY6210 *atg1Δ::HIS3 pRS-ATG1(406)::URA3*	This study
XLY317	SEY6210 *atg1Δ::HIS3 pRS-ATG1^{mut}(406)::URA3*	This study
XLY318	BY4742 *Fba1-GFP::HIS3*	This study
XLY319	BY4742 *Fba1-GFP::HIS3 dhh1Δ::URA3*	This study
XLY320	BY4742 *Fba1-GFP::HIS3 atg1Δ::URA3*	This study
XLY321	SEY6210 *DHH1-PA::HIS3*	This study
XLY322	SEY6210 *ATG1-ADH1 3'UTR::TRP1*	This study
XLY323	SEY6210 *ATG1-ADH1 3'UTR::TRP1 dhh1Δ::KANMX6*	This study
XLY323	SEY6210 *ATG1-ADH1 3'UTR::TRP1 DHH1-PA::HIS3*	This study
XLY324	SEY6210 *PGI1-GFP:TRP1 DHH1-PA::HIS3*	This study
XLY325	SEY6210 *PGI1-GFP:TRP1 DHH1(H395AR396A)-PA::HIS3*	This study
XLY336	WLY176 *ATG2-PA*	This study
XLY337	WLY176 *ATG2-PA dhh1Δ::URA3*	This study
ZYY101	WLY176 *pRS405-GFP-ATG8::LEU2*	[3]
ZYY201	WLY176 *pRS405-GFP-ATG8::LEU2 dhh1Δ::KAN*	This study
ZYY202	JMY114 *pRS406-ATG13-PA::URA3*	This study
ZYY203	JMY114 *pRS406-ATG13-PA::URA3 dhh1Δ::HIS3*	This study
ZYY204	JMY114 *pRS406-ATG13-PA::URA3 eap1Δ::HIS3*	This study
ZYY205	JMY114 *pRS406-ATG13^{mut}-PA::URA3*	This study
ZYY206	JMY114 *pRS406-ATG13^{mut}-PA::URA3 dhh1Δ::HIS3*	This study
ZYY207	SEY6210 *HIS3::ZEO1p-EAP1-PA::KAN*	This study
ZYY208	SEY6210 *DHH1-3HA::TRP1*	This study
ZYY209	SEY6210 *HIS3::ZEO1p-EAP1-PA::KAN DHH1-3HA::TRP1*	This study

References

1. Robinson, J.S., Klionsky, D.J., Banta, L.M., and Emr, S.D. (1988). Protein sorting in *Saccharomyces cerevisiae*: isolation of mutants defective in the delivery and processing of multiple vacuolar hydrolases. Mol Cell Biol *8*, 4936-4948.

2. Kanki, T., Wang, K., Baba, M., Bartholomew, C.R., Lynch-Day, M.A., Du, Z., Geng, J., Mao, K., Yang, Z., Yen, W.L., et al. (2009). A genomic screen for yeast mutants defective in selective mitochondria autophagy. Mol Biol Cell *20*, 4730-4738.

3. Yao, Z., Delorme-Axford, E., Backues, S.K., and Klionsky, D.J. (2015). Atg41/Icy2 regulates autophagosome formation. Autophagy *11*, 2288-2299.

Table S3.2. Primers for RT-qPCR analysis in the RNA immunoprecipitation assay

Primer	Sequence
ATG1 -480 F	TTAACCGCTCGGCTCTGATTTC
ATG1 -480 R	AAGCTCCTTTATGAGATGCTCGATTC
ATG1 -290 F	TAGGCCGAGGTTAATTCTAGAACG
ATG1 -290 R	ATAGTACTGTTCTCTGTTTCCCCAGA
ATG1 35 F	CTGTGAACCATAATCTAATGGCAAGTG
ATG1 35 R	TACTTCCTTTATGGCTACATGCTGAG
ATG1 800 F	GAGCTTCCAATCATTTGGAGTTATTC
ATG1 800 R	CTATTCTTTGGGCTGGATCAAATGTC
ATG1 2340 F	GGTAGTTCGGAAGAGCCAGTATAT
ATG1 2340 R	GTTGCATAAGCTAATTCACAGTTGTAC
ATG1 3UTR F	GAGGCAGAAGATGAACCACCAAA
ATG1 3UTR R	GTAAAGCATTTCGAGAGTAGCATAAC
ATG13 -10 F	AGCATGAGTCATGGTTGCCGAAG
ATG13 -10 R	ACTTGATTCGGTGGAGCATATTAG
ATG13 1000 F	CAACACCAGGTCCAGACACAAC
ATG13 1000 R	GTTGAACAGGTCTCGATATTGGATAG
ATG13 3'UTR F	GACGAGGATGATCAAGATGATGATCTAG
ATG13 3'UTR R	TCTTTTCTTGCATATCTATTTCACCTT
ATG1-ADH1$^{3'UTR}$ F	CCAAAATTAAGCGCGCCACTTC
ATG1-ADH1$^{3'UTR}$ R	TCGTTTTAAAACCTAAGAGTCACTT

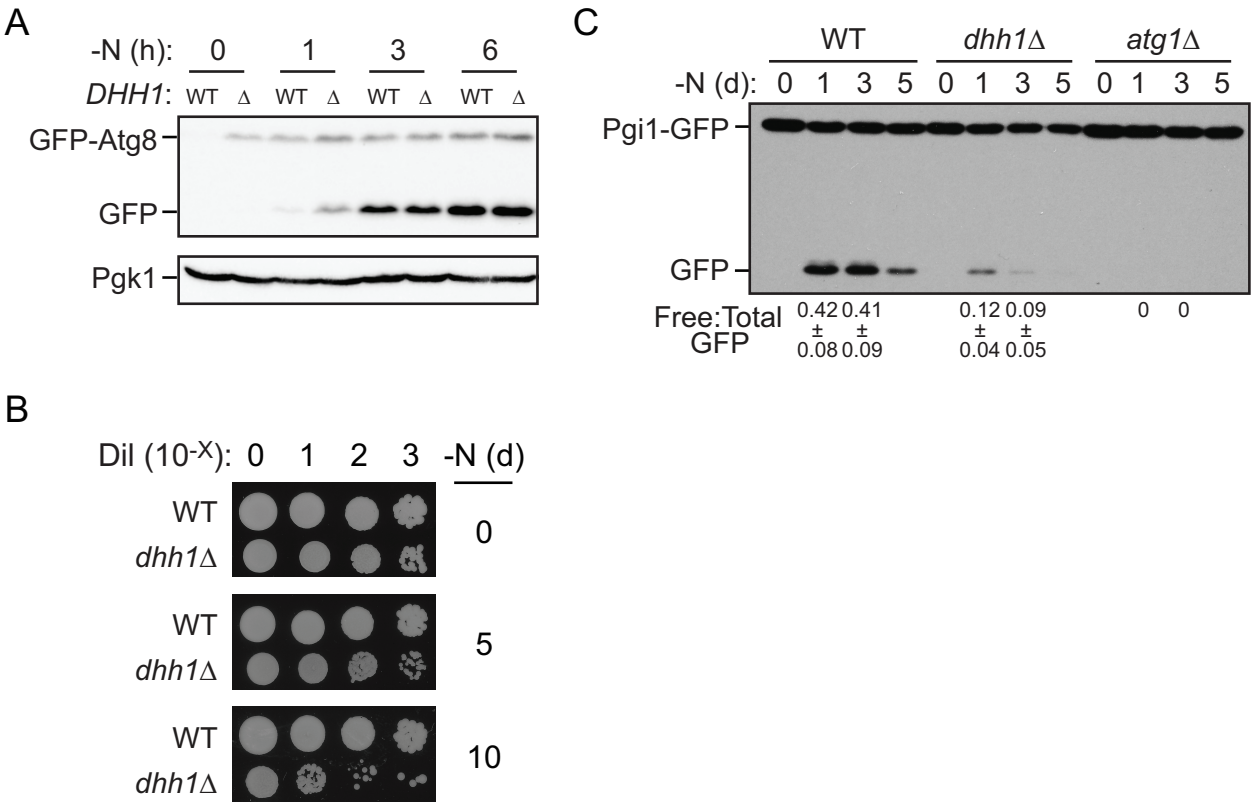

Figure 3.1. Dhh1 positively regulates autophagy under nitrogen starvation conditions. (A) GFP-Atg8 (ZYY101) and GFP-Atg8 *dhh1*Δ (ZYY201) cells were grown in YPD to mid-log phase (-N: 0 h) and then shifted to SD-N for 1, 3 and 6 h. Cell lysates were prepared, subjected to SDS-PAGE and analyzed by western blot. Pgk1 was a loading control. (B) WT (SEY6210) and *dhh1*Δ (XLY301) cells were grown in YPD to mid-log phase (-N: 0 d) and then shifted to SD-N for 5 and 10 d. The indicated dilutions of cells were plated on YPD plates and grown for 2 days. (C) Pgi1-GFP (XLY306), Pgi1-GFP *atg1*Δ (XLY307), and Pgi1-GFP *dhh1*Δ (XLY308) cells were grown in YPD to mid-log phase (-N: 0 d) and then shifted to SD-N for 1, 3 and 5 d. Cell lysates were prepared, subjected to SDS-PAGE and analyzed by western blot.

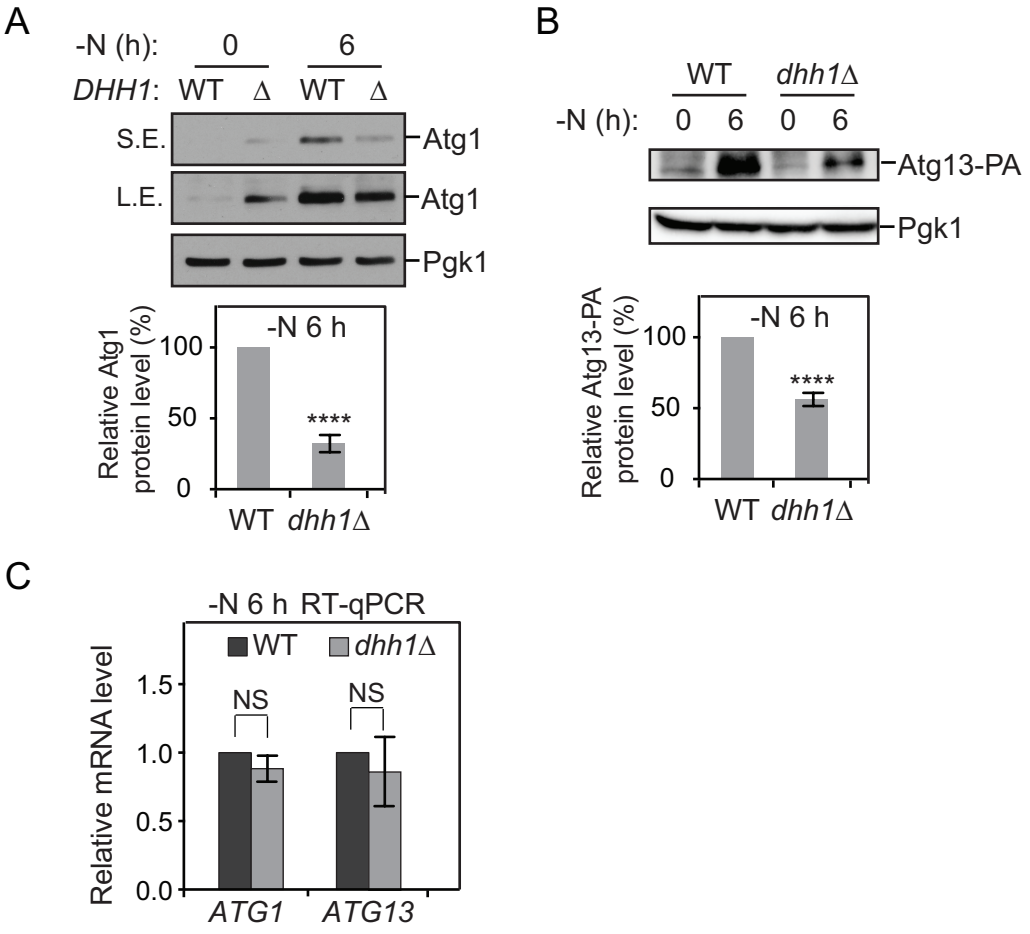

Figure 3.2. Dhh1 promotes the translation of Atg1 and Atg13.
(A) WT (SEY6210) and *dhh1*Δ (XLY301) cells were grown in YPD to mid-log phase (-N: 0 h) and then shifted to SD-N for 6 h. Cell lysates were prepared, subjected to SDS-PAGE and analyzed by western blot. For quantification of Atg1 protein level in cells after prolonged nitrogen starvation, Atg1 protein level was first normalized to the loading control Pgk1. The values of the *dhh1*Δ mutant samples were then normalized to that in WT cells. The error bars indicate the SD of 3 independent experiments. The result is examined by t-test, ****, $p < 0.0001$. S.E, short exposure; L.E, long exposure. (B) Atg13-PA (ZYY202) and Atg13-PA *dhh1*Δ (ZYY203) cells were grown in YPD to mid-log phase (-N: 0 h) and then shifted to SD-N for 6 h. Cell lysates were prepared, subjected to SDS-PAGE and analyzed by western blot. The quantification of Atg13 protein level was conducted as indicated in (A). (C) Atg13-PA and Atg13-PA *dhh1*Δ cells were grown in YPD to mid-log phase (-N: 0 h) and then shifted to SD-N for 6 h. Total RNA for each sample was extracted and the mRNA levels were quantified by RT-qPCR. The mRNA levels of the samples were first normalized to the level of the reference gene *TFC1*. Then, individual *ATG1,* and *ATG13* mRNA levels were normalized to the mRNA level of the corresponding gene in WT cells. The error bars indicate the SD of 3 independent experiments. The quantification was conducted as indicated in (A).

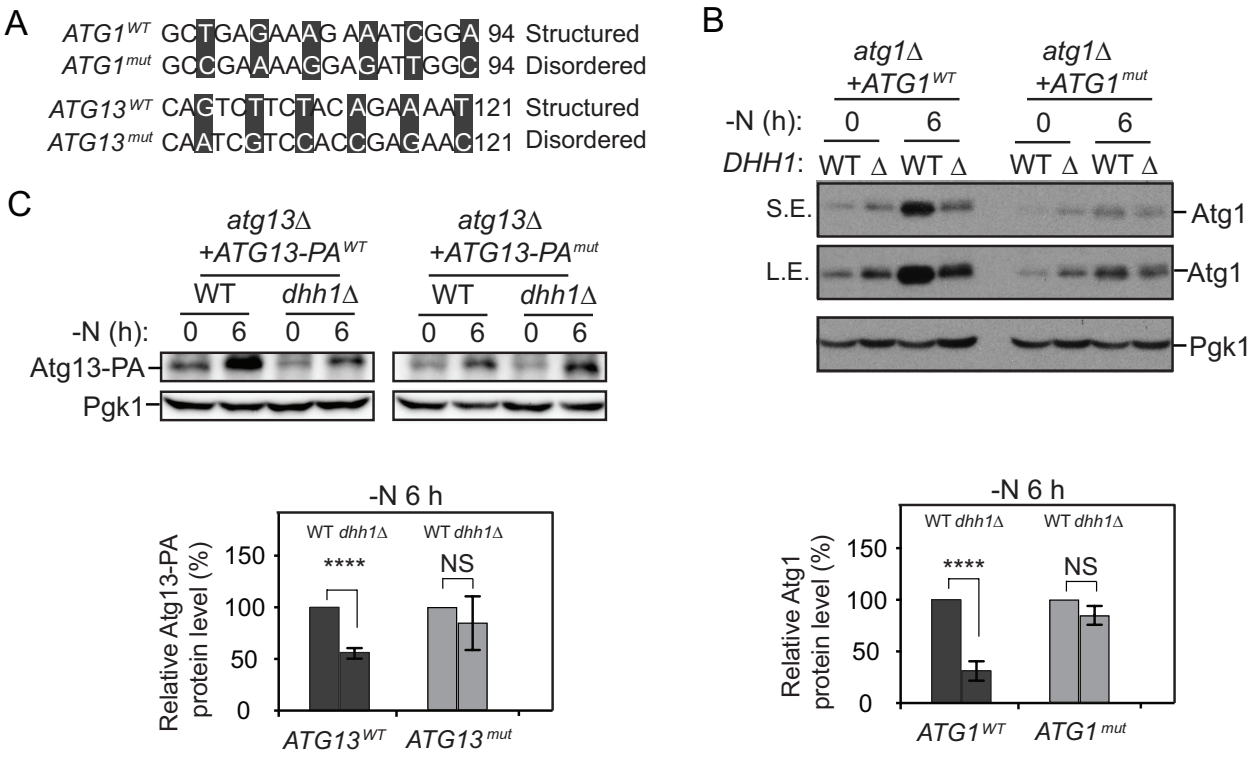

Figure 3.3. The structured regions in the *ATG1* and *ATG13* ORFs are necessary for the translational regulation by Dhh1.

(A) The mutations made in the structured regions of *ATG1* and *ATG13* ORFs are shown as indicated. (B) Atg1^{WT} (XLY316), Atg1^{WT} *dhh1*Δ (XLY317), Atg1^{mut} (XLY318) and Atg1^{mut} *dhh1*Δ (XLY319) cells were grown in YPD to mid-log phase (-N: 0 h) and then shifted to SD-N for 6 h. Cell lysates were prepared, subjected to SDS-PAGE and analyzed by western blot. The error bars indicate the SD of 3 independent experiments. The result is examined by t-test, ****, $p < 0.0001$. (C) Atg13^{WT}-PA (ZYY202), Atg13^{WT}-PA *dhh1*Δ (ZYY203), Atg13^{mut}-PA (ZYY205) and Atg13^{mut}-PA *dhh1*Δ (ZYY206) cells were grown in YPD to mid-log phase (-N: 0 h) and then shifted to SD-N for 6 h. Cell lysates were prepared, subjected to SDS-PAGE and analyzed by western blot. The quantification of Atg13-PA protein level was conducted as indicated in Figure 3B.

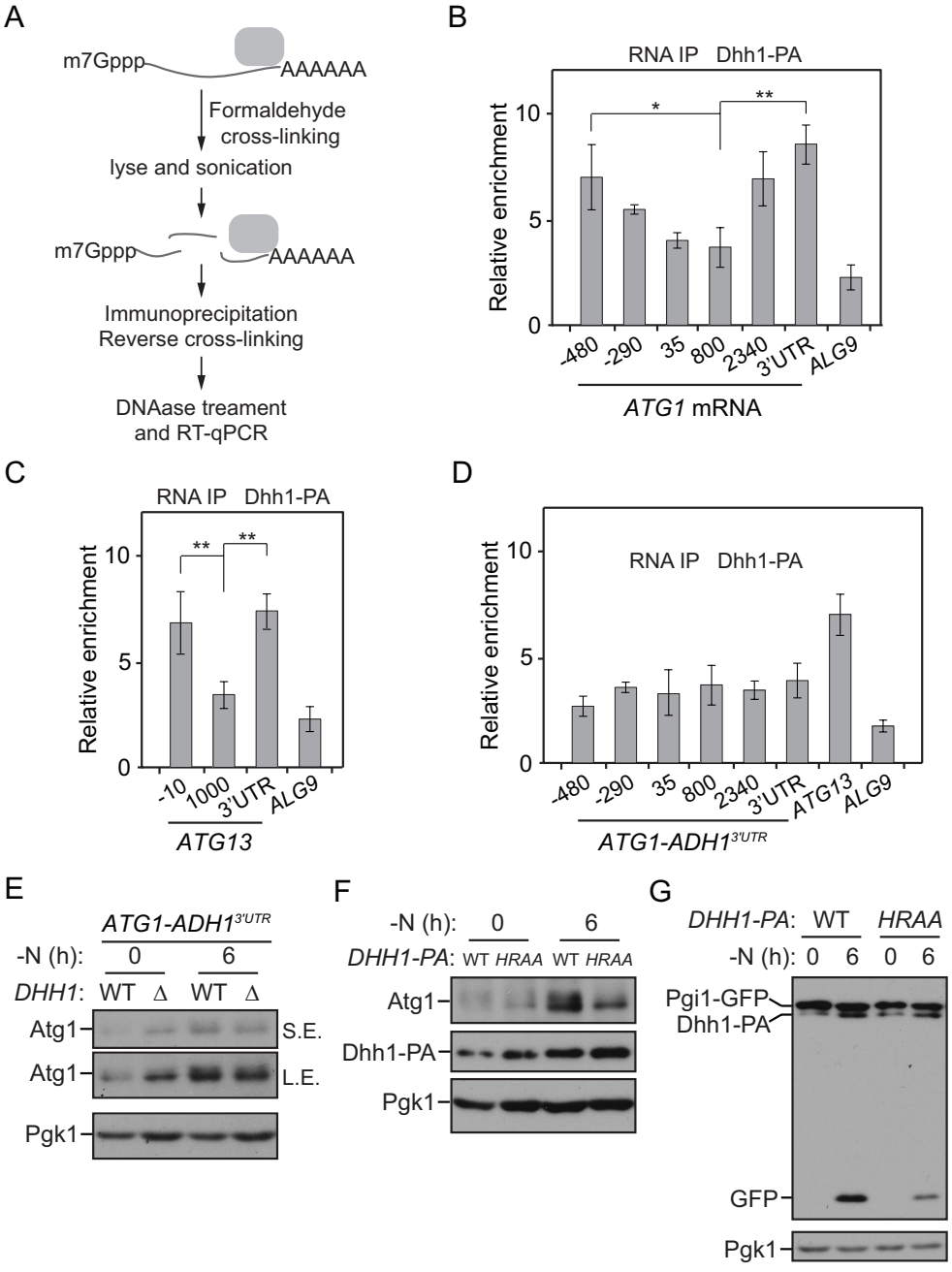
A
m7Gppp
AAAAAA
Formaldehyde cross-linking
lyse and sonication
m7Gppp
AAAAAA
Immunoprecipitation
Reverse cross-linking
DNAase treament and RT-qPCR
B
RNA IP Dhh1-PA
Relative enrichment
10
5
0
*
**
-480
-290
35
800
2340
3'UTR
ALG9
ATG1 mRNA
C
RNA IP Dhh1-PA
Relative enrichment
10
5
0
**
**
-10
1000
3'UTR
ALG9
ATG13
D
RNA IP Dhh1-PA
Relative enrichment
10
5
0
-480
-290
35
800
2340
3'UTR
ATG13
ALG9
ATG1-ADH1 3'UTR
E
ATG1-ADH1 3'UTR
-N (h): 0 6
DHH1: WT Δ WT Δ
Atg1
S.E.
Atg1
L.E.
Pgk1
F
-N (h): 0 6
DHH1-PA: WT HRAA WT HRAA
Atg1
Dhh1-PA
Pgk1
G
DHH1-PA: WT HRAA
-N (h): 0 6 0 6
Pgi1-GFP
Dhh1-PA
GFP
Pgk1

Figure 3.4. Dhh1 associates with *ATG1* and *ATG13* mRNAs.
(A) Workflow of the RNA immunoprecipitation assay. (B), (C) WT (SEY6210) and Dhh1-PA (XLY323) cells were grown in YPD to mid-log phase (-N: 0 h) and then shifted to SD-N for 2 h. Cells were subjected to the RNA immunoprecipitation procedures as described in Materials and Methods. RT-qPCR was performed to analyze the enrichment of RNA fragments as indicated. The values were first normalized to the input samples. Next, levels of affinity-isolated RNA fragments from the Dhh1-PA cells were normalized to that from WT cells. *ALG9* mRNA was a negative control. Enrichment of regions in *ATG1* and *ATG13* mRNAs are shown in (B) and (C), respectively. (D) *ATG1-ADH1*$^{3'UTR}$ (XLY324) and *ATG1-ADH1*$^{3'UTR}$ Dhh1-PA (XLY325) cells cultured and subjected to the RNA immunoprecipitation assay as described in (B) and (C). The relative enrichments of the indicated *ATG1-ADH1*$^{3'UTR}$ mRNA fragments are shown. *ATG13* mRNA is shown as a positive control. *ALG9* mRNA is a negative control. (E) *ATG1-ADH1*$^{3'UTR}$ and *ATG1-ADH1*$^{3'UTR}$ Dhh1-PA cells were grown in YPD to mid-log phase (-N: 0 h) and then shifted to SD-N for 6 h. Cell lysates were prepared, subjected to SDS-PAGE and analyzed by western blot. (F), (G) Pgi1-GFP Dhh1^{WT}-PA (XLY327) and Pgi1-GFP Dhh1^{H395AR396A}-PA (XLY328) cells were grown in YPD to mid-log phase (-N: 0 h) and then shifted to SD-N for 6 h. Cell lysates were prepared, subjected to SDS-PAGE and analyzed by western blot. The analysis of Atg1 protein levels and Pgi1-GFP processing are shown in (F) and (G), respectively.

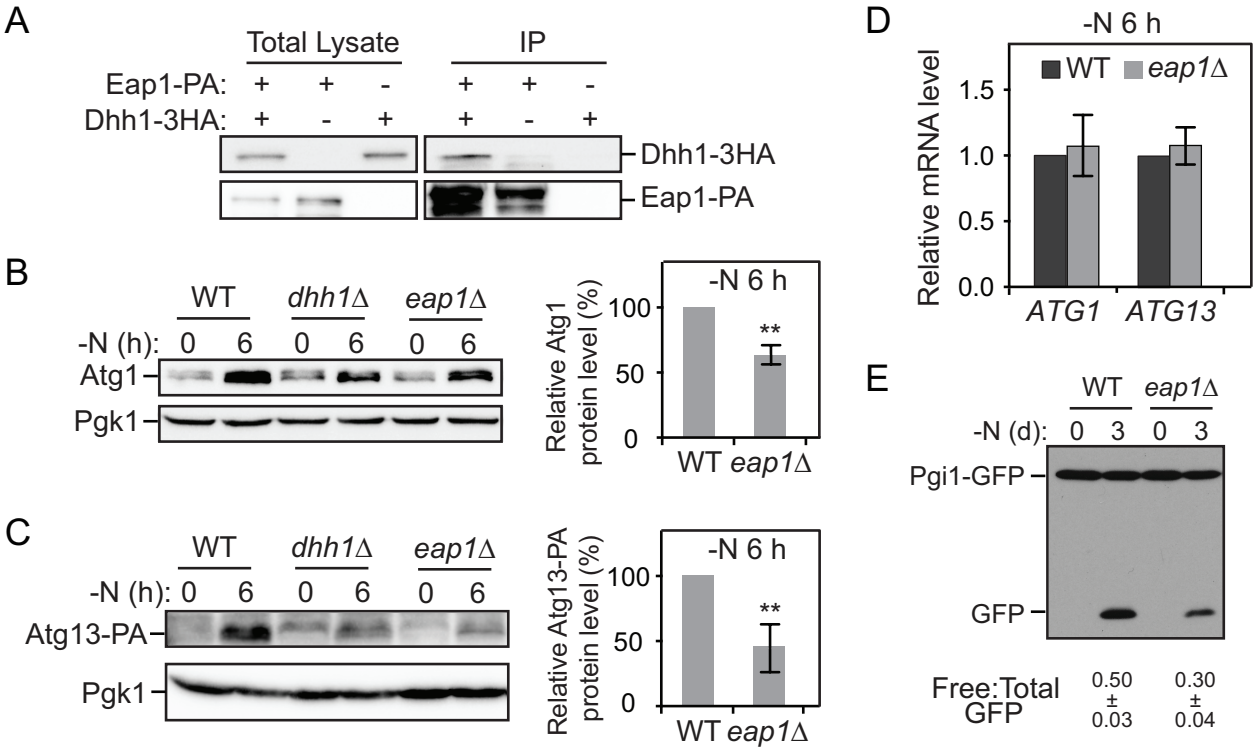

Figure 3.5. Eap1 interacts with Dhh1 and facilitates Atg1 and Atg13 translation during nitrogen starvation.

(A) Eap1-PA (ZYY207), Dhh1-3HA (ZYY208) and Eap1-PA Dhh1-3HA (ZYY209) cells were grown in YPD to mid-log phase (-N: 0 h) and then shifted to SD-N for 2 h. The samples were collected and subjected to the protein-protein immunoprecipitation procedures described in Materials and Methods. The analysis of the samples by western blot was shown. (B), (C) Atg13-PA (ZYY202) and Atg13-PA *eap1*Δ (ZYY204) cells were grown in YPD to mid-log phase (-N: 0 h) and then shifted to SD-N for 6 h. Cell lysates were prepared, subjected to SDS-PAGE and analyzed by western blot. Atg1 and Atg13-PA levels are shown in (B) and (C), respectively. The error bars indicate the SD of 3 independent experiments. The result is examined by t-test, **, $p < 0.01$. (D) Atg13-PA and Atg13-PA *eap1*Δ cells were grown in YPD to mid-log phase (-N: 0 h) and then shifted to SD-N for 6 h. Total RNA for each sample was extracted and the *ATG1* and *ATG13* mRNA levels were quantified by RT-qPCR. (E) Pgi1-GFP (XLY306) and Pgi1-GFP *eap1*Δ (XLY310) cells grown in YPD to mid-log phase (-N: 0 d) and then shifted to SD-N for 3 d. Cell lysates were prepared, subjected to SDS-PAGE and analyzed by western blot.

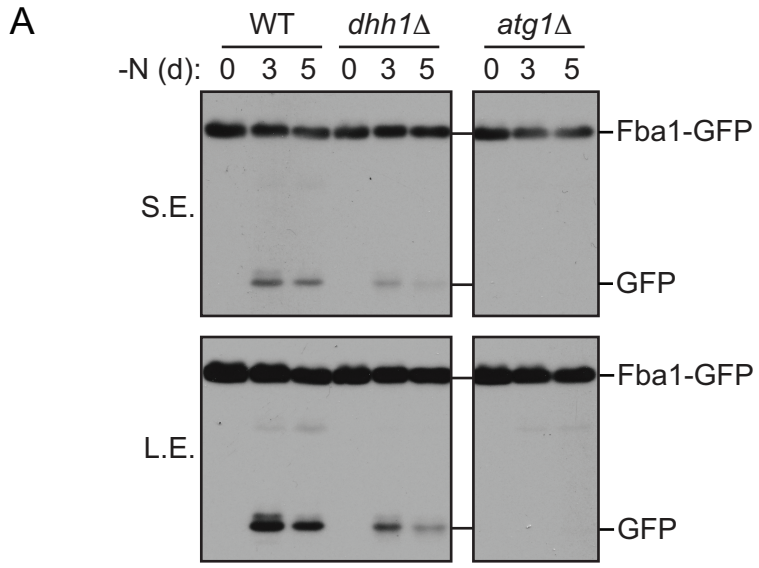

Figure S3.1 Dhh1 positively regulates autophagy under nitrogen starvation conditions. (A) Fba1-GFP (XLY320), Fba1-GFP *dhh1*Δ (XLY321) and Fba1-GFP *atg1*Δ (XLY322) cells were grown in YPD to mid-log phase (-N: 0 h) and then shifted to SD-N for 3 and 5 d. Cell lysates were prepared, subjected to SDS-PAGE and analyzed by western blot. The image shown is from one blot. Some unrelated lanes were cropped.

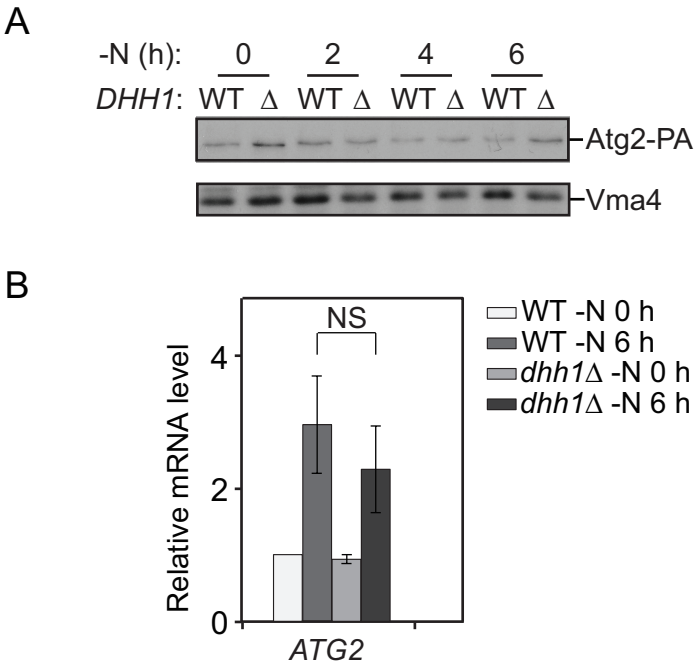

Figure S3.2. Dhh1 promotes the translation of Atg1 and Atg13. (A) Atg2-PA (XLY336) and Atg2-PA *dhh1*Δ (XLY337) cells were grown in YPD to mid-log phase (-N: 0 h) and then shifted to SD-N for 2, 4 and 6 h. Cell lysates were prepared, subjected to SDS-PAGE and analyzed by western blot. Vam4 was a loading control. The 5'-UTR and 3'-UTR of *ATG2* in these strains were not changed. (B) WT (SEY6210) and *dhh1*Δ (XLY301) cells were grown in YPD to mid-log phase (-N: 0 h) and then shifted to SD-N for 6 h. Total RNA for each sample was extracted and the *ATG2* mRNA levels were quantified by RT-qPCR.

Chapter 4 Summary[4]

Autophagy is a highly conserved degradation system that is required for cellular homeostasis in eukaryotes. Dysfunction of autophagy is tightly connected to a verity of diseases including neurondegeneration, heart failure and cancer. Autophagy process relies on a set of autophagy specific proteins, termed Atg proteins, to form autophagy machinery in a complicated manner. The fine control of the autophagy machinery is crucial to maintain proper autophagy level. Thus, studies on molecular basis of autophagy as well as regulation of autophagy are not only important to understand the mechanism of autophagy process but also helpful to provide insight to disease therapies. In my thesis, I use *Saccharomyces cerevisiae* as a model system to investigate 1) The function of Atg41/Icy2 in autophagy; 2) The translational regulation of Dhh1 to autophagy.

4.1. Atg41/Icy2 regulates autophagosome formation

Autophagy is best characterized by the formation of a double membrane structure termed autophagosome. The membrane source required for autophagosome and the detailed mechanism of donating membrane are still under investigation. Over past decades, more than 40 Atg proteins has been identified in yeast. These proteins function in different steps in autophagy. Among them Atg9 was reported to be involved in membrane donation for

[4] This chapter is reprinted partly from Z Yao, E Delorme-Axford, SK Backues, DJ Klionsky. Atg41/Icy2 regulates autophagosome formation. *Autophagy* 11 (12), 2288-2299 and the manuscript X Liu*, Z Yao*, M Jin*, DJ Klionsky. Dhh1 promotes autophagy-related protein translation and autophagy during nitrogen starvation, with some modifications.

autophagosome formation. However, the mechanism and molecular partners for Atg9 membrane donation is not fully elucidated.

Based on a previous screening, we targeted Atg41/Icy2 as a novel member in autophagy machinery. In the absence of Atg41/Icy2, autophagy defect is observed under nitrogen starvation. Huge increase of Atg41/Icy2 mRNA level and protein level is observed when autophagy is induced and this up-regulation is necessary for autophagy. Autophagosome number but not size is affected when Atg41/Icy2 is absent or express in a low level. Atg41/Icy2 is observed to localize near mitochondrial, which shows a similar localization of Atg9. Further analysis indicates Atg41/Icy2 associate with Atg9 near mitochondria and affect Atg9's anterograde traffic. The C terminal of Atg41/Icy2 is important for its localization and function. Since truncation of last Atg41/Icy2 C termini results in its mis-localization, lost interaction with Atg9 and autophagy defect. Atg41/Icy2 is under transcriptional control under starvation. Gcn4, a master regulator under stress is shown to directly activate Atg41/Icy2 when autophagy is induced.

However, there are questions remained to be answered. Although Atg41/Icy2 is shown to increase a lot during autophagy, we don't know how these proteins are consumed. We have not detected this protein within the vacuole, suggesting that it may be degraded by the proteasome. Future studies may provide further information on the mechanism(s) involved in regulating the expression and stability of Atg41 and in determining its role in autophagy. Although homologs of Atg41/Icy2 are found in different fungal species, no homolog is reported in higher eukaryotes based on sequence analysis. Even though many Atg proteins are conserved from yeast to mammals, a number of Atg proteins in yeast lack the corresponding homologs in mammals; however, in many cases the potential functional

counterparts of these Atg proteins in mammals exist. Furture studies may include identification of functional counterparts of Atg41 in mammals.

4.2. RNA helicase Dhh1 functions in translational regulation of Atg proteins to promote autophagy

Autophagy is a fine tuned process. Abnormal levels of autophagy will lead to disruption of cellular homeostasis. Autophagy is tightly controlled in multiple aspects including transcriptional, post-transcriptional, translational and post-translational regulations. These controlling mechanisms function through targeting ATG genes and their products. Thus autophagy activity remains low in nutrient replete condition and quickly goes up when the stress is applied. Compared to other 3 types of regulations, translational regulation of autophagy is barely investigated.

Here we reported the DExD/H-box RNA helicase, Dhh1, is required for translational activation of Atg1 and Atg13 proteins and autophagy activity during nitrogen starvation. Autophagy activity decreased when Dhh1 is absent. Atg1 and Atg13 protein levels are decreased in the dhh1 deletion strain while mRNA levels of them remained similar to wild type. The structured regions shortly after the start codon of the two mRNAs are necessary for their regulation by Dhh1. In addition, Dhh1 directly associates with *ATG1* and *ATG13* mRNAs via the 3' untranslated region (UTR) regions. Moreover, Dhh1 physically interacts with an EIF4E binding protein, Eap1, and facilitates the delivery of the Dhh1-*ATG* mRNA complex to the translation initiation machinery. In the absent of Eap1, autophagy activity and Atg1/Atg13 protein levels decreased. These results demonstrate a model of how some *ATG* genes bypass the general translational suppression by TOR inhibition during nitrogen starvation to maintain a proper level of autophagy.

There are several questions remained to be answered. Both Dhh1 and Eap1 are found to serve as a negative regulator in nutrient rich conditions. Eap1 specifically, was found as the yeast homolog of EIF4EBP in mammals. In mammals, EIF4EBP activates in stress condition to inhibit the protein translation through disrupting Cap-dependent translation initiation. However, our result indicates Eap1 positive regulates Atg protein translation. Eap1 has a unique long C-terminal domain that is absent in its mammal homologs. This domain may distinct Eap1 as a positive regulator of ATG1 and ATG13 mRNAs. It would be interesting to identify the functional counterpart of the C-terminal part of Eap1 in higher eukaryotes. It is possible that the domain's function is executed by some unknown protein(s) in mammals. Another interesting question arises about the multiple roles Dhh1 plays in different conditions. The switch mechanism between its transcriptional and translational roles is still unclear. Whether it is under post-translational modification or undergoes conformational change during the switch of conditions needs further investigation.

4.3. Contribution of the thesis

In this thesis, questions about autophagy machinery and regulation of autophagy are investigated. For the autophagy machinery, this thesis focuses on autophagosome generation. By identifying a novel protein, Atg41, this thesis enlarges the knowledge about the membrane donation process in autophagy. Meanwhile, this study also indicates that membrane near mitochondria serves as a potential membrane donor for autophagosome formation, which is consistant with previous reports from the Klionsky lab. Moreover, the Atg9 complex is less understood in both yeast and mammals compared to other autophagy machineries. Studies of the Atg9 cycling system can be an interesting topic for this field in the future. By elucidating the relationship between Atg41 and Atg9, this study provides a

potential path for further investigation of this Atg complex. Recently, more and more attention has been drawn to the regulation of autophagy. In this thesis, both transcriptional and tranlational regulation of autophagy are studied. This thesis provides evidence about the quick reaction of transcriptional regulation and relativly long-term effect of translational regulation. The results not only show the control of autophagy at mutiple levels, but also indicate that different kinds of regulation serve in different time frames. Specifically, translational regulation of autophagy is poorly understood compared to other kinds of regulation. This thesis provides important hints for translational regualtion of autophagy, which will benefit this field and provide potential direction for future studies.